Talanta 257 (2023) 124324

Contents lists available at ScienceDirect

Talanta

journal homepage: www.elsevier.com/locate/talanta

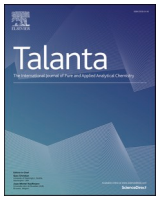

Hyphenation of Fourier transform ion cyclotron resonance mass spectrometry (FT-ICR MS) with separation methods: The art of compromises and the possible - A review

Clarisse Gosset-Erard [a,b], Frédéric Aubriet [a], Emmanuelle Leize-Wagner [b], Yannis-Nicolas François [b], Patrick Chaimbault [a,*]

[a] Université de Lorraine, LCP-A2MC, F-57000, Metz, France
[b] Laboratoire de Spectrométrie de Masse des Interactions et des Systèmes (LSMIS) UMR 7140 (Unistra-CNRS), Université de, Strasbourg, France

ARTICLE INFO

Handling Editor: J. L. Burguera

Keywords:
FT-ICR MS hyphenation
Liquid chromatography (LC)
Capillary electrophoresis (CE)
Gas chromatography (GC)
Omics
Environment

ABSTRACT

This review provides an overview of the online hyphenation of Fourier Transform Ion Cyclotron Resonance Mass Spectrometry (FT-ICR MS) with separation methods to date. The online coupling between separation techniques (gas and liquid chromatography, capillary electrophoresis) and FT-ICR MS essentially raises questions of compromise and is not look as straightforward as hyphenation with other analyzers (QTOF-MS for instance). FT-ICR MS requires time to reach its highest resolving power and accuracy in mass measurement capabilities whereas chromatographic and electrophoretic peaks are transient. In many applications, the strengths and the weaknesses of each technique are balanced by their hyphenation. Untargeted "Omics" (e.g. proteomics, metabolomics, petroleomics, …) is one of the main areas of application for FT-ICR MS hyphenated to online separation techniques because of the complexity of the sample. FT-ICR MS achieves the required high mass measurement accuracy to determine accurate molecular formulae and resolution for isobar distinction. Meanwhile separation techniques highlight isomers and reduce the ion suppression effects extending the dynamic range.

Even if the implementation of FT-ICR MS hyphenated with online separation methods is a little trickier (the art of compromise), this review shows that it provides unparalleled results to the scientific community (the art of the possible), along with raising the issue of its future in the field with the relentless technological progress.

1. Introduction

It is a long time since, the first spectrum obtained by Fourier Transform Ion Cyclotron Resonance Mass Spectrometry (FT-ICR MS) was published by Comisarow and Marshall [1] in 1974. With the relentless progress in this technology, nowadays, evoking FT-ICR MS is immediately synonymous of extreme resolution mass spectrometry (with typical resolving powers higher than 1 000 000 and up to 24 000 000 [2]) and very high mass measurement accuracy (sub parts-per-million enabling the determination of molecular formulae). FT-ICR MS provides indubitable benefits for the molecular profiling of any type of complex mixtures. Direct flow injection FT-ICR MS is widely used in many "omic" studies such as proteomic [3], metabolomics [4], foodomic [5] petroleomic [6] and environmental analyses [7]. This non-exhaustive list of applications deserves the inclusion of Mass Spectrometry Imaging for which, the unique FT-ICR MS resolving power enables the specific localization of isobaric compounds in human [8] or plant tissues [9]. At last, different fragmentation modes, such as sustained off-resonance irradiation collision-induced dissociation (SORI-CID), infrared multiple photon dissociation (IRMPD) or electron-capture dissociation (ECD), are often implemented to complete the structural information obtained by direct infusion [10] and thus, to confirm the identification of specific analytes.

If the FT-ICR MS story began in the middle of 1970s, the chapter concerning its hyphenation with separation methods started being written a little later. Indeed, very high-resolution mass measurement

* Corresponding author. Laboratoire de Chimie et Physique, Approche Multi-échelle des Milieux Complexes (UR 4632), ICPM, Université de Lorraine, 1 boulevard Arago, BP 95823 57078, METZ, Cedex 3, France.
E-mail addresses: clarisse.gosset-erard@univ-lorraine.fr (C. Gosset-Erard), frederic.aubriet@univ-lorraine.fr (F. Aubriet), leize@unistra.fr (E. Leize-Wagner), yfrancois@unistra.fr (Y.-N. François), patrick.chaimbault@univ-lorraine.fr (P. Chaimbault).

https://doi.org/10.1016/j.talanta.2023.124324
Received 28 October 2022; Received in revised form 31 January 2023; Accepted 2 February 2023
Available online 3 February 2023

requires long acquisition times, which have long been an obstacle to the implementation of the coupling between FT-ICR MS and separation methods. Ledford et al. were the first to attempt the adventure of the hyphenation with gas chromatography (GC) in 1980 [11]. Getting a high-resolution ICR mass spectrum from a GC peak was not easy at that time, mainly due to vacuum problems when GC is interfaced with FT-ICR MS. However, since 1983, Sack and Gross succeeded in reaching a resolution of 63 000 (full width at half maximum, FWHM) at m/z 128.062 (for naphthalene) in GC-FT-ICR MS [12]. The first coupling of FT-ICR MS with liquid chromatography (LC) was achieved in the early 1990's by Stockston et al. [13] using electrospray (ESI) as ion source. In 1994, the LC-ESI-FT-ICR MS analysis of peptides carried out by Stacey et al. reached a resolution of 35 000 (FWHM) [14] even as it appears quite low compared with current performance in LC-FT-ICR MS. The detection sensitivity was also not entirely satisfactory but, thanks to the progress in ion trapping, this drawback was slowly overcome. Since 2004, a review in this field claimed that "the coupling of liquid chromatography (LC) to mass spectrometry (MS) is nowadays well established in routine analysis" [15]. The "routine" characterization may seem a bit excessive as of today for LC-FT-ICR MS, even if true, this view is shared by a very limited number of specialized research groups. Capillary electrophoresis (CE) was the last online separation method coupled to FT-ICR MS. Even if CE is still today less widespread than LC, its hyphenation with FT-ICR MS was developed almost simultaneously by Hofstadler et al. who published the first papers in CE-FT-ICR MS in 1993 [16].

Online hyphenation of FT-ICR MS with separation methods raises at least two questions: Fisrtly from a chromatographer's point of view - why would it be necessary to use such an expensive instrument as a detector when cheaper alternatives are available? Secondly, from a mass spectrometrist point of view, why would it be necessary to use a time-consuming separation method when the resolving power of FT-ICR mass spectrometer is doing the job? This review will try to answer both questions before moving on to the matter of applications.

2. Fourier transform ion cyclotron resonance mass spectrometry (FT-ICR MS)

The first article dealing with gas chromatography coupled with FT-ICR MS has been published for more than 25 years now. However, with the exception of Schrader et al. in 2004 [15] and Hertzog et al. in 2021 [17], the published reviews FT-ICR MS generally focused on the recent research and technological developments in MS instrumentation rather than on hyphenation with separation methods. It is not the intention of this review to cover all theoretical aspects of FT-ICR MS. Nevertheless, to understand the challenges, the instrumental specificities, and the benefits of online FT-ICR MS hyphenation with separation methods, it is essential to dive into few simplified theoretical aspects of FT-ICR MS.

2.1. FT-ICR MS principle

As depicted in Fig. 1, the analyte ions produced in the source are first accumulated and then transferred by packets into the ion cyclotron resonance (ICR) cell. The ion transfer (including their accumulation) between the source and the FT-ICR MS cell is a crucial step to understand the challenge of coupling FT-ICR MS with separation methods, but this issue will be discussed later in section 3.

The ICR cell is placed in an ultra-high vacuum region (typically lower than 10^{-9} Torr) located itself inside a superconducting magnet generating a high-field intense magnetic field (B_0). At its simplest, the cell is composed of two trapping plates, two excitation plates and two detection plates. After their transfer, the ions are located close to the center of the ICR cell, on relatively small orbits around B_0 axis. The ions, whose circular motion is uniformly distributed (non-coherent motion), are then excited due to a swept RF pulse orthogonal to the magnetic field. As a result, ions having the same mass-to-charge (m/z) ratio acquire a coherent motion and bundles together on a higher gyration orbit allowing their detection by the detection plates.

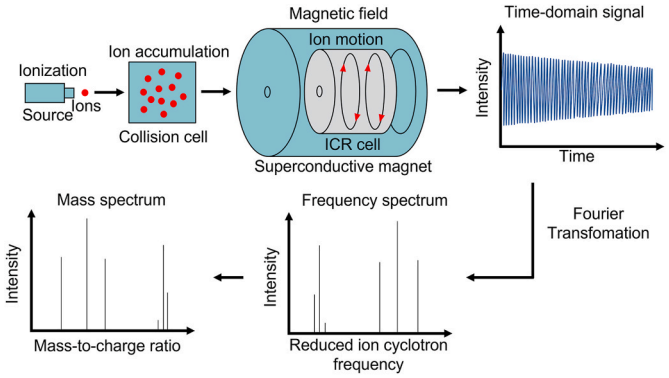

Fig. 1. Brief principle of the ultra-high-resolution mass spectrometry using FT-ICR MS. Ionized analytes are accumulated in the collision cell and send by packet into the ICR cell. Then, the trapped ions are excited to synchronize their cyclotron motion and increase their gyration radius to ensure their detection by the detection plates. The frequencies of gyration are deconvoluted by Fourier-transform and the frequency spectrum is converted into a mass spectrum. Reproduced and adapted from Ref. [18].

This motion, called the cyclotron motion, is the basis of the m/z measurement in FT-ICR MS. The ion packets are rotating at their own cyclotron frequencies w_c which are inversely proportional to their m/z ratios (Eq. (1)) [19]:

$$w_c = \frac{eB_0}{m/z} \tag{1}$$

with w_c the ion cyclotron frequency e the elementary charge and B_0 the magnetic field value.

The sinusoidal signal induced by the ion motion recorded close to the detection plates is called time domain signal or transient. This transient acquisition is the longest step in FT-ICR MS analysis since the resolution and the mass measurement accuracy increase with low acquisition rate. The time domain signal is then converted into cyclotron frequencies by Fourier transformation and finally, the mass spectrum is deduced from cyclotron frequencies.

In practice, the overall motion of the ions in the cell is much more complex due to the combined action of an electrostatic field (application of potential on the trapping plates) and the magnetic field. Harmonic oscillations, called trapping motion, are created by the electrical potential applied between the two trapping plates required to confine the ions in the ICR cell. The trapping frequency is defined by Eq. (2) [19]:

$$w_T = \sqrt{\frac{2\, e\propto V_T}{m/z}} \tag{2}$$

with w_T the ion trapping frequency, $\propto V_T$ a coefficient proportional to the trapping voltage V_T, e the elementary charge, V_T the trapping voltage and m/z the ion mass-to-charge ratio.

Because of the trapping motion, the real frequency of the ion cyclotron motion is modified compared to the theoretical one. The recorded frequency is actually the reduced ion cyclotron frequency w_+ (from which the mass spectrum is deduced) defined by Eq. (3) [19]:

$$w_+ = \frac{w_c}{2} + \sqrt{\frac{w_c^2}{4} - \frac{w_T^2}{2}} \tag{3}$$

with w_+ the reduced ion cyclotron frequency, w_T the ion trapping frequency and w_c the ion cyclotron frequency.

Finally, the combination of the magnetic field B_0 and the electrical potential created by the trapping plates induces the magnetron motion

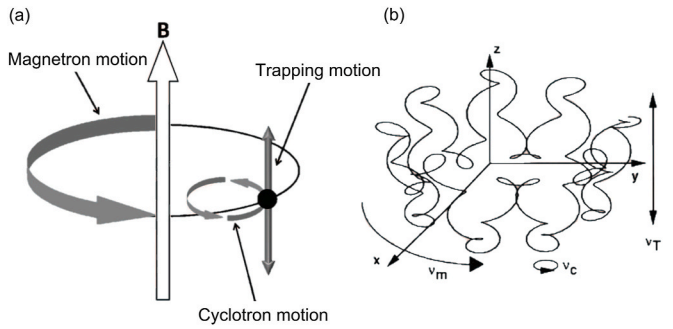

Fig. 2. Schematic representation of (a) the three natural motions of an ion confined in an ICR cell and (b) the resulting ion trajectory. Figure and caption are extracted and adapted from Ref. [20].

around the magnetic field axis. The magnetron frequency w_- is described by Eq. (4) [19]:

$$w_- = \frac{w_c}{2} - \sqrt{\frac{w_c^2}{4} - \frac{w_T^2}{2}} \quad (4)$$

with w_- the ion magnetron frequency, w_T the ion trapping frequency and w_c the ion cyclotron frequency.

The consequence of the superposition of these three motions is a very complex trajectory (represented in Fig. 2). Notwithstanding the specific issues of hyphenation with separation methods, even with an ICR cell properly shimmed and gated, additional peaks appear on the mass spectra because of these harmonic oscillations. They can be limited but not eliminated adding complexity of the data interpretation for the uninitiated users. More details on the deep theory of FT-ICR MS can be found in Marshall et al. [10].

2.2. Advantages of FT-ICR MS

Even if FT-ICR mass spectrometers are more user-friendly than they were in the past, their use is still trickier than other mass spectrometers. This is largely compensated by the advantages they provide. FT-ICR mass spectrometers provide the highest resolution and mass measurement accuracy, at least in low *m/z* range [21,22]. Indeed, the use of a strong magnetic field enables FT-ICR MS to provide an ultra-high resolution and a high mass measurement accuracy. Already in the beginning of the 2010's, the resolving power of a 7 T FT-ICR MS equipped with the dynamically harmonized ICR cell reported by Nikolaev et al. reached 24 000 000 at *m/z* 609 (protonated reserpine) with a mass measurement accuracy of 0.9 ppm for a detection time of 180 s [2]. Concerning higher mass compounds such as proteins, in 1997, Kelleher et al. achieved the unit mass resolution with a 3 Da-accuracy for a 112 kDa-protein (Chondroitinase II) applying a detection time of 100–150 s on a custom built 9.4 T FT-ICR mass spectrometer. Such a performance corresponds to a resolution power of 170 000 [23]. Later on, Nikolaev et al. achieved isotopic resolution for a 186 kDa tetrameric enolase with a 7 T FT-ICR MS [24]. The key to reaching such ultra-high resolutions is the progress in very high vacuum technologies (a typical vacuum around 10^{-10}-10^{-11} bar is required in the ICR cell to enable such long acquisition times) as well as the more recent instrumental and data processing developments. These issues will be discussed later in this review.

The high mass measurement accuracy achieved by the FT-ICR enables the reliable assignment of a molecular formula to each detected feature, and the high resolution achieves the distinction of very close isobaric species. Indeed, only high-resolution mass spectrometry enables the separation of overlapping isotopologue peaks containing ^{13}C, ^{2}H, ^{18}O, ^{15}N, ^{31}P and ^{34}S, as shown in Fig. 3. The isotopic peak pattern gives crucial information on the elemental composition. Therefore, the high resolution is helping to narrow down the number of candidates for elemental compositions until the assignment of an unambiguous elemental formula especially for small molecules [18,25,26]. Another advantage of the FT-ICR MS is the availability of numerous fragmentation techniques. Indeed, besides the common collision induced dissociation (CID) and electron-transfer dissociation (ETD) fragmentation techniques, ultraviolet photodissociation (UVPD), infrared multiphoton dissociation (IRMPD) and electron-capture dissociation (ECD) fragmentation techniques are available in the ICR cell. All those techniques produce complementary MS^n data, enabling an easier and deeper structural elucidation of analytes [27].

2.3. Limits of FT-ICR MS overcome by hyphenation with separation methods

FT-ICR MS is a powerful tool for the assignment of elemental composition and structural elucidation thanks to its ultra-high resolution, its sub-ppm mass measurement accuracy, and its multiple fragmentation modes. However, this technique still has some limitations when used in direct infusion.

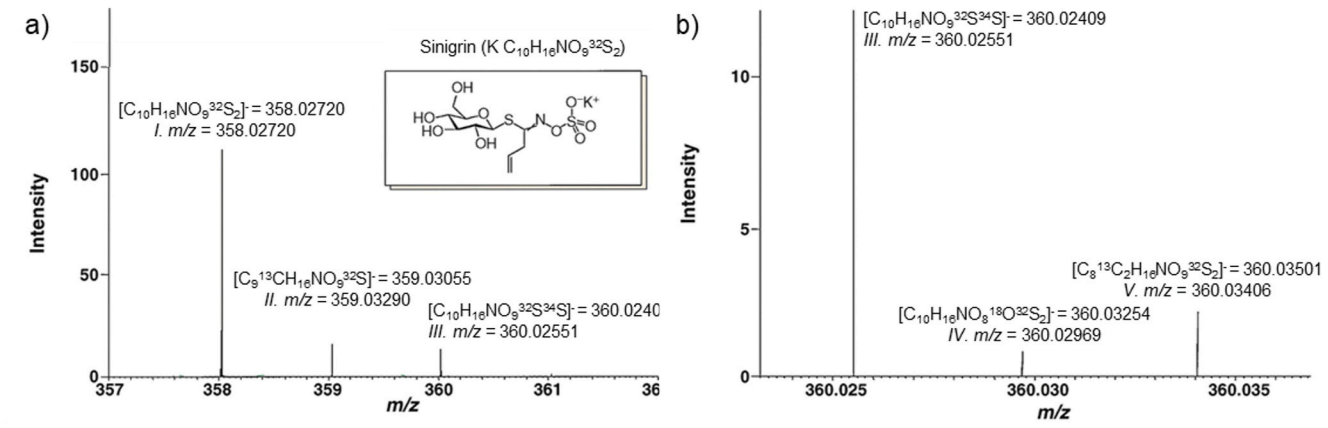

Fig. 3. (a) Example of ultra-high-resolution MS analysis using a FT-ICR MS. The MS spectra were obtained using an LTQ-FT-ICR MS (Thermo Scientific). A glucosinolate produced by the *Brassicaceae* plants, sinigrin ($KC_{10}H_{16}NO_9S_2$), was subjected to the separation of isotope ion peaks in an ESI-negative mode. In a broadband spectrum, the detected ions of I (*m/z* 358.02890), II (*m/z* 359.03290), and III (*m/z* 360.02539) corresponded to $[C_{10}H_{16}NO_9S_2]^-$, $[C_9{}^{13}CH_{16}NO_9{}^{32}S_2]^-$, and $[C_{10}H_{16}NO_9{}^{32}S^{34}S]^-$, respectively. (b) Resolution of isotope ions using a FT-ICR MS. Magnification of the *m/z* window near the ion III ($C_{10}H_{16}NO_9{}^{32}S^{34}S$, *m/z* 360.02551) further revealed the presence of ions of V (*m/z* 360.02969) and VI (*m/z* 360.03406) corresponding to $[C_{10}H_{16}NO_8{}^{18}O^{32}S_2]^-$ and $[C_8{}^{13}C_2H_{16}NO_9{}^{32}S_2]^-$, respectively. Figure and caption are extracted from Ref. [18].

There are two essential "prerequisites" for the specific detection and identification of a given analytes in mass spectrometry and FT-ICR MS is no exception to this rule.

The first rule concerns the charge "z" itself: no charge means no ion, making the *m/z* measurement impossible. The direct infusion of complex mixtures is often subject to the well-known ion suppression effect. Indeed, during the ionization step, the analytes of interest can compete with other compounds to become electrically charged, leading to reduction of their ionization efficiency and thus a poor detection sensitivity. Such ionization suppression was nicely demonstrated by Guillemant et al. in a recent publication dealing with the analysis of N and S hydrocarbons in gasoline [28]. A separation prior MS detection limits the ion suppression phenomenon because fewer molecules are present simultaneously in the ion source [29–33]. Thus, in spite of the chromatographic dilution, the number of detected compounds is higher than in direct infusion. For example, during their proteomic study of cerebrospinal fluid tryptic digest, Wetterhal et al. succeeded in identifying by CE-FT-ICR MS twice the number of identified compounds than by direct infusion [34]. The authors attributed this difference to a better selectivity but also to a lower ion suppression in CE-MS.

Precisely the above-mentioned conclusion leads to the second issue which concerns the discrimination of isomers that cannot be achieved solely by MS detection irrespective of resolving power of the mass spectrometer. Unless ion-mobility is used, structural isomers cannot be distinguished since they have the same exact mass. The solution is their chromatographic or electrophoretic separation before their MS detection. Then, the isomers can be discriminated and identified based on their retention/migration time. This approach may be associated with MS^2 and MS^n data, and eventually also compared to commercially available standards [35–38]. Mass spectra can be very complex, particularly with extreme resolution mass spectrometer such as FT-ICR MS. The selectivity achieved by a separation method, regardless of the presence of isomers, reduces the complexity of the individual mass spectra obtained along the run and thus facilitates the assignment of a molecular formula for each detected ion. Despite this, Zacs et al. identified more than 5000 *m/z* values in every GC-FT-ICR MS data point of their untargeted analysis of brominated and chlorinated flame retardants in food [39], which still represents a huge work of data interpretation. In their studies, the assignment of the elemental compositions was facilitated by the specific isotope patterns of $^{79/81}Br$ and $^{35/37}Cl$ atoms. However, it is easy to imagine how tremendous a task it would have been to process the data in case of the compounds overlapping.

Apart from these two critical points, there are still a few additional advantages in the hyphenation. As already mentioned, the separation technique reduces the number of compounds simultaneously present in the ion source. Consequently, it also helps limiting the peak coalescence of ions having close *m/z* values which is observed when the charge load is too high in the ICR cell. When the ion clouds are too dense, the MS peaks tend to merge together. The chromatographic dilution decreases the amount of ions in the ICR cell and the peak coalescence phenomenon is less likely to happen [40]. In the same idea, the hyphenation of ultra-high resolution mass spectrometry with separation methods increases the dynamic range since the number of ions in the cell is reduced [31,41–44]. Limiting the number of ions in the ICR cell reduces the space-charge effect (Coulombic interactions between ions) which can cause frequency shifts, and therefore mass-to-charge ratio shifts [45]. Direct infusion is thus less accurate in the quantification of the analytes, and relative and absolute quantification is rather performed by hyphenation with a separation method [39,41,46–50]. At last, direct infusion is limited for low concentrated and small volume samples contrary to hyphenated methods [34]. Sensitivity can be even improved using miniaturized and low flow rate separation techniques [51]. Such hyphenation is essential when working with samples in very restricted/limited available quantities, which is a common issue with biological or environmental samples.

As a conclusion to this part, the hyphenation of a separation method to a FT-ICR mass spectrometer enables the separation of isomers, extends the dynamic range of the detection, reduces the complexity for each spectrum obtained along the analytical run, eases data interpretation and quantification. Hence, the hyphenation of separation methods with FT-ICR mass spectrometers has been increasingly developed over the past few years for various applications. Hyphenation of liquid chromatography (LC) [30,31,43,49,52–54], gas chromatography (GC) [39,55,56] and capillary electrophoresis (CE) [16,41,57–59] with FT-ICR MS are used in multiple studies. In order to reach the best selectivity and sensitivity, the separation technique is chosen based on the analytes, the sample matrix and the requested sample preparation.

3. Challenges of the hyphenation of FT-ICR MS and separation methods

The historical chapter about the hyphenation of FT-ICR MS with separation techniques started in 1980 with gas chromatography (GC) [15]. The main problem was to maintain a sufficient vacuum state (typically less than 10^{-8} Torr) for the optimal mass analysis when GC is interfaced with FT-ICR MS. In the following years, there has been an explosion of tips (home-made most of the time) dedicated to circumvent this challenge. Even if the ionization step is still sometimes carried out in the ICR cell (internal ionization) in few studies, external ionization techniques are nowadays dominating, making possible the use of atmospheric pressure ionization (API) sources and the coupling with LC and CE. With the external ionization techniques, the ion source is separated from the ICR cell by several stages of differential pumping in order to reach the required extreme low pressure (Fig. 4). However, this solution implies to guide ions towards the ICR cell. If such interfaces provide advantages, the ion transfer from the source to the ICR cell can be long and also bring other drawbacks concerning the hyphenation with separation techniques. This will be discussed later in section 3.2.

3.1. Compatibility of ion sources

Having solved the problem of vacuum, there are no technical barriers to the coupling. Each separation techniques can be used with its traditional ionization sources. Thus, many studies have been carried out in gas chromatography with electron impact (EI) either in external [55,56] or even in internal ionization [61]. The chemical ionization, which is "softer" than EI and consequently eases access to the molecular weight, is less widespread in GC-FT-ICR MS. However, Szulejko et al. [61] introduced ethanol vapors as chemical ionization reagent and Luo et al. [35] employed this strategy to characterize multicomponent gasoline

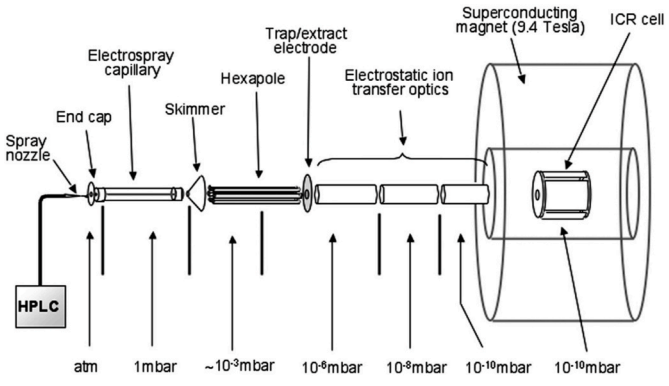

Fig. 4. Schematic view of an HPLC-ESI-FT-ICR MS and its differential pumping stages from the atmospheric pressure ion source to the of 10^{-10} mbar-ultra-high vacuum of the ICR cell (Bruker Daltonics BioAPEX −94e fitted with a 9,4T magnet). Ions formed at atmospheric pressure are transferred through a glass capillary and then through a skimmer into a hexapole ion trap where they are stored before their further transfer to the ion cyclotron resonance cell. Extracted from Ref. [60].

samples. Among the atmospheric pressure ionization (API) sources, atmospheric pressure chemical ionization (APCI) is likely the most used ionization source in GC-FT-ICR MS [39,62,63]. As expected with a soft ionization technique, APCI reduces the fragmentation compared to EI and preserves the intact molecule, either as protonated [62] or deprotonated ions [39] depending on the chosen ion mode. APCI is rather used to analyze mid polar compounds comprising few heteroatoms such as phenols, terpenoids, flame retardants, long chain alkyl and alkylene carboxylic acids. Atmospheric photoionization laser ionization (APLI) is the latest developed among atmospheric ionization methods. In the world of ion sources dedicated to apolar compounds, APLI is the immediate rival of Atmospheric Pressure Chemical Ionization (APPI) and yet APLI, with its stepwise two-photon process, is much more efficient and selective for the ionization of non-polar compounds such as

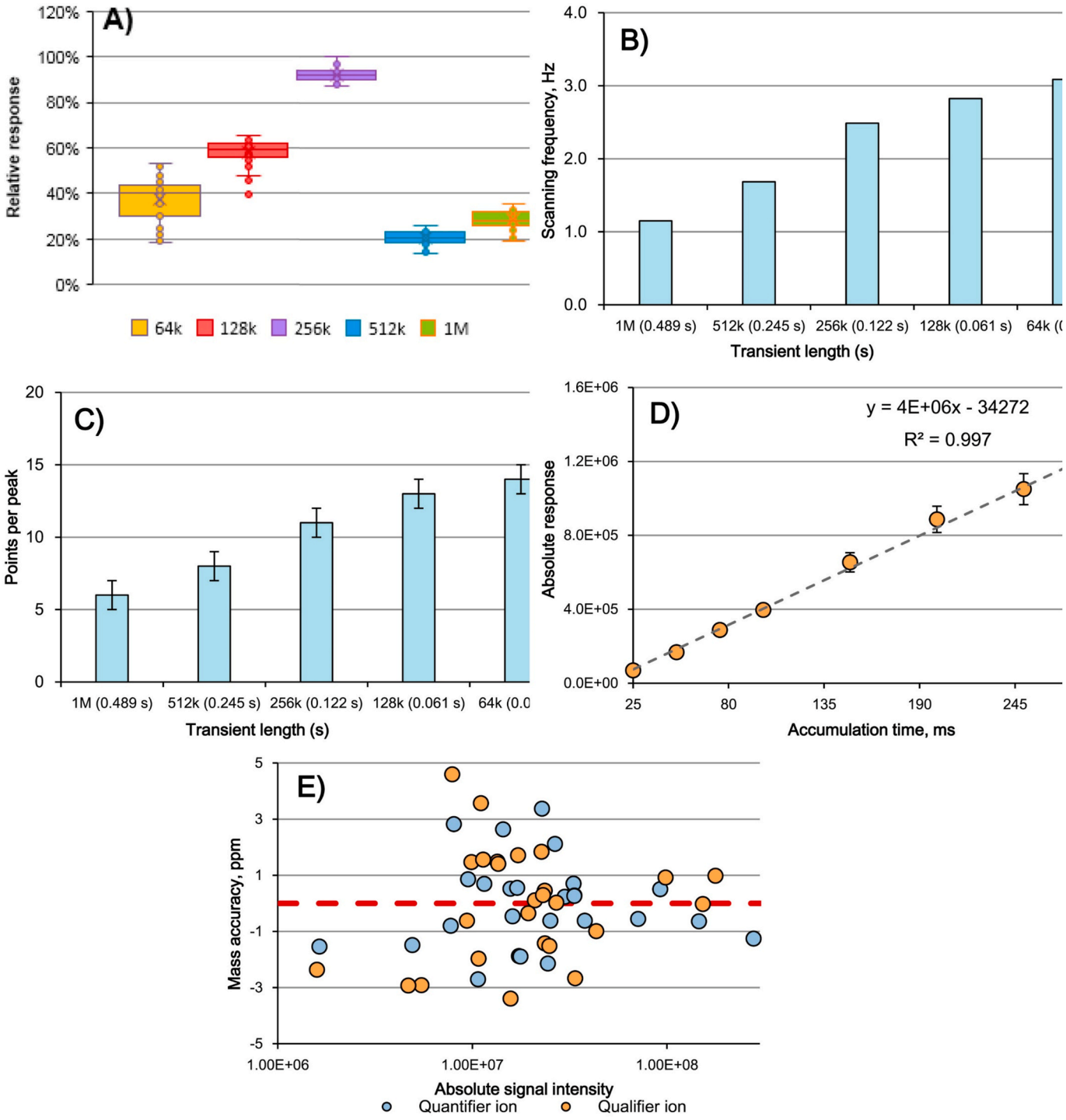

Fig. 5. Design of results of the method optimization experiments from the analysis of PBDE-99, a brominated flame retardant, (50 pg on-column): (A) instrumental response of the system obtained by the applying different transient lengths; (B) relationship between the scanning speed and transient length; (C) relationship between the number of data points per chromatographic peak and different transient lengths; (D) relationship between the observed instrumental response and accumulation time; (E) mass measurement accuracy for targeted analyte fragment ions observed with the optimized method. Figure and caption are extracted from Ref. [39].

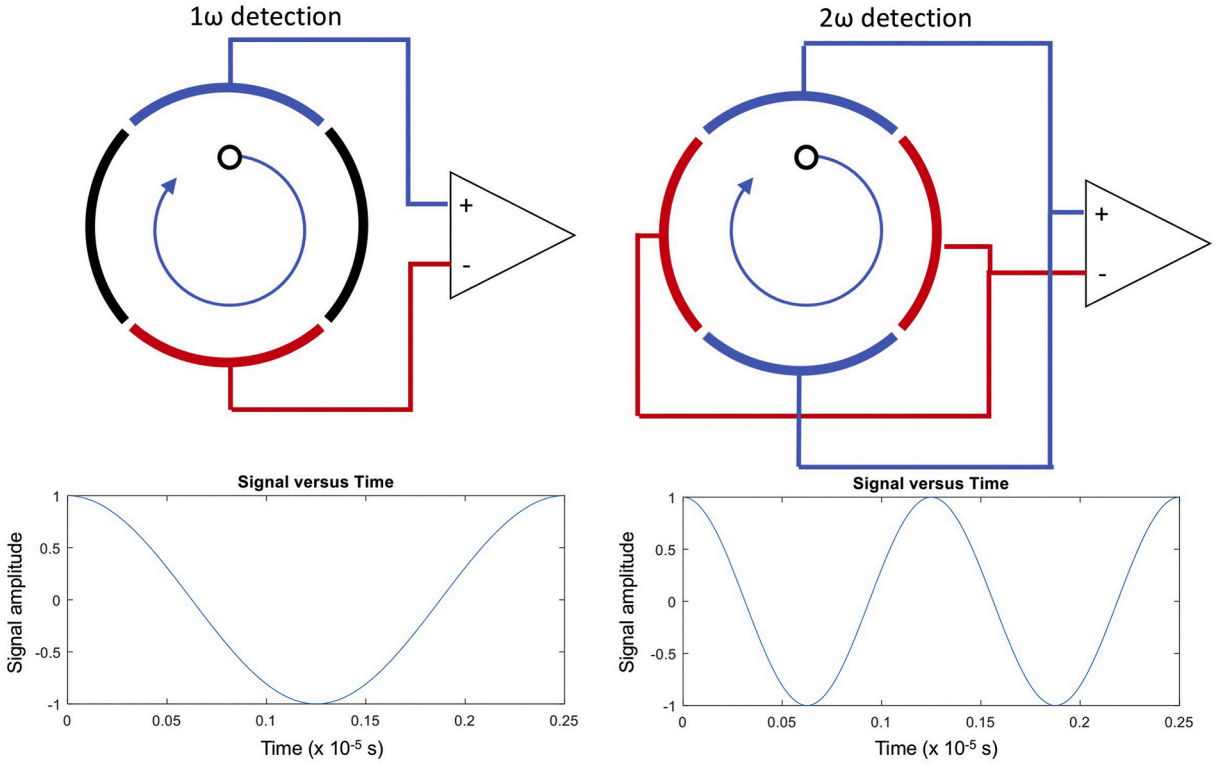

Fig. 6. (Top) Detection set-up for normal detection (1ω) and for detection at twice the cyclotron frequency (2ω). (Bottom) The image current resulting from one revolution of the ion packet for both 1ω and 2ω detection schemes. Figure and caption extracted from Ref. [89].

polycyclic aromatic hydrocarbons (PAHs) [64]. Not surprisingly, GC-APLI-FT-ICR MS has been successfully employed to improve the molecular coverage in PAHs in fossil oil [65].

For its part, the hyphenation of mass spectrometry with liquid chromatography (including UPLC or nanoLC) takes "the lion's share" with around 70% of the published papers and requires exclusively API sources among which electrospray ionization (ESI) and its declination (e.g. ultrasonic assisted nebulization ESI). This high percentage is explained by the involvement of FT-ICR MS in omics studies such as proteomics or metabolomics (targeted and untargeted, including specific declination like lipidomics) but also foodomics where highly polar molecules play essential roles. This will be illustrated in the last part of this review. Decreasing the polarity of the analytes compound, APCI may also be employed in LC-FT-ICR MS. For example, UPLC-APCI-FT-ICR MS was used for the qualitative/quantitative characterization of *Spirulina* pigments dietary supplements [66]. Another example is the analysis by LC-APCI-FT-ICR MS of toxicants (e.g. hydroxyl or amino PAH) in complex environmental mixtures [67]. The coupling of LC with APPI- and APLI-FT-ICR MS is rare and to the best of our knowledge, there are only very few published studies. Lababidi and Schrader [68] showed normal-phase LC-FT-ICR MS ion chromatograms of complex crude oil mixtures obtained with ESI, APPI, APCI and APLI. Their study highlights the complementarity of each source regarding the analyte polarity and aromaticity.

Due to its principle, capillary zone electrophoresis (CZE) is dedicated to the separation of ionic and ionizable compounds. It is easy to understand that ESI is the source of predilection for its hyphenation with mass spectrometry. However, CE is probably the separation technique with the less obvious compatibility for online hyphenation with mass spectrometry. Indeed, the principle of the two techniques is based on electrical charge circulation and the first challenge in CE-MS is to combine both electrical circuits, while maintaining two independent voltages (for the CE separation and for the MS ionization). The history of CE-FT-ICR MS illustrates the host of ideas and the progress in this matter. In the early phases, Hofstadler et al. published the first CE-FT-ICR MS analyses of proteins using sheathless CE interfaces [16,69,70]. Few centimeters of the external protecting polyacrylamide coating were removed from the outlet of the separation capillary and the nude fused silica was etched using hydrofluoric acid to taper it. Then, a gold conductive coating was deposited allowing the electrical contact with the buffer solution and ensuring the electrospray process. Much less frequently, CE-ESI-FT-ICR MS was also implemented using the liquid junction interface [48]. However, the majority of the currently published method in CE-ESI-FT-ICR MS have mainly resorted to the coaxial liquid junction interface (sheath flow or sheath liquid) [42,58,71–75]. The make-up (or sheath-liquid) is delivered independently of the CE effluent flow rate. It provides a robust and reproducible spray [76] compared to the liquid junction and its composition can be carefully optimized to improve significantly the sensitivity of detection [77]. The main drawback of the sheath liquid interface is the dilution effect brought by the addition of the make-up. The porous tip interface developed by Whitt and Moini is the most recently developed one [78]. There are many similarities in the capillary preparation. The external protecting polyimide coating was removed from the outlet, and the nude fused silica was also etched using hydrofluoric acid until it reaches a porosity allowing a contact closure with a conductive liquid. No conducting coating is then required and only nitrogen was introduced into the capillary during the etching process to protect the capillary inner wall. The commercial version of porous tip interfaces from Sciex Separations (CESI 8000) is now available and applied by Gstöttner et al. [59] recently in CE-FT-ICR MS for the analysis of bispecific antibodies subunits.

3.2. *Mass measurement accuracy, resolving power and sensitivity: the art of compromise in hyphenation*

If there is no apparent technical limitation, hyphenating a separation technique with FT-ICR MS is somehow like squaring the circle and

Table 1
Applications using LC hyphenated to FT-ICR MS. (RPLC: reversed-phase liquid chromatography, NPLC: reversed-phase liquid chromatography, HIC: hydrophobic interaction chromatography; GCC: graphited carbon column; EC: electochemical cell; CZE: capillary zone electrophoresis; A: isomers separation, B: quantification, C: high sensitivity; D: high dynamic range, E: easier data interpretation; n.d.:not disclosed).

Applications			Instrumental parameters							Advantages brought by the LC hyphenation				References		
Domain	Application	Sample	LC mode	Ionization source (polarity)	FTICR magnetic field (T)	MS mode	Other parameters	MS resolution (FWHM)	Mass measurement accuracy (ppm)	Advantages brought by LC hyphenation	Number of detected compounds	Number of unambiguous formula assignments	Number of identifications	Authors	Year	Reference
Proteomics	Peptides analysis	Standard peptides in artificial cerebrospinal fluid	RPLC	ESI (+)	n.d.	MS	Accumulation during 0.5–3 s, up to 100% duty cycle	n.d.	n.d.	C	n.d.	n.d.	n.d.	Senko et al.	1997	[142]
Proteomics	Peptides identification	Neuroactive peptides mixture	RPLC	ESI (+)	9.4	MS, MS^2 (IRMPD)	64 k - 128 k data points	8000–1100	n.d.	C	n.d.	n.d.	n.d.	Emmet et al.	1998	[143]
Proteomics	Proteins identification	Mixtures of standard proteins	RPLC	ESI (n.d.)	9.4	MS, MS^2 (IRMPD)	256 k data points, 5 s/scan	n.d.	n.d.	n.d.	5	n.d.	5	Li et al.	1999	[144]
Proteomics	Proteome analysis	Tryptic digests of fractionated *S. cerevisiae* cell lysate	RPLC	ESI (n.d.)	11.5	MS, MS^2 (n.d.)	128 k data points, 5 s/spectrum	n.d.	0.3–4.5	B, C	n.d.	n.d.	n.d.	Gao et al.	2000	[46]
Proteomics	Proteins identification	Digest of protein mixture (β-lactoglobulin, β-casein, bovine serum albumin, carbonic anhydrase II, cytochrome *c*, glyceraldehyde-3-phosphate dehydrogenase)	RPLC	ESI (+)	n.d.	MS, MS^2 (IRMPD)	64 k data points, 2 s/spectrum	n.d.	<0.01 Da	C	n.d.	n.d.	n.d.	Martin et al.	2000	[145]
Proteomics	Bottom-up identification of proteins	Cytosolic tryptic digest of *S. cerevisiae*	RPLC	ESI (n.d.)	11.5	MS, MS^2 (n.d.)	5.7 s/spectrum	n.d.	<1	C, D, E	110000	n.d.	~1000	Shen et al.	2001	[44]
Proteomics	Proteome analysis	Tryptic digest of *D. radiodurans* cell lysate	RPLC	ESI (+)	3.5	MS, MS^2 (n.d.)	2.5 s/spectrum	n.d.	n.d.	C, D	48664	n.d.	n.d.	Shen et al.	2001	[43]
Proteomics	Peptides and proteins identification	Tryptic digests of *D. radiodurans* cell lysate and bovine serum albumine	RPLC	ESI (+)	7	MS, MS^2 (IRMPD, SORI-CID)	256 k data points	n.d.	1.1–35.1	D	44	n.d.	44	Li et al.	2001	[104]
Proteomics	Peptides analysis	Biological peptide mixtures	RPLC	ESI (+)	7	MS	64 k data points, 2 s/spectrum	n.d.	n.d.	C	n.d.	n.d.	n.d.	Quenzer et al.	2001	[146]
Proteomics	Proteins identification	Tryptic digest of diacetyl reductases in the human liver cytosol	RPLC	ESI (+)	n.d.	MS	*m/z* range 400–2400, 256 k data points, 6 s/2 spectra, accumulation during 0.5–4.8 s	n.d.	0.0–3; 5	n.d.	n.d.	n.d.	n.d.	Tanaka et al.	2001	[147]
Proteomics	Peptides characterization	BSA tryptic digest	RPLC	ESI (n.d.)	3.5	MS	Accumulation during 0.105 s	n.d.	0.059–4.997	C, D	83	n.d.	83	Belov et al.	2002	[148]
Proteomics	Peptides characterization	Mixture of standard peptides and bovine serum albumin tryptic digest	RPLC	ESI (n.d.)	9.4	MS, MS^2 (ECD)	128 k – 512 k data points, 17.5–28.1 s/spectrum	n.d.	n.d.	n.d.	75	n.d.	n.d.	PalmbLad et al.	2002	[149]
Proteomics	Identification of intact proteins	Yeast large ribosomal subunits	RPLC	ESI (n.d.)	7	MS	n.d.	n.d.	0.5–20.3	n.d.	71	n.d.	62	Lee et al.	2002	[106]

(*continued on next page*)

Table 1 (*continued*)

Applications			Instrumental parameters							Advantages brought by the LC hyphenation				References		
Domain	Application	Sample	LC mode	Ionization source (polarity)	FTICR magnetic field (T)	MS mode	Other parameters	MS resolution (FWHM)	Mass measurement accuracy (ppm)	Advantages brought by LC hyphenation	Number of detected compounds	Number of unambiguous formula assignments	Number of identifications	Authors	Year	Reference
Proteomics	Proteome analysis	Tryptic digests of *D. radiodurans* cell lysate	RPLC	ESI (+)	11.4	MS, MS^2 (n. d.)	n.d.	n.d.	≤1	C, D	n.d.	n.d.	n.d.	Lipton et al.	2002	[102]
Proteomics	Proteome characterization	Tryptic digest of *Deinococcus radiodurans* cell lysate	RPLC	ESI (+)	11.5	MS, MS^2 (n. d.)	5 s/spectrum	100000	<1	B, C	n.d.	n.d.	n.d.	Smith et al.	2002	[150]
Proteomics	Analysis of protein digest	Cytochrome *c* digest	RPLC	ESI (+)	7	MS (broadband ECD)	*m/z* range 292–2000, 512 k data points, accumulation during 0.5	n.d.	n.d.	n.d.	n.d.	n.d.	n.d.	Davidson et al.	2002	[151]
Proteomics	Proteins analysis	Protein mixture from COS-6 membranes	RPLC	ESI (+)	7	MS	*m/z* range 400–2000	n.d.	0.4–4.0	E	n.d.	n.d.	n.d.	Ihling et al.	2003	[152]
Proteomics	Proteins identification	Tryptic digests of cerebrospinal fluid samples	RPLC	n.d.	9.4	n.d.	n.d.	n.d.	~2	C, D	6551	n.d.	n.d.	Ramström et al.	2003	[97]
Proteomics	Proteins identification	BSA tryptic digest	RPLC	ESI (+)	7	MS	Infinity ICR cell, *m/z* 790–3000, 512 k data points.	n.d.	≤5 (external calibration), ≤2 (internal calibration°	n.d.	n.d.	n.d.	n.d.	Witt et al.	2003	[153]
Proteomics	Bottom-up analysis	Deinococcus radiodurans cell lysate	RPLC	ESI (n.d.)	9.4	MS, MS^2 (n. d.)	Infinity ICR Cell, 512 k data points, transient of 0.8 s, accumulation during 0.6 s, 1.6 s/scan	n.d.	≤10	C, D	n.d.	n.d.	n.d.	Belov et al.	2004	[100]
Proteomics	Analysis of complex biological samples	Tryptic digests of BSA and cerebrospinal fluid samples	RPLC-CZE	ESI (n.d.)	9.4	n.d.	7.5 s/ spectrum	n.d.	≤10	n.d.	10–3126	n.d.	10 n.d. 3126	Bergström et al.	2006	[154]
Proteomics	Characterization of proteins (potential biomarkers or vaccine antigens)	Tryptic digest of *Helicobacter pylori* outer membrane proteins	RPLC	ESI (+)	7	MS, MS^2 (n. d.)	*m/z* range 400–1600	60000 at *m/z* 600	≤5	C, D, E	n.d.	n.d.	60	Carlsohn et al.	2006	[52]
Proteomics	Bottom-up characterization of the proteome	Tryptic digest of *S. oneidensis* MR-1 cell lysates	RPLC	ESI (n.d.)	7	MS, MS^2 (CID)	Open cylindrical ICR cell, time of flight of 0.150 s	n.d.	MS: ≤10 MS^2: ≤25	n.d.	94	n.d.	n.d.	Kang et al.	2007	[99]
Proteomics	Datasets processing	Tryptic digests of savinase, a protein mixture and cerebrospinal fluid	RPLC	ESI (+)	7	n.d.	Infinity ICR Cell, time of flight of 0.4 s, 1.3 s/scan	n.d.	≤20	n.d.	n.d.	n.d.	34	Burgt et al.	2007	[155]
Proteomics	Characterization of oxidized forms of a protein	Calmodulin from activated macrophage lysates	RPLC	ESI (n.d.)	12	MS, MS^2 (n. d.)	*m/z* range 400–2000, 2 s/spectrum	10 000	<15	n.d.	n.d.	n.d.	n.d.	Smallwood et al.	2007	[156]
Proteomics	Analysis of glycopeptides	Typtic digest of a HIV-1 envelope protein	RPLC	ESI (+)	7	MS, MS^2 (CID)	*m/z* range 800–2000	50000 at *m/z* 400	n.d.	n.d.	215	n.d.	215	Irungu et al..	2008	[94]

(*continued on next page*)

Table 1 (*continued*)

Applications			Instrumental parameters							Advantages brought by the LC hyphenation				References		
Domain	Application	Sample	LC mode	Ionization source (polarity)	FTICR magnetic field (T)	MS mode	Other parameters	MS resolution (FWHM)	Mass measurement accuracy (ppm)	Advantages brought by LC hyphenation	Number of detected compounds	Number of unambiguous formula assignments	Number of identifications	Authors	Year	Reference
Proteomics	Top-down identification of proteins	*A. flavus* cell lysate	RPLC	ESI (n.d.)	7	MS, MS^2 (CID)	n.d.	100000 at *m/z* 400	0.44–2.34	B	659	n.d.	22	Collier et al.	2008	[118]
Proteomics	Bottom-up characterization of the proteome	Tryptic digest of proteins in mouse bronchoalveolar lavage fluid	RPLC	n.d.	9.4	MS, MS^2 (n.d.)	n.d.	n.d.	≤5	n.d.	n.d.	n.d.	1797	Pounds et al.	2008	[98]
Proteomics	Top-down characterization of the degree of nitration and oxidation of intact calmodulin	Calmodulin in macrophage lysates	RPLC	ESI (+)	12	MS, MS^2 (CID)	Infinity ICR Cell, accumulation during 0.2 s, 2 s/spectrum	n.d.	0.31–23.98	B	266	n.d.	144	Lourette et al.	2010	[120]
Proteomics	Characterization of glycopeptides	Typtic digest of fetal bovine serum	RPLC	ESI (+)	14.5	MS, MS^2 (CID)	Accumulation during 0.2 s	100000 at *m/z* 400	0.01–2.08	n.d.	n.d.	137	n.d.	Wang et al.	2010	[96]
Proteomics	Proteoforms identification	α-synuclein from human brain tissue	RPLC	ESI (+)	7	MS, MS^2 (CID)	*m/z* range 600–1500 or 350 - 1500	MS: 100000 MS^2: 50000	2–5	n.d.	3	n.d.	3	Örhfelt et al.	2011	[157]
Proteomics	Top-down analyses of endogenous Amyloid β peptide species and other proteolytic cleavage products of amyloid precursor protein	Human and cat cerebrospinal fluid samples	RPLC	ESI (+)	7	MS, MS^2 (CID, IRMPD, ECD)	*m/z* range 350–1500	MS: 100000 MS^2: 50000	0.0–9.3	B	n.d.	n.d.	n.d.	Brinkmalm et al.	2012	[116]
Proteomics	Top-down identification of proteins	HeLa cell lysate	n.d.	ESI (+)	14.5	MS, MS^2 (CID)	Transient of 1.8 s	n.d.	≤10	n.d.	n.d.	n.d.	n.d.	Tipton et al.	2012	[119]
Proteomics	Top-down identification of proteins	Human 20S and 19S proteasome complexes	RPLC	ESI (+)	15	MS, MS^2 (FS-CAD, CASI-CAD)	*m/z* range 150–3000, 1 M data points, transient of 0.34 s, accumulation during 0.2 s, 0.63 s/spectrum	45000 – 50000	0.4–17	n.d.	n.d.	n.d.	n.d.	Lakshmanan et al.	2014	[121]
Proteomics	Glycan structural analysis of a glycoprotein	Ovalbumin	GCC-LC	ESI (+)	n.d.	MS, MS^2 (CID)	n.d.	n.d.	n.d.	n.d.	n.d.	n.d.	n.d.	Xin et al.	2015	[95]
Proteomics	Characterization of protein disulfide bonds	β-lactoglobulin and ribonuclease B	RPLC-EC	ESI (+)	15	MS, MS^2 (CID)	ParaCell, *m/z* range 307–3000, 1 M data points, accumulation during 3 s	n.d.	n.d.	n.d.	n.d.	n.d.	n.d.	Switzar et al.	2016	[158]
Proteomics	Top-down analysis of protein	Human Mitochondrial Branched-Chain Amino Acid Aminotransferase 2	RPLC	miESI (+)	21	MS, MS^2 (ETD, CID)	Dynamically harmonized ICR cell, transient of 0.76 s	300000 at *m/z* 400 110000 at *m/z* 920	0.1–3.6	n.d.	n.d.	n.d.	n.d.	Anderson et al.	2017	[159]
Proteomics	Top down/middle down analysis of mAbs	mAbs in human serum	RPLC	ESI (+)	21	MS, MS^2 (ETD, CID)	*m/z* range 650–2000 or 300–2000,	150000 at *m/z* 400	MS: 0.2–0.4 MS^2: 2.9–4.7	B	n.d.	n.d.	n.d.	He et al.	2017	[114]

(*continued on next page*)

Table 1 (*continued*)

Applications			Instrumental parameters							Advantages brought by the LC hyphenation				References		
Domain	Application	Sample	LC mode	Ionization source (polarity)	FTICR magnetic field (T)	MS mode	Other parameters	MS resolution (FWHM)	Mass measurement accuracy (ppm)	Advantages brought by LC hyphenation	Number of detected compounds	Number of unambiguous formula assignments	Number of identifications	Authors	Year	Reference
							transient of 0.76 s or 0.38 s									
Proteomics	Proteome top-down analysis	Fractionated human colorectal cancer cells lysate	RPLC	ESI (+)	21	MS, MS^2 (ETD, CID)	Transient of 0.381–0.762 s, duty cycle (1MS + 2 MS/MS) of 3–6 s	150000 - 300000 at *m/z* 400	n.d.	n.d.	n.d.	n.d.	141 n.d. 593	Anderson et al.	2017	[115]
Proteomics	Top-down analysis of mAbs	Deglycosylated IgG1	HIC	n.d. (+)	12	MS, MS^2 (ECD)	ParaCell, *m/z* range 200–10000 or 500–10000, 1 M data points, accumulation during 1.3 s, time of flight of 2 ms	n.d.	n.d.	n.d.	n.d.	n.d.	n.d.	Chen et al.	2018	[117]
Proteomics	Middle-down analysis of mAbs	universal antibody standard human IgG1	RPLC	nanoESI (+)	12	MS, MS^2 (ECD/CAD)	*m/z* range 100–3000, 1 M data points, accumulation during 0.04 s	Isotopic resolution	n.d.	n.d.	6	n.d.	6	Jin et al.	2019	[113]
Proteomics	Analysis of mAbs at intact level	4 mAbs intacts	FcγRIIIa affinity	ESI (+)	15	MS	*m/z* range 506–20000, 128 k data points, accumulation during 1 s, 2.6 data points/min	n.d.	n.d.	n.d.	n.d.	n.d.	n.d.	Lippold et al.	2019	[105]
Targeted metabolomics	Profiling of N-acyl-homoserine lactones	*Pseudomonas aeruginosa* isolates	RPLC	ESI (+)	7	MS, MS^2 (IRMPD)	*m/z* range 100–500	50000 at *m/z* 400	0.10–4.92	A, B, C, D	12	n.d.	12	Cataldi et al.	2007	[30]
Targeted metabolomics	Targeted and untargeted analysis of amine containing metabolites	Human urine	RPLC	ESI (+)	9.4	MS	n.d.	n.d.	0.00–1.95	A, B, D	438	n.d.	18	Guo et al.	2007	[160]
Targeted metabolomics	Targeted bile acids profiling in bodyfluids and tissues	Human urine, plasma, liver tissue methanol extracts	RPLC	ESI (−)	n.d.	MS	n.d.	100000 at *m/z* 400	0.10–0.37	A, B	20	n.d.	17	Bobeldijk et al.	2008	[161]
Targeted metabolomics	Analysis of N-acyl-homoserine-lactones and cognate lactone-opened compounds	*Pseudomonas aeruginosa* isolates	RPLC	ESI (+)	7	MS, MS^2 (CID)	*m/z* range 150–500	50000 at *m/z* 400	0.07–1.79	A, B	13	n.d.	n.d.	Cataldi et al.	2009	[162]
Targeted metabolomics	Quantitative profiling of amine and phenol metabolites using 12C/13C isotope dansylation labeling	Human urine samples	RPLC	ESI (+)	9.4	MS	n.d.	n.d.	<1.5	A, B, D	672	n.d.	121	Guo et al.	2009	[163]
Targeted metabolomics	Metabolites profiling using 13C/12C isotope	Human cerebrospinal fluid	RPLC	ESI (+)	9.4	MS	n.d.	n.d.	<2	A, B	1132	n.d.	85	Guo et al.	2011	[164]
Targeted metabolomics	Targeted analysis of monoterpene indole alkaloids	Extracts of C. roseus and U. rhynchophylla	RPLC	ESI (+)	7	MS^2(QCID)	Infinity ICR Cell, *m/z* range 100–600, 0.4893 s,	66000 at *m/z* 400	n.d.	A, C, D, E	n.d.	19	n.d.	Nakabayashi et al.	2015	[128]

(*continued on next page*)

Table 1 (*continued*)

Applications			Instrumental parameters							Advantages brought by the LC hyphenation				References		
Domain	Application	Sample	LC mode	Ionization source (polarity)	FTICR magnetic field (T)	MS mode	Other parameters	MS resolution (FWHM)	Mass measurement accuracy (ppm)	Advantages brought by LC hyphenation	Number of detected compounds	Number of unambiguous formula assignments	Number of identifications	Authors	Year	Reference
							accumulation during 0.1 s for MS and 2 s for MS/MS, time of flight of 0.4 s									
Targeted metabolomics	Cannabinoids characterization	Extracts of Cannabis sativa	RPLC	ESI (+)	7	MS, MS^2 (CID, IRMPD)	*m/z* range 50–1000	100000 at *m/z* 400	0.02–1.22	A, B	6	n.d.	6	Lelario et al.	2021	
Untargeted metabolomics	Profiling of N-acyl-homoserine lactones	*Pseudomonas aeruginosa* isolates	RPLC	ESI (+)	7	MS, MS^2 (IRMPD)	*m/z* range 100–500	50000 at m/z 400	0.10–4.92	A, B, C, D	12	n.d.	12	Cataldi et al.	2007	[30]
Untargeted metabolomics	Profiling of metabolites	Peel and flesh extracts of tomato	RPLC	ESI (±)	n.d.	MS, MS^2 (CID)	*m/z* range 100–1500	100000 at m/z 400	0.00–3.86	A, B	869	493	31	Iijima et al.	2008	[36]
Untargeted metabolomics	Profiling of flavonoids	Lotus japonicus extracts	RPLC	ESI (+)	n.d.	MS, MS^2 (CID)	*m/z* range 200–1500	100000 at m/z 400	0.006–0.435	A, B	61	59	14	Suzuki et al.	2008	[165]
Untargeted metabolomics	Analysis of N-acyl-homoserine-lactones and cognate lactone-opened compounds	*Pseudomonas aeruginosa* isolates	RPLC	ESI (+)	7	MS, MS^2 (CID)	*m/z* range 150–500	50000 at *m/z* 400	0.07–1.79	A, B	13	n.d.	n.d.	Cataldi et al.	2009	[162]
Untargeted metabolomics	Metabolites profiling	Leaf of *Arabidopsis thaliana*	RPLC	ESI (±)	n.d.	MS	*m/z* range 100–1300, transient ≤0.5 s	Set at 50000	≤1	A, B, C, D	643	94 over 98 most abundant	n.d.	Giavalisco et al.	2009	[50]
Untargeted metabolomics	Metabolites profiling of ginsenosides *in vitro* models of the gastrointestinal tract	Red ginseng extracts	RPLC	ESI (−)	n.d.	MS, MS^2 (CID)	*m/z* range 300–1500	n.d.	≤1.2	A, B	n.d.	n.d.	42	Kong et al.	2009	[37]
Untargeted metabolomics	Profiling of metabolites triterpene saponins	Hairy roots of *Medicago truncatula* extracts	RPLC	ESI (−)	n.d.	MS, MS^2, MS^3 (CID)	*m/z* range 120–1400	Set at 100000	1.352–6.539	A	79	n.d.	79	Pollier et al.	2011	[125]
Untargeted metabolomics	Analysis of sulfur-containing metabolites	Allium cepa extracts	RPLC	ESI (+)	7	MS, MS^2 (n.d.)	*m/z* range 50–1500, 4 M MS data points (transient 1.9573 s), 1 M MS/MS data points, MS transient 1.9573 s, MS/MS transient of 0.2621 s, accumulation during 0.001 s, MS time of flight of 0.5 ms, MS/MS time of flight of 0.7 ms	MS: 260000 at *m/z* 400 MS^2: 35000 at *m/z* 400	<1	n.d.	67	22	6	Nakabayashi et al.	2013	[122]
Untargeted metabolomics	Profiling of *in vivo* metabolites of flavonoids after oral admission of extracts of ziziphi spinosae semen to rats and dogs	Feces and urine from rats and dogs	RPLC	ESI (+)	n.d.	MS, MS^2, MS^3 (CID)	*m/z* range 100–1000	Set at 50000	0.03–3.83	A	15	15	9	Ren et al.	2013	[123]

(*continued on next page*)

Table 1 (*continued*)

Applications			Instrumental parameters							Advantages brought by the LC hyphenation				References		
Domain	Application	Sample	LC mode	Ionization source (polarity)	FTICR magnetic field (T)	MS mode	Other parameters	MS resolution (FWHM)	Mass measurement accuracy (ppm)	Advantages brought by LC hyphenation	Number of detected compounds	Number of unambiguous formula assignments	Number of identifications	Authors	Year	Reference
Untargeted metabolomics	Profiling of *in vivo* metabolites of 2-(2 hydroxypropanamido) benzoic acid	Plasma, urine, feces, bile from rats	RPLC	ESI (+)	7	MS, MS^2 (CID)	*m/z* range 50–1000	n.d.	0.07–0.94	A, C	13	13	n.d.	Guan et al.	2015	[124]
Untargeted metabolomics	Chemical constituant profiling	Rhodiola crenulate extract	RPLC	ESI (±)	7	MS, MS^2 (CID)	*m/z* range 50–3000	n.d.	0.01–1.43	D	48	n.d.	48	Han et al.	2016	[166]
Untargeted metabolomics	Analysis of sulfur-containing metabolites	Allium cepa, Allium fistulosum and Allium sativum extracts	RPLC	ESI (+)	7	MS, MS^2 (n.d.)	*m/z* range 50–1500, 4 M MS data points (transient 1.9573 s), 1 M MS/MS data points, MS transient 1.9573 s, MS/MS transient of 0.2621 s, accumulation during 0.001 s, MS time of flight of 0.5 ms, MS/MS time of flight of 0.7 ms	MS: 260000 at *m/z* 400 MS^2: 35000 at m/z 400	<1	A	69	n.d.	11	Nakabayashi et al.	2016	[167]
Untargeted metabolomics	Profiling of *in vivo* metabolites of esculin after oral administration	Plasma, urine, feces and bile from rats	RPLC	ESI (+)	7	MS, MS^2 (CID)	*m/z* range 100–1000	n.d.	0.03–3.00	A	19	19	n.d.	Wang et al.	2016	[168]
Untargeted metabolomics	Metabolites profiling of pyrexia for biomarkers identification	Plasma of rats after subcutaneous administration of pyrexia	RPLC	ESI (+)	7	MS	*m/z* range 50–1000, accumulation during 0.15 s	n.d.	0.01–2.83	n.d.	52	n.d.	52	Liu et al.	2017	[169]
Untargeted metabolomics	Profiling of metabolites of erysolin after intragastric administration	Plasma, urine, feces and bile from rats	RPLC	ESI (+)	7	MS, MS^2 (CID)	*m/z* range 50–1500	n.d.	0.08–0.45	A, E	6	6	n.d.	Li et al.	2018	[170]
Untargeted metabolomics	Profiling of metabolites of Gegenqinlian decoction after oral administration	Plasma, urine, bile and feces from rats	RPLC	ESI (+)	7	MS, MS^2 (CID)	*m/z* range 50–3000	n.d.	0.00–3.87	A, C, D	174	n.d.	≥19	Liu et al.	2018	[171]
Untargeted metabolomics	Metabolites profiling of paeoniflorin	Human intestinal microflora	RPLC	ESI (+)	7	MS	*m/z* range 100–1000	n.d.	0.00–2.28	A, C	31	n.d.	16	Sun et al.	2018	[38]
Untargeted metabolomics	Metabolites profiling of Palbociclib after oral administration	Urine, feces and bile from rats	RPLC	ESI (+)	7	MS, MS^2 (n.d.)	*m/z* range 150–1000	n.d.	0.04–1.64	A	29	n.d.	29	Yao et al.	2019	[172]
Targeted lipidomics	Study of the triglyceride dynamics during the ovarian previtellogenic stage	ovaries of *Aedes aegypti*	RPLC	ESI (+)	14.5	MS	Hexapolar detection ICR cell	>1 000 000 at m/z 800	0.065–0.440	A, B	19	n.d.	19	Valadares Tose et al.	2021	[91]
Untargeted lipidomics	Lipids profiling	Murine primary hepatocytes	RPLC	ESI (±)	7	MS, MS^2 (CID)	*m/z* range 400/ 350–1050	200000 at *m/z* 400	<2	A, B, C, D	242	n.d.	n.d.	Fauland et al.	2011	[29]
Foodomics	Analysis of glucosinolates	Extracts of wild bud flowers of *Capparis spinosa*	RPLC	ESI (−)	7	MS, MS^2 (IRMPD)	*m/z* range 50–1000	100000 at *m/z* 400	0.23–1.56	B, C	n.d.	8	n.d.	Bianco et al.	2012	[126]

(*continued on next page*)

Table 1 (*continued*)

Applications			Instrumental parameters							Advantages brought by the LC hyphenation				References		
Domain	Application	Sample	LC mode	Ionization source (polarity)	FTICR magnetic field (T)	MS mode	Other parameters	MS resolution (FWHM)	Mass measurement accuracy (ppm)	Advantages brought by LC hyphenation	Number of detected compounds	Number of unambiguous formula assignments	Number of identifications	Authors	Year	Reference
Foodomics	Analysis of intact glucosinolates	Brassicaceae (broccoli, cauliflower, rocket salad) extracts	RPLC	ESI (−)	n.d.	MS, MS^2 (CID)	*m/z* range 70–1000	100000 at *m/z* 400	0.1–2.0	A, B, C	n.d.	n.d.	24	Lelario et al.	2012	[53]
Foodomics	Analysis of flavan-3-ols	Extracts of seeds of grape pomace	RPLC	ESI (−)	7	MS	*m/z* range 200–2000 or 150–1500	100000 at *m/z* 400	0.01–2.00	A	n.d.	251	n.d.	Rockenbach et al.	2012	[127]
Foodomics	Profiling of glycoalkaloids	Eggplants extracts	RPLC	ESI (+)	n.d.	MS, MS^2 (IRMPD)	*m/z* range 50–1300	n.d.	0.2–1.3	A, B	n.d.	19	n.d.	Lelario et al.	2019	[47]
Environment	Organic aerosol characterization	VOCs from gas-phase ozonolysis of α-pinene, sabinene and cyclohexane	RPLC	ESI (−)	7	MS, MS^2 (CID)	*m/z* range 100–500	100000 at *m/z* 400	0.1–2.1	A	58	58	n.d.	Müller et al.	2009	[173]
Environment	Mutagenic polycyclic aromatic compounds analysis	Fractions of aquatic sediment extract	RPLC	APCI (±)	n.d.	MS (SIM), MS^2	*m/z* range 100–400	25000	≤1	A	17	n.d.	17	Bataineh et al.	2010	[67]
Environment	Dissolved and natural organic matter analysis	Coastal seawater from the Tasman Peninsula and Suwannee River natural organic matter	RPLC	ESI (−)	n.d.	MS	*m/z* range 50–1000	Target at 30000	≤2	A	2200	n.d.	n.d.	Sandron et al.	2018	[54]
Environment	Natural organic matter analysis	Suwannee River fluvic acid and Upper Mississippi River natural organic matter	RPLC	ESI (−)	7 (2XR)	MS	2ω detection, *m/z* range 100–1500, 2 M data points, transient of 0.524 s, accumulation during 0.2 s, 0.803 s/scan	170000 at *m/z* 400	≤1	B	n.d.	n.d.	n.d.	Kim et al.	2019	[129]
Environment	Soil organic matter characterization	Soil extracts	RPLC	ESI (−)	12	MS	*m/z* range 200–1200	n.d.	n.d.	C, D	n.d.	n.d.	n.d.	Shen et al.	2019	[174]
Environment	Siderophore profiling of soil bacteria	Soil extract after enrichment culture	RPLC	ESI (+)	21	MS, MS^2 (CID)	*m/z* range 220–1400, transient of 1–2 s	600000 at *m/z* 400	n.d.	D	46	n.d.	n.d.	Boiteau et al.	2019	[32]
Environment	Geographical origin determination	Raw propolis samples	UPLC	ESI (+)	15	MS	*m/z* range 150–1000, 4 M data points, transient of 1.398 s, accumulation during 50 ms	n.d.	0.0–1.098	B	n.d.	n.d.	43	Kim et al.	2019	[175]
Environment	Photodegradation products of benzisothiazolinone monitoring	Delaware River to the Sargasso Sea	RPLC	ESI (±)	9.4	MS, MS^2 (CID)	*m/z* range 57.7–1000, 4 M data points, accumulation during 0.02s	n.d.	n.d.	A	15	n.d.	15	Varga et al.	2020	[176]
Environment	Dissolved organic matter analysis	Surface water from Yongding River and rainwater from Shanghai	RPLC	ESI (−)	7 (2XR)	MS, MS^2 (CID)	*m/z* range 200–800	n.d.	≤0.5	A, B, D, E	n.d.	n.d.	n.d.	Qi et al.	2021	[49]
Petroleomics	Component analysis of crude oil	Deasphalted crude oil rich in nitrogen	NPLC	APLI (+)	12	MS	n.d.	200000 at *m/z* 400	n.d.	C	1438	n.d.	n.d.	Lababidi et al.	2013	[135]

(*continued on next page*)

Table 1 (*continued*)

Applications			Instrumental parameters							Advantages brought by the LC hyphenation				References		
Domain	Application	Sample	LC mode	Ionization source (polarity)	FTICR magnetic field (T)	MS mode	Other parameters	MS resolution (FWHM)	Mass measurement accuracy (ppm)	Advantages brought by LC hyphenation	Number of detected compounds	Number of unambiguous formula assignments	Number of identifications	Authors	Year	Reference
Petroleomics	Component analysis of crude oil	Deasphalted crude oil rich in nitrogen	NPLC	ESI, APPI, APCI, APLI (+)	12	MS	*m/z* range 150–800, 3 s/spectrum	n.d.	n.d.	A	n.d.	150–939	n.d.	Lababidi et al.	2014	[68]
Petroleomics	Component analysis of crude oil	Heavy gas oil distillate and bitumen distillate	NPLC-SCX	APPI (+)	21	MS	Dynamically harmonized ICR cell, *m/z* range 150–2000, transient of 6.2 s, absorption mode	3 200 000 at *m/z* 400	RMS: 0.120	A, C, D	49356	n.d.	n.d.	Rowland et al.	2021	[31]
Miscalleneous	Assignment of compounds produced by combinatorial chemistry	Mixture of pyrazole carboxylic acids	RPLC	ESI (+)	4.7	MS	*m/z* range 250–2500, 64 k data points, 3 s/scan	95 000 at *m/z* 361	n.d.	n.d.	120	n.d.	n.d.	Schmid et al.	2001	[33]
Miscalleneous	Oligosaccharides characterization	Rat brain	GCC-LC	ESI (±)	7	MS, MS^2, MS^3, MS^4 (n.d.)	*m/z* range 700–2000	n.d.	n.d.	A	103	n.d.	n.d.	Itoh et al.	2006	[177]
Miscalleneous	Identification of microcystin toxins produced by a cyanobacteria	Extract of Microcystis aeruginosa cell lysate	RPLC	n.d.	7	MS, MS^2 (CAD)	*m/z* range 400–1200, MS: 0.2 s/scan, MS/MS: 0.4 s/scan	MS: 100000 at *m/z* 400 MS/MS: 25000	MS: 0.11–0.76 MS^2: 0.00–7.8	n.d.	8	n.d.	8	Diehnelt et al.	2006	[178]
Miscalleneous	Cell therapy products quality control	N-glycolylneuraminic acid incorporated into human cells	RPLC	ESI (+)	n.d.	MS, MS^2 (n.d.)	*m/z* range 400–450	n.d.	n.d.	B, C	n.d.	n.d.	n.d.	Hashii et al.	2007	[179]
Miscalleneous	Criteria determination for hormone and veterany drug residue analyses	Stanozolol and designer β-agonist "Clenbuterol-R″	RPLC	ESI (+)	7	MS, MS^2 (CID)	*m/z* range 75–400	250000 at *m/z* 161	MS^2: 0.1–0.5	n.d.	n.d.	n.d.	n.d.	Nielen et al.	2007	[180]
Miscalleneous	Ruthenium complexes characterization	Ruthenium arene anticancer complexes	RPLC	ESI (+)	9.4	MS	*m/z* range 90–3000, 512 k data points	n.d.	n.d.	n.d.	2	n.d.	2	Wang et al.	2008	[181]
Miscalleneous	Drug impurities identification	Moxifloxacin (drug substance)	RPLC	ESI (+)	n.d.	MS, MS^2, MS^3 (n.d.)	*m/z* range 100–1000	50000	n.d.	n.d.	11	n.d.	11	Wu et al.	2012	[182]

means some compromises.

Let us go back to ultra-high mass measurement accuracy and resolving power, which are the ultimate performances expected from an FTICR mass spectrometer. The mass measurement accuracy requires a mandatory distinction between the peak of interest and the others. Consequently, the accurate measurement is strongly depending on the mass resolving power R (Eq. (5)).

$$R = \frac{m/z}{\Delta m/z} = \frac{w_c}{\Delta w_c} \tag{5}$$

where m/z is the mass-to-charge ratio of the peak of interest and $\Delta m/z$ the peak width at half maximum (FWHM).

The relation is obviously also true when expressed as cyclotron frequency. By combining Eq (1) with Eq. (5), Eq. (6) shows the well-known dependence of the magnetic field strength on the resolution (for a given m/z).

$$R = \frac{eB_0}{m/z \bullet \Delta w_c} \tag{6}$$

However, without getting too specific, Marshall et al. have shown that the resolving power of any peak is also depending on the time-domain ICR signal acquisition period T [79]. The relationship between resolution and the time-domain ICR signal acquisition period can be expressed as (Eq. (7)):

$$R = \frac{k\, z\, B_0\, T}{m} \tag{7}$$

where k is a peak width constant (e.g. $k = 1274{\cdot}10^{-7}$ for the resolution at FHWM and at low pressure).

As an example, Hendrickson et al. obtained a resolving power about 150 000 for intact bovine serum albumine (66 kDa) with detection period of 0.38 s with a 21 T FT-ICR MS. The resolution went up to more than 2 000 000 for a detection time of 12 s [80].

From Eq. (7), it can be deduced that the highest time-domain ICR signal acquisition period leads to the highest resolution. That is the very paradox of coupling FT-ICR MS to separation methods. High resolution is time demanding but the continuous flow of the separation technique required fast analyses and therefore some compromises. There are only few articles involving FT-ICR MS hyphenation illustrating this dichotomy. The effect of transient duration on resolution is well known in direct infusion [10]. Nevertheless, Zacs et al. published an interesting paper in 2019 showing how the transient length also influences many other key parameters in hyphenation. In this case, the study was carried out in GC-APCI-FT-ICR MS [39], which is reputed for its high separation efficiency (narrow peak width of only a few seconds), and chromatographic resolving power. Drawing an accurate chromatogram requires commonly around 10 to 15 points per peaks, below which the chromatographic peak often looks angular (rather than Gaussian shaped) and most of the time truncated at the top, reducing the chromatographic signal-to-noise ratio (S/N). Fig. 5 shows very well that such number of points per peak can only be achieved by drastically reducing the transient length (only from 256 thousand data points and lower), at the expense of the resolving power. In their study, the mass resolving power was only around 40 000 (FWHM) for 256 thousand data points at m/z 486 whereas it reached around 100 000 (FWHM) for 1 million data points. Still on this particular subject, whatever the separation technique (GC, LC including UPLC, and CE), the number of points per peak is a key parameter to monitor very low concentrated compounds particularly automated MS/MS experiments are required to achieve structural elucidation, for instance in non-targeted "omics". This is even truer in case of partial coelution of analytes.

Another issue is the sensitivity of detection in qualitative and, above all, in quantitative studies. The signal intensity and more precisely the limit of detection or quantification, which are linked to the signal-to-noise (S/N) ratio, are the key values. In FT-ICR MS, the signal-to-noise ratio is a function of the data acquisition time T and a collisional damping constant τ (depending on the frequency of collision between the measured ions with other ions and gas molecules in the cell) as shown by Eq. (8).

$$S/N \propto \frac{\tau}{\sqrt{T}} \bullet \left(1 - e^{-T/\tau}\right) \tag{8}$$

Whereas a high acquisition time T significantly improves the resolving power R, a too high value of T impairs the S/N of the mass spectra [81]. The sampling rate is also a reality in separation sciences [82]. With high sampling frequencies, chromatographic peaks are well defined but the background noise is increased. On the contrary, small sampling frequencies reduce the noise on the chromatographic baseline but when the number of points per peak is too small, the signal is truncated and the signal-to-noise ratio also decreases. Both for mass spectrometry and chromatographic reasons, the "optimal T value" must be considered as a compromise between the MS resolving power, on the one hand, and, the signal-to-noise ratio and the number of points per peak in the other hand. Of course, in many commercial FT-ICR mass spectrometers, the signal itself can be increased using ion accumulation (e.g. in a hexapole ion trap as proposed in Fig. 4) along their way towards the ICR cell as depicted in Fig. 5D. Nevertheless, the reader should be aware that ion accumulation takes time at the expense of the acquisition time T and thus at the expense of the resolving power as well as the number of points per chromatographic peak: once more the art of compromise.

4. Recent developments of FT-ICR MS improving the performances in hyphenation

Efficient separation methods do not allow low MS acquisition rates because, contrary to direct infusion, they provide small retention or migration time windows for the detection of analytes. With very few data points, chromatographic or electrophoretic peaks can be distorted, and their intensities can be biased. Accordingly, some of the less concentrated compounds might not be detected at all. The question is then how to improve the resolving power without increasing acquisition time too much.

Obviously, during the implementation of the hyphenation with FT-ICR MS, it is critical to spend time on the optimization of all available parameters in order to make the best of both techniques. However, from the initial concept in 1974 [1] to the present day, the many technical developments in FT-ICR MS have made the hyphenation with separation methods more friendly (even as they are still challenging), and also contributes to reducing the loss of resolution that accompanies it.

All the historic instrumentation developments of FT-ICR MS were well described by Marshall et al. [83] and Wanczel et al. [84] in their respective reviews. In this review, the focus is rather put on the technical advances benefiting to the implementation of the hyphenation of FT-ICR MS with separation techniques in order to increase the MS resolving power, the mass measurement accuracy or/and acquisition rate.

From Eq. (7), the increase in the magnetic B_0 field strength is one of the first ways to improve the resolving power R independently of the transient duration T. The implementation of superconductive magnets of higher strength is thus beneficial for the hyphenation of FT-ICR MS with a separation method. Indeed, higher magnetic field strength enables higher resolution and higher mass measurement accuracy, but also increases the acquisition speed, the dynamic range and the resistance to peak coalescence [85]. The first FT-ICR system was home built with a magnet of 0.32 T [1]. Nowadays, the highest magnetic field commercially available is 15 T, however custom-built FT-ICR MS with 21 T magnet also exist. For instance, Smith et al. analyzed samples containing dissolved organic matter by 9.4 T FT-ICR MS and 21 T FT-ICR MS, and results showed that the 21 T superconductive magnet helped to increase the resolution by 2.2, the mass measurement accuracy by 2.6 and the number of assigned molecular formulae by 1.3 compared to the 9.4 T

Table 2
Applications using CE hyphenated to FT-ICR MS. (CZE: capillary zone electrophoresis; CIEF: capillary isoelectric focusing; CEC: capillary electrochromatography; tITP: transient isotachophoresis; PMS: pH-mediated stacking; RPLC: reversed-phase liquid chromatography; A: isomers separation, B: quantification, C: high sensitivity; D: high dynamic range, E: easier data interpretation; n.d.: not disclosed).

Applications			Instrumental parameters							Advantages brought by the LC hyphenation				References		
Domain	Application	Sample	LC mode	Ionization source (polarity)	FTICR magnetic field (T)	MS mode	Other parameters	MS resolution (FWHM)	Mass measurement accuracy (ppm)	Advantages brought by LC hyphenation	Number of detected compounds	Number of unambiguous formula assignments	Number of identifications	Authors	Year	Reference
Proteomics	Intact proteins analysis	Mixture of standard proteins	CZE	ESI (+)	7	MS	*m*/z range 800–1800, transient of 0.3–0.4 s, 6 s/spectrum	>30000	n.d.	C	6	n.d.	6	Hofstadler et al.	1993	[16]
Proteomics	Proteins analysis	Mixtures of standard proteins and peptides	CZE	ESI (+)	7	MS, MS^2 (SORI-CAD)	5 s/spectrum	50000	n.d.	n.d.	n.d.	n.d.	n.d.	Hofstadler et al.	1994	[70]
Proteomics	Cells analysis	Human erythrocyte single cell	CZE	ESI (+)	7	MS	*m*/z range ≥690, 256 k data points, transient of 0.836 s	≥100000	n.d.	n.d.	n.d.	n.d.	n.d.	Hofstadler et al.	1995	[69]
Proteomics	Intact proteins analysis	Mixture of standard peptides and proteins	CZE	ESI (+)	7	MS	64 k data points, 6 s/spectrum	≥45000	n.d.	n.d.	n.d.	n.d.	n.d.	Wahl et al.	1995	[183]
Proteomics	Proteins top-down analysis	Mixture of standard proteins	CZE	ESI (+)	6	MS, MS^2 (n.d.)	*m*/z range 500 - >2500	50000 – 60000	n.d.	C	n.d.	n.d.	n.d.	Valaskovic et al.	1996	[184]
Proteomics	Single cell analysis	Human erythrocyte cells	CZE	ESI (+)	7	MS	256 k data points, pulse sequence of 12.6 s	≥45000	n.d.	C	n.d.	n.d.	n.d.	Hofstadler et al.	1996	[110]
Proteomics	Intact proteins analysis	Mixture of standard proteins and *E. coli* cell lysate	CIEF	ESI (+)	7	MS	*m*/z range 700–3000, 128 k – 256 k data points, transients of 0.435–0.835 s, accumulation during 0.4 s, 2.24 s/scan	≥45000 (256 k)	1–5	C, D	112	n.d.	n.d.	Yang et al.	1998	[71]
Proteomics	Proteome top-down analysis	*E. coli* cell lysate	CIEF	ESI (+)	7	MS, MS^2 (SORI CID)	256 k data points, 3.5 s/spectrum	n.d.	n.d.	C, D	1500	n.d.	n.d.	Jensen et al.	1999	[42]
Proteomics	Intact proteins analysis	*E. coli* cell lysate	CIEF	n.d.	7	MS	n.d.	n.d.	n.d.	n.d.	n.d.	n.d.	n.d.	Pasa-Tolic et al.	1999	[109]
Proteomics	Intact proteins analysis	Mixture of standard proteins and *E. coli* cell lysate	CIEF	ESI (+)	7	MS	*m*/z range 150–2000, 16 k data points, 3 s/spectrum	n.d.	n.d.	n.d.	100	n.d.	n.d.	Zhang et al.	2000	[108]
Proteomics	Proteome analysis	*E. coli* cell lysate	CIEF	ESI (+)	7	MS	4 s/spectrum	n.d.	n.d.	n.d.	n.d.	n.d.	n.d.	Veenstra et al.	2000	[185]
Proteomics	Analysis of intact protein complexes	Protein complexes mixture	CIEF	ESI (+)	7	MS	4 s/spectrum	n.d.	n.d.	n.d.	n.d.	n.d.	n.d.	Martinovic et al.	2000	[112]
Proteomics	Analysis of intact enzymes	Human liver alcohol dehydrogenase isoenzymes	CIEF	ESI (+)	7	MS	4 s/spectrum	n.d.	n.d.	n.d.	n.d.	n.d.	9	Martinovic et al.	2000	[72]
Proteomics	Intact proteins analysis	*E. coli* and D. radiodurans cell lysates	CIEF	ESI (+)	7	MS	256 k data points, 3.5 s/spectrum	n.d.	n.d.	B, C, D	400–1000	n.d.	n.d.	Jensen et al.	2000	[41]
Proteomics	Peptide characterization	Mixture of standard peptides and human serum albumine tryptic digest	n.d.	ESI (+)	9.4	MS^2 (ECD)	128 k data points, transient of 0.2 s, accumulation during 0.6–1.0 s, time of flight <0.01 s, 0.4–0.5 s/scan, 2–4 s/spectrum	n.d.	n.d.	E	n.d.	n.d.	n.d.	Tsybin et al.	2002	[103]

(*continued on next page*)

Table 2 (*continued*)

Application			Instrumental parameters							Advantages brought by the LC hyphenation				References		
Domain	Application	Sample	LC mode	Ionization source (polarity)	FTICR magnetic field (T)	MS mode	Other parameters	MS resolution (FWHM)	Mass measurement accuracy (ppm)	Advantages brought by LC hyphenation	Number of detected compounds	Number of unambiguous formula assignments	Number of identifications	Authors	Year	Reference
Proteomics	Protein identification	Tryptic digests of cerebrospinal fluid samples	CZE	ESI (n.d.)	9.4	n.d.	256 k data points, 4.5 s/spectrum	n.d.	≤5	C, D	1497	n.d.	n.d.	Wetterhall et al.	2002	[34]
Proteomics	Identification of intact proteins	Protein extract of *E. coli* and *S. cerevisiae*	CIEF	ESI (+)	7	n.d.	4 s/spectrum	n.d.	≤10 (resolved peaks), ≤100 (unresolved peaks)	n.d.	n.d.	n.d.	n.d.	Martinovic et al.	2002	[107]
Proteomics	Protein identification	Tryptic digest of *S. oneidensis* cell lysate	tITP/CZE	ESI (n.d.)	7	MS	256 k data points	n.d.	n.d.	C, D	n.d.	n.d.	3071	Mohan et al.	2003	[101]
Proteomics	Characterization of olygosaccharides from glycoproteins	Mixture oligosaccharides from bovin mucin and bile salt-stimulated lipase	CEC	ESI (+)	7	MS, MS^2 (SORI-CID)	Infinity ICR Cell, 256 k data points, 1.6–1.8 s/scan	30 000	0.00–9.13	n.d.	27	n.d.	27	Que et al.	2003	[186]
Proteomics	Identification of biomarkers for renal disease (bottom-up and top-down)	Urine samples	CZE	ESI (+)	9.4	MS, MS^2 (ECD, IRMPD)	512 k data points, accumulation during 2–30 s, time of flight of 0.012 s	n.d.	3–6.5	n.d.	4	n.d.	n.d.	Chalmers et al.	2005	[73]
Proteomics	Analysis of complex biological samples	Tryptic digests of BSA and cerebrospinal fluid samples	RPLC-CZE	ESI (+)	9.4	n.d.	7.5 s/spectrum	n.d.	≤10	n.d.	10–3126	n.d.	10–3126	Bergström et al.	2006	[154]
Proteomics	Polypeptides identification	Polypeptides from rat urine	n.d.	ESI (n.d.)	12	MS	*m/z* range 300–2000, 1 M data points, 0.5 s of accumulation, 5 s/scan	n.d.	≤0.5	n.d.	100	n.d.	n.d.	Frommberger et al.	2007	[57]
Proteomics	Characterization of intact glycoproteins	Intact α subunit of recombinant human chorionic gonadotrophin	CZE	ESI (+)	n.d.	MS	*m/z* range 1400–2000, accumulation during 0.2 s	55000 at *m/z* 1800	n.d.	B	n.d.	n.d.	n.d.	Thakur et al.	2009	[48]
Proteomics	Bottom-up characterization of muropeptide variants	Bacillus licheniformis peptidoglycan	CZE	ESI (+)	7	MS, MS^2 (CID), MS^3 (CID, ETD)	*m/z* range 400–2000 or 200 - 2000	50000 at *m/z* 400	0.01–2.26	A	25	n.d.	25	Boulanger et al.	2019	[75]
Proteomics	Middle up and intact analyses of bispecific antibodies	2 bispecific antibodies	CZE	ESI (+)	12	MS	ParaCell, *m/z* range 202.70–3000 or 405.41–3000 or 589.68–3000, 1 M data points, transient of 0.144 s or 1.25 s or 1.78 s, accumulation during 0.1 s, time of flight of 1.2 ms	140000 at *m/z* 1100	n.d.	n.d.	18–19	n.d.	18–19	Gstöttner et al.	2020	[59]
Targeted metabolomics	Targeted cationic metabolites profiling	*D. vulgaris* lysate	PMS-tITP	ESI (+)	9.4	MS	*m/z* range 65–1000, 131 k data points, transient of 0.0328 s, 1 s of accumulation, 1.3 s/spectrum	15000 at *m/z* 250, 30000 at *m/z* 125	0.08–3.08	A, B	n.d.	n.d.	28	Baidoo et al.	2008	[58]
Lipidomics			CZE	ESI (−)	7	MS		n.d.	0.11–5.30	A, C	15	n.d.	n.d.	Hübner et al.	2009	[74]

(*continued on next page*)

Table 2 (*continued*)

Applications			Instrumental parameters						Advantages brought by the LC hyphenation			References	
Domain	Application	Sample	LC mode	Ionization source (polarity)	FTICR magnetic field (T)	MS mode	Other parameters	MS resolution (FWHM)	Mass measurement accuracy (ppm)	Advantages brought by LC hyphenation	Number of detected compounds	Number of unambiguous formula assignments	Number of identifications	Authors	Year	Reference
	Characterization of lipopolysaccharides and lipids	Isolated lipopolysaccharides from *Escherichia coli* and *Salmonella enterica*					512 k data points, accumulation during 2 s, 3.3 s/spectrum									

magnet [86]. To increase the acquisition rate and the mass measurement accuracy while keeping the same resolution, higher magnetic field strength has a significant advantage for the implementation of the hyphenation of FT-ICR MS with a separation method. Indeed, magnets of higher strength limit the "sacrifice" of resolution required for the hyphenation. The only drawback is the tremendous cost of such systems.

Another way to bypass the problem of short time-domains "T" requested by the hyphenation is the design of the ICR cell itself. Several ICR cells have been designed over the time. The dynamically harmonized cell called ParaCell [19], first design in 2011, is now commercially available (Bruker Daltonics, Bremen, Germany). This ICR cell offers the best ion stability and coherence in ion cyclotron motion than any other cells by dynamically harmonizing the potential. This harmonization is performed by averaging the hyperbolic electrical field over the cyclotron motion. Unharmonized potential influences the ion cyclotron motion and causes phase shift. During the phase shift of ion cyclotron motion, MS peaks become wider and distorted, leading to lower resolution. As the design of this cell enables the dynamic harmonization of the potential, it enables higher resolving power [19]. An adaptation of the dynamically harmonized cell was proposed by Kostyukevich et al. in 2012. It is based on the addition of supplemental shaped electrodes adapting the electrical field (flat-bottom potential well) in order to compensate the inhomogeneity of the magnetic field inside the ICR cell. This adaptation further reduces the phase shift of ion cyclotron motion [87].

Besides the usual detection with a single pair of plates, a multiple detection is achieved by the modification of the ICR cell design. Quadrupole detection is based on an ICR cell using two pairs of opposite detection plates instead of a single pair. The set-up of the detection plates and the resulting image current for an ion cloud of both traditional (1ω) and 2ω ICR cells are presented in Fig. 6. In a conventional ICR cell (1ω), the reduced cyclotron frequency is measured by the pair of detection plates, whereas the second harmonic of the reduced cyclotron frequency is measured by the two pairs of detection plates in quadrupole detection. This second harmonic is the double of the reduced cyclotron frequency and enables to double either the acquisition rate while conserving the same resolution or the resolution while conserving the same acquisition rate [88–90]. The only commercially available instrument using this 2ω detection technology is the 7 T SolariX 2xR FT-ICR MS (Bruker Daltonics, Bremen, Germany). However, Valadores Tose et al. used a 3ω detection (hexapolar detection) during LC-FT-ICR MS 14.5 T, resolution higher than 1 000 000 (FWMH) at m/z 800 and mass measurement accuracy lower than 0.5 ppm [91]. Shaw et al. also published a study using 4ω detection with a home-build analyzer cell and obtained a resolution of 150 000 at m/z 200 with a transient of 200 ms [92]. Therefore, using multiple detection is a strong asset for the hyphenation of FT-ICR MS with separation methods to reach very high resolution and mass accuracy while using short acquisition times. Nevertheless, the rise of undesired harmonics of the reduced cyclotron frequencies is more likely with FT-ICR MS instruments using multiple detection [88]. Hence, to reduce the intensity of the undesired harmonic signals, the ICR cell must be frequently and finely shimmed and gated. It enables the control and reduction of the magnetron motion and helps to center the ion cyclotron motion in the ICR cell. Moreover, with the tremendous advances in signal processing, m/z signals corresponding to harmonics are indicated on the mass spectra by software and these peaks can be automatically removed from the lists of the peak of interests. Finally, with 3ω or 4ω detection, loss of sensitivity can also occur [89].

Advances may also result from the signal processing. Besides the classical data processing method called "magnitude mode", another method called "absorption mode" is based on the complex impedance of the measured signal [31]. The real part of the signal is extracted and plotted to obtain frequency and mass spectra. This processing method increases the resolution by a factor up to 2, the signal-to-noise by a factor of 1.4. and the mass measurement accuracy by a factor of 1.3. However, the signal extracted in absorption mode needs to be phased with the

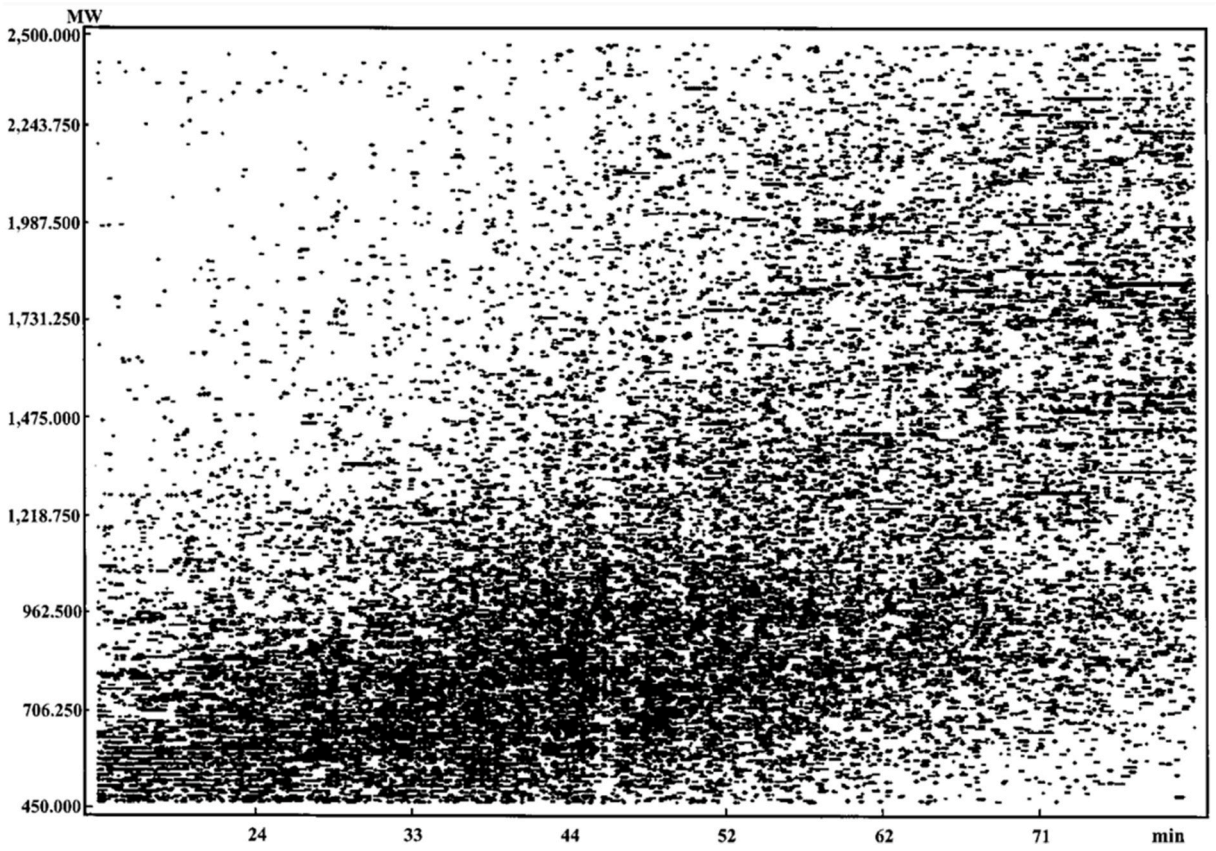

Fig. 7. Capillary LC-FTICR 2-D display for a portion of the analysis of a yeast global soluble protein tryptic digest that contained a total of ~110 000 detected components. Figure and caption reprinted with permission from Ref. [44]. Copyright 2001 American Chemical Society.

signal of magnitude mode to prevent peak distortion. Therefore, phase correction of the absorption signal must be performed and can make the reprocessing more complex. It should be noted that the ParaCell is extremely compatible with the absorption mode as the phasing of the ion cyclotron motion is more efficiently maintained than with other cell designs [90]. Therefore, the combination of the absorption mode and the quadrupole detection improves by a factor of nearly four, either the acquisition rate while conserving the same resolution, or the resolution while conserving the same acquisition rate [90]. This can benefit the hyphenation of FT-ICR MS with a separation method by increasing the compatibility and the performances of both techniques.

Another strategic development is ion accumulation during detection [93]. Indeed, the acquisition time is the longest in FT-ICR MS meaning that no ion accumulation during detection can lead to a loss of information. This parameter is often called "LC capture" or "Accumulate During Detect" in the software. The user can choose how the accumulation time is distributed during the acquisition. However, this feature is mainly useful only in MS mode only. If some MS/MS fragmentation is carried out after a full scan MS, the next full scan MS will not be able to accumulate ions during the MS/MS analysis.

5. The application field: the art of the possible in hyphenation

By way of introduction to this last section, it is interesting to keep in mind that in coupling, the separation methods and mass spectrometry are supporting each other to compensate their weaknesses and add their strengths. Thus, it is not always necessary to reach the ultimate resolving power that the FT-ICR MS handles and in the same way, a full chromatographic separation is not always required to explore in-depth the molecular content of complex samples. However, it is essential to ensure that the minimal MS resolution, sensitivity and separation are reached to achieve the objectives. Over the past years, the use of LC, GC or CE hyphenated to FT-ICR MS has been expanded in various application domains from proteomics, metabolomics and other "omics" subdivision (e.g. lipidomics) to petroleomics and environmental studies. The last part of this review is dedicated to the applications showing the art of the possible in coupling FT-ICR MS with separation techniques.

5.1. Proteomics applications

Proteomics studies are not only the first but also the most common applications of hyphenation with FT-ICR MS. This is likely due to the need of high-resolving power and mass measurement accuracy that, in the early days of MS instrumentation, could not be achieved otherwise than by a FT-ICR mass spectrometer. Because of their high polarity and molecular weight, peptides and proteins are commonly ionized by electrospray implying LC (Table 1) or CE-FT-ICR MS (Table 2) analyses.

Proteomics analyses can be categorized according to strategies chosen for the study. In the following paragraphs, some illustrations of the bottom-up, middle-up, intact, middle-down and top-down strategies will be presented.

5.1.1. Bottom-up analyses

The bottom-up strategy consists in digesting the protein into peptides, typically with trypsin, before analyzing them by MS and MS/MS fragmentation. In bottom-up analyses, the digestion step results in a complex mixture of peptides. Thus, the analytical challenge of the final peptide mixture is rapidly increasing with the number of proteins in the initial sample. Separation methods are especially useful to reduce the complexity of the mass spectra recorded along the analytical run.

The bottom-up strategy is, for instance, useful to identify the modifications present on a protein. Irungu et al. [94] characterized the 31

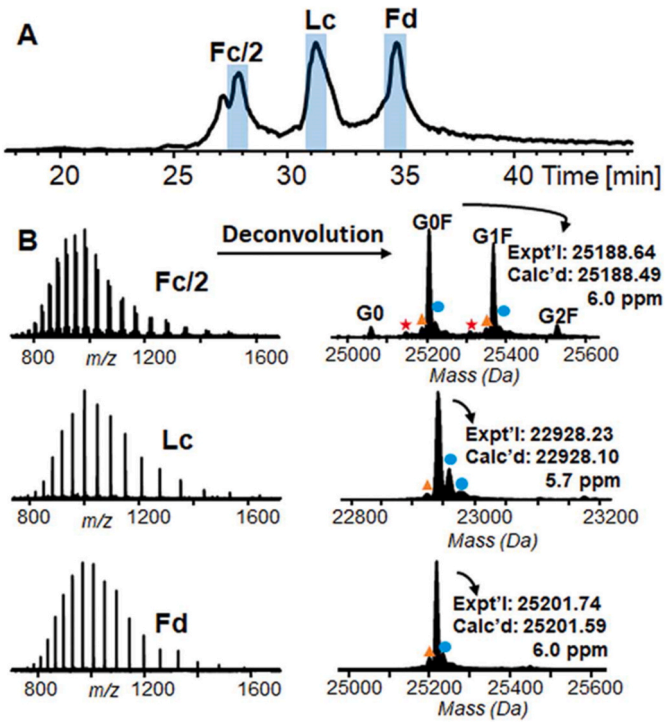

Fig. 8. Chromatogram and mass spectra of proteolytic subunits from IdeS digestion. (A) TIC chromatogram of three proteolytic subunits, Fc/2, Lc and Fd, from online LC/MS analysis. (B) Left, experimental mass spectra of Fc/2, Lc, and Fd. Right, deconvoluted mass spectra of Fc/2, Lc, and Fd. Asteroid, −58 Da from C-terminal glycine clipping and proline amidation; triangle, −18 Da from neutral loss of water; dot, +16 Da from oxidation. Expt'l, experimental monoisotopic mass based on data from MS experiments. Calc'd, calculated monoisotopic mass based on amino acid sequences. Figure and captions are extracted from Ref. [113], available at www.tandfonline.com.

potential glycosylation sites of the HIV-1 envelope glycoprotein structure (*CON–S gp140ΔCFI*) by analyzing its tryptic digest by LC-FT-ICR MS/MS. In this application, the LC separation helped to reduce ion suppression effects due to non-glycosylated peptides, enabling the detection of various low abundance glycoforms. Two hundred and fifteen glycans were detected and identified, corresponding to 18 of 31 potential sites. Combined with an offline LC/MALDI-TOF/TOF approach, a total of 341 glycans were identified. Other bottom-up analyses of glycopeptides hyphenating a separation method to FT-ICR MS have been carried out [95,96]. Another example is Boulanger et al. [75] who characterized by CZE-FT-ICR MS the modifications on muropeptides from muramidase digestion of *Bacillus lichenformis* cell wall. The high resolution (50 000 at *m/z* 400) and mass measurement accuracy (0.01–2.26 ppm) provided by the FT-ICR MS enabled confident identification of 49 peptidoglycans separated in 25 electrophoretic peaks. Several modifications such as deacetylations and particularly isomer muropetides differing by their amidation sites were identified after their separation by CZE. FT-ICR MS/MS (CID) and FT-ICR MS^3 (ECD or ETD) enabled the final discrimination of these isomers.

The proteome identification of a complex mixture such as body fluids [34,97,98] or cell lysate [43,44,99–104] is also possible by the bottom-up strategy. For example, as the environment or the development state of a given micro-organism can impact its proteome, multiple analyses are often necessary to obtain comprehensive results. This requires high throughput methods. In 2001, Shen et al. [44] developed a new strategy for high throughput bottom-up analysis based on capillary LC-FT-ICR MS in which two LC columns were used in parallel (one column is regenerated while the other one is employed for the analysis). This new strategy was tested on a trypsic digest of *Saccaromyces cerevisiae* cell lysate. The additional dimension provided by LC increased the dynamic range and simplified the mass spectra. Around 110 000 peptides were identified in this cell lysate (Fig. 7).

On their own, Calrsohn et al. [52] performed a nanoLC-FT-ICR MS/MS profiling of the outer membrane proteome of several strains of *Helicobacter pylori* to find potential markers or target proteins for vaccine development. The different strains of *H. pylori* were collected from asymptomatic patients and others suffering from duodenal ulcers or gastric cancer. A total of 60 membrane proteins, including the low-abundant ones, were identified by database searching, MS and MS/MS matching. One of these proteins was found as a potential marker for all strains. Furthermore, the strains causing duodenal ulcers seemed to be characterized by the presence of one specific protein and the absence of another one.

5.1.2. Middle-up analyses

Middle-up analyses are based on the partial digestion of proteins into large subunits followed by MS analysis.

To the best of our knowledge, the only use of separation methods hyphenated to FT-ICR MS for middle-up analyses is the structural characterization of bispecific antibodies subunits. In 2020, Gstöttner et al. [59] used CE-FT-ICR MS to study the heterogeneity of subunits. All 25 kDa subunits (Fd_1, Fd_2, Lc_1, Lc_2, $Fc/2_1$ and $Fc/2_2$) were partially separated by CE, detected, and identified with great mass measurement accuracy (2–13 ppm) and high resolution (145 000 at *m/z* 1100). Several modifications were identified such as pyroglutamate formation on Lc and Fd subunits, or K-clips and glycosylations on both Fc/2 subunits.

5.1.3. Intact protein analyses

The intact protein strategy consists in analyzing by MS the whole protein without any digestion step and without MS/MS fragmentation. This approach usually investigates the various proteoforms. For instance, in 2009, Thakur et al. [48] analyzed the various glycoforms of the α subunit of intact recombinant human chorionic gonadotropin from murine cell line by CE-LTQ-FT-ICR MS. Initially, the analysis was performed by CE-LTQ-MS to delineate the *m/z* range of interest for FT-ICR MS analysis. Using a narrower mass range for CE-FT-ICR MS analysis enabled a faster acquisition and a higher sensitivity of detection while achieving a resolution power of 55 000 at *m/z* 1800. More than 60 glycoforms were detected and identified. The relative abundance of the variants was achieved thanks to LC separation. The authors reported that the 20 most abundant glycoforms represented 90% of the whole protein content. Another example of protein heterogeneity studies is Lippold et al. [105] who hyphenated the FcγRIIIa affinity chromatography to FT-ICR MS to study the influence of glycosylation heterogeneity on the FcγRIIIa affinity of a therapeutic monoclonal antibody (mAb).

Glycosylations are not the only modifications leading to various proteoforms. There are also smaller modifications such as methylations or oxidations. A good illustration is provided by the work of Lee et al. [106] who characterized by LC-FT-ICR MS the proteins from the large ribosomal subunit of yeast. Thanks to the high mass measurement accuracy and resolution of FT-ICR MS coupled to the LC separation of isoforms with high structural similarity, it was possible to identify 42 proteins and 58 isoforms, including their various modifications (mostly methylations, phosphorylations, N-terminal modifications).

The analyses of intact proteins are also carried out for their identification in complex mixtures such as cell lysates [41,69,71,107–110]. Jensen et al. [41] hyphenated a capillary isoelectric focusing separation (CIEF) to FT-ICR MS to study complex protein mixtures. Their method was based on an isotope depletion strategy. To demonstrate the usefulness of their method, the response to a cadmium (Cd^{2+}) stress of the proteomes from *E. coli* and *D. radiodurans* cell lysates were evaluated. Stressed and unstressed cell lysates were mixed in equal proportions and the relative abundances of proteins were measured after 0 min, 45 min and 150 min of exposure to Cd^{2+}. From the stressed/unstressed ratio, it has been deduced which proteins are induced or suppressed by the Cd^{2+}

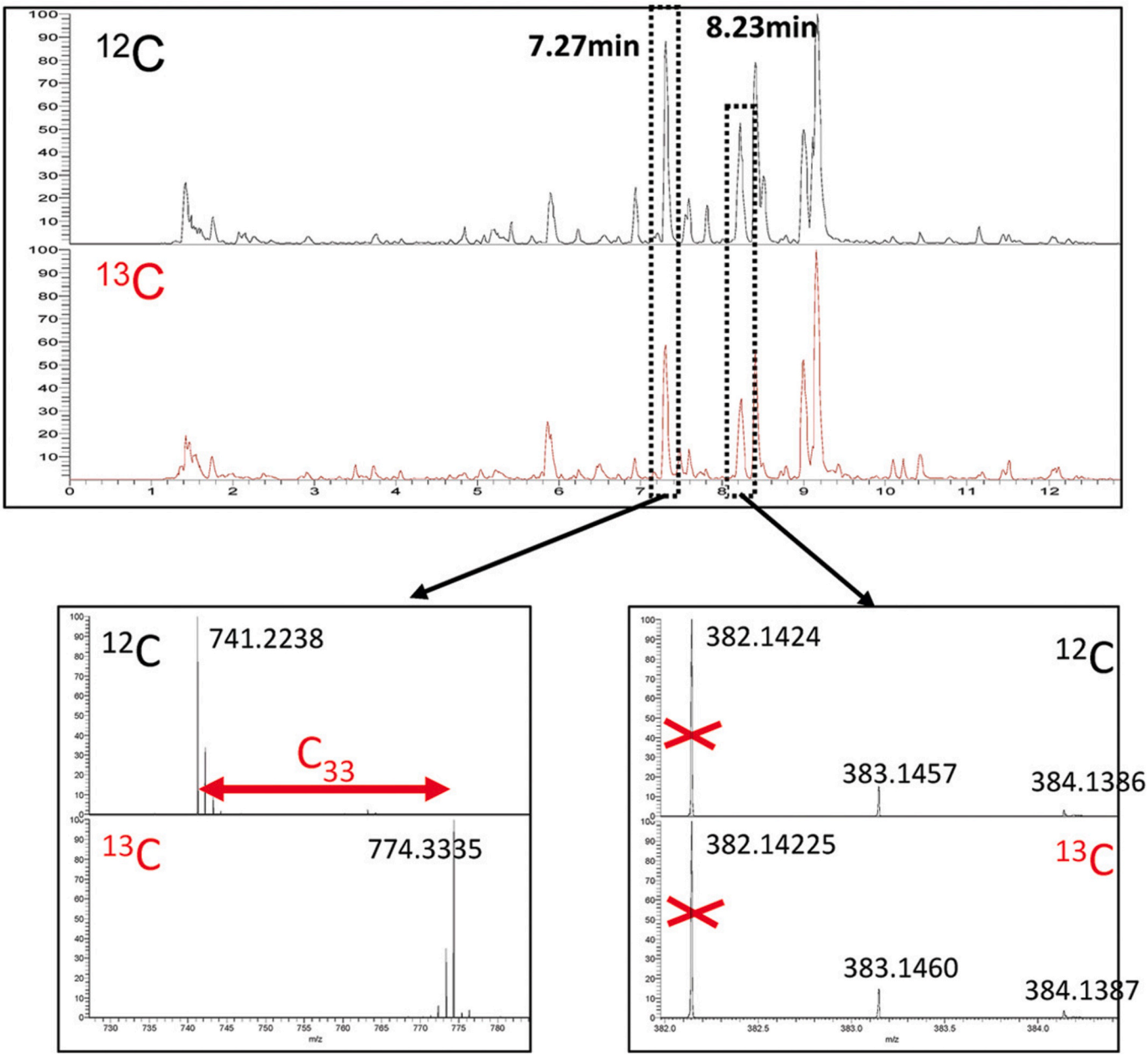

Fig. 9. Positive ion mode spectra of leaf metabolites from *A. thaliana*. The upper chromatogram represents the total ion chromatogram (TIC) of the ^{12}C (black) and ^{13}C (red) sample. Spectra in the bottom left-hand corner show the ^{12}C and ^{13}C mass spectra at the apex of the chromatographic peak at 7.27 min, while the spectra at the bottom right show the ^{12}C and ^{13}C mass spectra of the peak at 8.31 min. The presence/absence of a mass shift between the displayed masses in the upper (^{12}C) and lower (^{13}C) row of each mass spectrum indicates the biological (a)/non-biological (b) origin of the compound, and in case a mass shift is detectable, the number of carbon atoms of the measured compound. Figure and caption are reprinted with permission from Ref. [50]. Copyright 2009 American Chemical Society.

stress. As shown by Marshall et al. in 1997, the isotope depletion strategy associated with FT-ICR MS detection can improve the mass measurement accuracy [111]. CIEF prior to FT-ICR MS not only extended the dynamic range for their detection and but also enabled their relative quantification. CIEF-FT-ICR MS was also used by Hofstadler et al. [69,110] to analyze whole single cells (human erythrocytes) without preliminary lysis. The whole cells were directly lysed in the CE capillary due to an osmotic shock. By injecting several cells, partial CIEF separation of proteins succeeded in the detection of low abundance proteins like carbonic anhydrase (approx. 7 amol/cell), compared to hemoglobin which was the most abundant in the sample (approx. 450 amol/cell) [69]. By injecting one single cell, both α and β chains of hemoglobin could be detected [110].

The intact protein analyses are also implemented to study and characterize non-covalent protein complexes. In 2000, Martinovic et al. [72,112] analyzed non-covalent protein complexes by CIEF-FT-ICR MS. In native condition, CIEF enabled the separation of the different non-covalent complexes according to their isoelectric point. Depending on the composition of the sheath liquid at the CE-MS interface, it was possible to keep intact or to dissociate the complex to identify non-covalent protein complexes and their corresponding subunits.

5.1.4. *Middle-down analyses*

Middle-down analyses are based on the partial digestion of proteins into large subunits followed by MS analysis and MS/MS fragmentation.

To our knowledge, the only use of separation methods hyphenated to

FT-ICR MS for middle-down analyses is a structural characterization of monoclonal antibodies (mAbs) subunits. In 2019, Jin et al. [113] characterized the 25 kDa subunits (Fc/2, Fd and Lc) of an IgG1 mAb by LC-FT-ICR MS/MS. The middle-down analyses (Fig. 8) highlighted and led to the identification of various glycoforms and other micro-variants (oxidation, loss of water, C-terminal glycine clipping and proline amidation). Additional top-down analysis with direct infusion and offline middle-down analysis were carried out to increase bond cleavage and confidence in identification. He et al. [114] also used LC-FT-ICR MS for middle-down analysis of 25k Da subunits of adalimumab spiked into human serum.

5.1.5. Top-down analyses

The top-down strategy is based on the MS/MS fragmentation of intact protein enabling the structural characterization of protein proteoforms. This analytical strategy is more difficult to implement than previous ones, mainly due to the high sample complexity and the size of intact proteins.

The work of Anderson et al. [115] on a human colorectal cancer cell lysate is a perfect illustration of the relevance of LC-FT-ICR MS/MS for the top-down characterization of proteoforms. Before the online LC-FT-ICR MS analysis, an electrophoretic gel of the lysate was run to simplify the original protein mixture into 8 fractions according to their molecular weight. Collision-induced dissociation (CID) and electron-transfer dissociation (ETD) fragmentation modes were both used for LC-FT-ICR MS/MS top-down analyses. With a total of 40 analyses in LC-FT-ICR MS/MS, the authors detected and identified in the lysate 684 unique proteins, including proteins larger than 30 kDa, and 3238 proteoforms, with a false discovery rate of 1%. For their part, in 2012, Brinkmalm et al. [116] hyphenated FT-ICR MS with nanoLC to highlight potential biomarkers of Alzheimer's disease in human cerebrospinal fluids. The abnormal degradation of amyloid β and amyloid precursor protein in cerebrospinal fluid could be characteristic of Alzheimer's disease. Top-down analyses were carried out with CID, ECD and IRMPD fragmentation. The ultra-high resolution provided by FT-ICR achieved the isotopic resolution of >3000 Da peptides, while the extra dimension provided by LC enabled their semi-quantification.

Top-down analyses can also be used to get information about 3D structures of proteins. Indeed, in 2018, Chen et al. [117] coupled the hydrophobic interaction chromatography (HIC) with FT-ICR MS/MS using ECD broadband fragmentation to analyze a mixture of two deglycosylated mAbs. The conditions for the separation of the two studied mAbs were adapted to be compatible with mass spectrometry while maintaining their native conditions. The ECD fragmentation preserved disulfide bonds and noncovalent interactions limiting the fragmentation. Consequently, it was possible to obtain information about the localization of the binding sites of the complementary-determining regions (CDR). Comparing ECD results with crystallographic 3D structure, hypotheses have been put forward concerning the role of N- and C-termini of light and heavy chains in interaction interface.

Other top-down analyses using a separation method hyphenated to FT-ICR MS have been carried out on cell lysates [42,118–120] and human ribosome [121]. Additional information on those is available in Table 1 for LC and, Table 2 for CE.

5.2. Metabolomics and other related omics disciplines

Metabolomics is the study of all metabolites in various samples derived from living organisms, from plants to animals, from bacteria to fungi, etc. Two strategies are usually implemented in this kind of study: the untargeted approach, which generally explores the metabolome as comprehensively as possible, and the targeted approach, which focus on already known specific metabolites. Both approaches aim at understanding metabolic pathways on the basis of the collected information (molecular formulae, structure).

Untargeted and targeted applications for metabolomics and other related omics disciplines carried out using hyphenation of a separation method to FT-ICR MS are gathered Table 1 for LC and Table 2 for CE. Some of them have been taken as illustrations in the following paragraphs.

5.2.1. Untargeted metabolites profiling

Compared to the targeted approach, untargeted analyses highlight hundreds of known but, more interestingly, of unknown compounds as well. Chromatography is especially useful to reduce the complexity of each mass spectrum recorded along the analytical run. The data interpretation remains a huge work and it often requires specific identification procedures and the assistance of dedicated software.

In 2008, Iijima et al. [36] developed an annotation procedure for untargeted metabolic profiling using LC-FT-ICR MS in *Solanum*

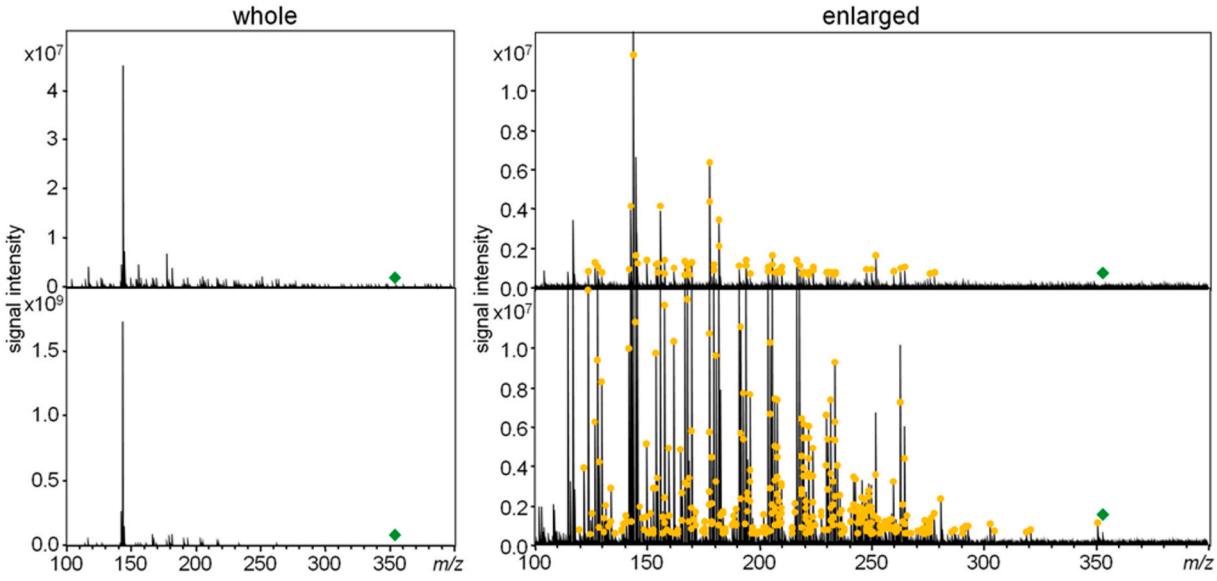

Fig. 10. Comparison of productions of ajmalicine in the MS/MS analysis (upper) and the MS/MS boost analysis (lower). The yellow circles indicate chemically assigned monoisotopic ions. The green diamond indicates the precursor ion. Figure and caption are reprinted with permission from Ref. [128]. Copyright 2009 American Chemical Society.

Table 3
Applications using GC hyphenated to FT-ICR MS. (A: isomers separation, B: quantification, C: high sensitivity; D: high dynamic range, E: easier data interpretation; n.d.: not disclosed).

Applications			Instrumental parameters						Advantages brought by the LC hyphenation				References		
Domain	Application	Sample	Ionization source (polarity)	FTICR magnetic field (T)	MS mode	Other parameters	MS resolution (FWHM)	Mass measurement accuracy (ppm)	Advantages brought by GC hyphenation	Number of detected compounds	Number of unambiguous formula assignments	Number of identifications	Authors	Year	Reference
Foodomics	Analysis of flame retardants as food contaminants	Food extracts (meat, whole milk, eggs, cereals, cod liver, fish liver oil, soybean meal)	APCI (+)	7	MS	*m/z* range 100–1000, 256 k data points, transient of 0.122 s, accumulation during 0.2 s, time of flight of 0.7 s	40000 at *m/z* 560	0.23–3.81	A, B, C, D	n.d.	n.d.	18	Zacs et al.	2019	[39]
Environment	Naphthenic acids analysis	Oil sand processed water and groundwater from the Athabasca River region	EI/CI (n.d.)	9.4	MS	*m/z* range 75–650, transient of 0.524 s, cycle time of 1.5	100000–150000	≤5	A	1300–2200	n.d.	n.d.	Ortiz et al.	2014	[130]
Environment	Flora VOC analysis	Headspace from pine tree twig samples	EI/SCI (+)	7	MS	Duty cycle of 0.06–29 s	140000–185000	0.07–0.88	A, C	7	n.d.	7	Solouki et al.	2004	[132]
Environment	Control of maternal transfer of contaminants in Europeans eels	Eggs and gonads extracts from eels	EI (+)	n.d.	MS	*m/z* range 75–650, transient of 0.524 s	100000–150000	n.d.	n.d.	n.d.	n.d.	n.d.	Sürhing et al.	2016	[134]
Environment	Dioxinx analysis	Industrial fire fallout exposed vegetation extract	n.d.	9.4	MS	*m/z* range 250–850, transient of 0.262 s, cycle time of 1.5 s	50000–100000	≤1	n.d.	n.d.	n.d.	n.d.	Taguchi et al.	2010	[56]
Environment	Petroleopic profiling of soil extracts	Extracts of Salt marsh soil from Staten Island in New York	APCI (+)	7 (2XR)	MS	ParaCell, *m/z* range 107–3000, 2 M data point	300000 at *m/z* 200	n.d.	C	n.d.	n.d.	n.d.	Thomas et al.	2019	[131]
Environment/ Petroleomics	Characterization of oil sands process water and groundwater compounds	Oil sands process water and groundwater from Athabasca oil sands area	APCI (+)	12	MS	*m/z* range 98–3000, transient of 0.56 s, 1 s/scan	330000 at *m/z* 200, 220000 at *m/z* 300	n.d.	A	n.d.	n.d.	n.d.	Barrow et al.	2014	[62]
Environment/ Petroleomics	Data processing	Oil sands process water and groundwater from Athabasca oil sands area	APCI (+)	7 (2XR)	MS (2w)	ParaCell	n.d.	n.d.	n.d.	n.d.	n.d.	n.d.	Gavard et al.	2020	[187]
Petroleomics	Multicomponent characterization of gasoline samples	Gasoline	Internal CI, EI (+)	7	MS	128 k - 512 k data points	n.d.	<6	A, C	≥50	≥25	≥5	Luo et al.	2009	[35]
Petroleomics	Characterization of pyrolysis oil	Pyrolysis oil from German brown coal	APCI (−)	15	MS	*m/z* range 46–500, 2 M data points,	n.d.	0.021–0.427	A	n.d.	n.d.	32	Zuber et al.	2016	[63]

(*continued on next page*)

Table 3 (*continued*)

Applications			Instrumental parameters						Advantages brought by the LC hyphenation				References		
Domain	Application	Sample	Ionization source (polarity)	FTICR magnetic field (T)	MS mode	Other parameters	MS resolution (FWHM)	Mass measurement accuracy (ppm)	Advantages brought by GC hyphenation	Number of detected compounds	Number of unambiguous formula assignments	Number of identifications	Authors	Year	Reference
Petroleomics	Polyaromatic hydrocarbons (PAH) analysis	Fossil oils (organics in shale oil, petroleum crude oil, and heavy sweet crude oil)	APLI (+)	7	MS	accumulation during 0.3 s, 1.003 s/ spectrum *m/z* range 100–900, 2 M data points, transient of 1 s, accumulation during 0.1 s	264000 at *m/z* 400	≤0.5	A, C	1655–1734	n.d.	n.d.	Benigni et al.	2016	[65]
Petroleomics	Fingerprinting of complex mixtures	Automobile gasoline and aviation jet fuel samples	Internal EI (+)	7	MS	Cylindrical ICR cell, 128 k data points	30000 at *m/z* 58	0.0–18.1	A	n.d.	37	n.d.	Szulejko et al.	2002	[55]
Miscalleneous	Low-mass ions detection	Grob sample (mixture of 12 organic compounds)	EI (n.d.)	9.4	n.d.	256 k data point	n.d.	n.d.	n.d.	n.d.	n.d.	n.d.	Zekavat et al.	2014	[188]

lycopersicum cv. Micro-Tom. Tomato has been used as a model but the procedure can be used in any other untargeted metabolites analysis. The annotation of each metabolite included mass spectra, predicted molecular formulae and structures, and each metabolite received a confidence grade (A, B or C) based on the eventual ambiguity of its identification. This procedure enabled the annotation of 869 metabolites including 496 new ones after comparison with public databases. The authors also performed the semi-quantification of flavonoids and glycoalkaloids after having compared their relative signal intensities in several samples.

Another example is relative to Giavalisco et al. [50] who developed a new strategy for untargeted qualitative and semi-quantitative analysis of metabolites in *Arabidopsis thaliana* leaves using LC-FT-ICR MS. Their approach is based on the $^{12}C/^{13}C$ ratio to determine the number of carbon atoms for each component. Knowing the number of carbon atoms in an elemental composition reduced the number of potential molecular formulae to a unique one or at least a few ones. Thanks to the LC separation and the $^{12}C/^{13}C$ sample labeling, the relative quantification was demonstrated to be reliable for 20 compounds. Moreover, the LC separation of isomers allowed discriminating biological from non-biological signals. Furthermore, the number of annotated non-redundant elemental compositions was multiplied by two compared to FT-ICR MS direct infusion (2304 vs 1024). As shown in Fig. 9, MS spectra for ^{12}C and ^{13}C samples were compared at similar retention time, and the number of carbons for each compound was deduced from the difference in mass-to-charge ratio between both spectra (Fig. 9a). If there is no difference between both spectra (Fig. 9b), the signal is determined as non-biological.

In 2013, Nakabayashi et al. [122] used a similar approach to study the sulfur-containing metabolites in onion bulb (*Allium cepa*). The chemical assignment of these metabolites was performed based on a ^{13}C labeling. The high mass measurement accuracy (>1 ppm) and the ultra-high resolution (>250 000 FHWM) enabled the distinction of S-monoisotopic ions from other species. Based on the natural abundance of ^{32}S and ^{34}S and their mass difference, the elemental compositions of various S-monoisotopic ions were assigned. The use of the hyphenation with LC led to the assignment of 67 S-containing monoisotopic ions among 4693 chromatographic compounds.

If the high mass measurement accuracy and the ultra-high resolution of FT-ICR MS are crucial to assign raw molecular formulae, the chromatographic separation is essential to highlight the presence of isomers.

For instance, Kong et al. [37] investigated by LC-FT-ICR MS the degradation and bioconversion of ginsenosides from red ginseng extract in *in vitro* gastrointestinal tract in order to have a better understanding of its pharmacological activity. Based on the mass measurement accuracy and MS/MS data from FT-ICR MS as well as their retention time in LC, 42 compounds were tentatively identified. The additional LC dimension was primordial to discriminate isomers with similar fragmentation pattern. All the identified compounds were also relatively quantified over time using some ginsenoside standards. Ren et al. [123] investigated the metabolism of flavonoids from *Ziziphi spinosae* semen extracts in urine and feces samples after oral administration to rats and dogs by using for the first time LC-FT-ICR MS. *Ziziphi spinosae* semen is used in traditional Chinese medicine to treat insomnia and anxiety. FT-ICR MS enabled the prediction of elemental composition and structures thank to both the mass measurement accuracy and the multistage fragmentation. A total of 15 compounds were detected and 9 were identified, including some never reported before in *Ziziphi spinosae* semen extracts. Among them, several isomers have been discriminated with the LC separation prior to MS detection and flavonoids metabolomic pathways could have been suggested.

Guan et al. [124] profiled with UPLC-FT-ICR MS *in vivo* metabolites of 2-(2-hydroxypropanamido)benzoic acid, a drug isolated from marine fungus *Penicillium chrysogenum*, in rat plasma, urine, feces and bile samples after oral administration. The additional dimension brought by

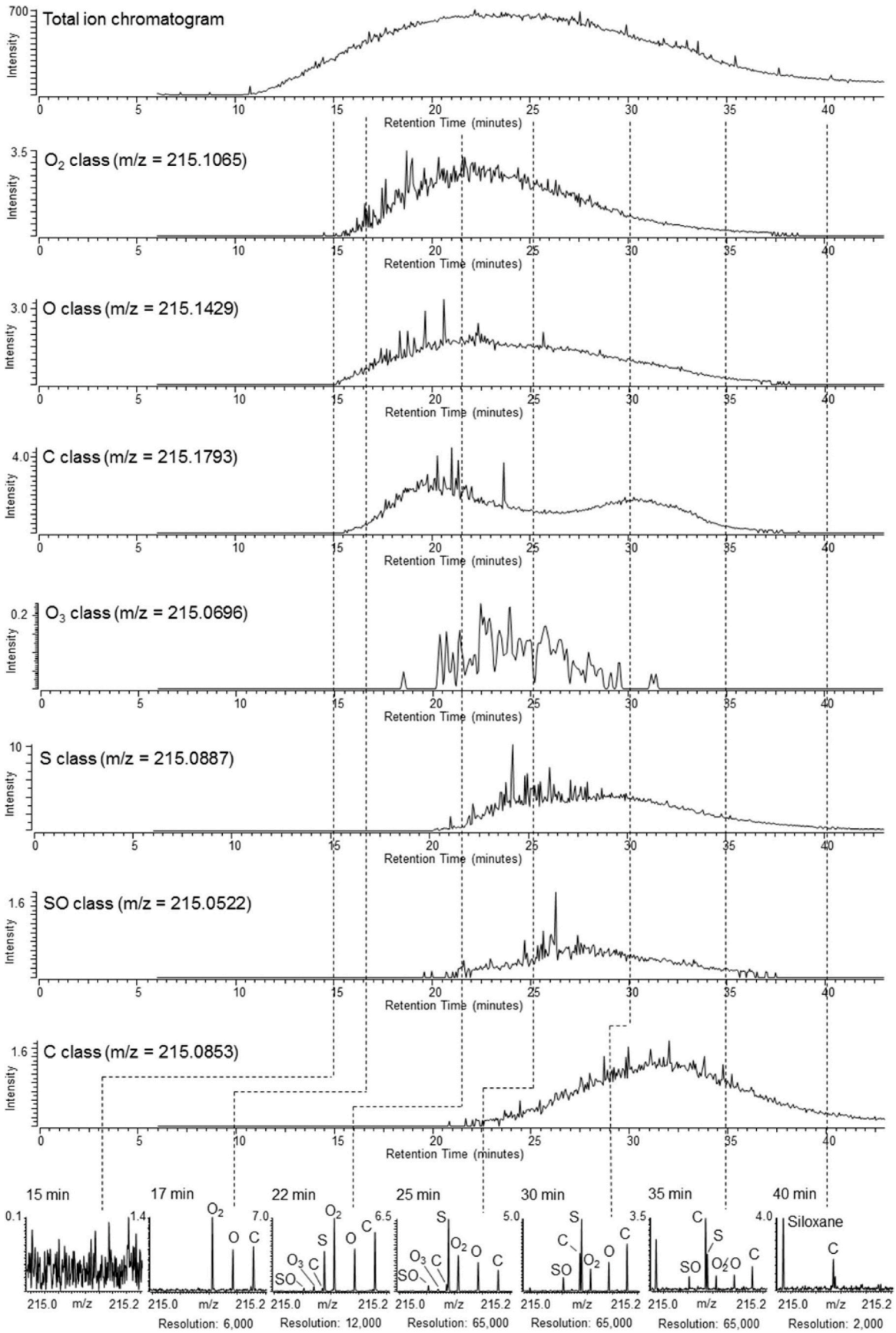

Fig. 11. Total ion chromatogram and extracted ions chromatograms of an oil sands processed water sample showing separation of several isomers within O, O2, O3, C, S and SO classes. Figure reprinted with permission from Ref. [130]. Copyright 2014 American Chemical Society.

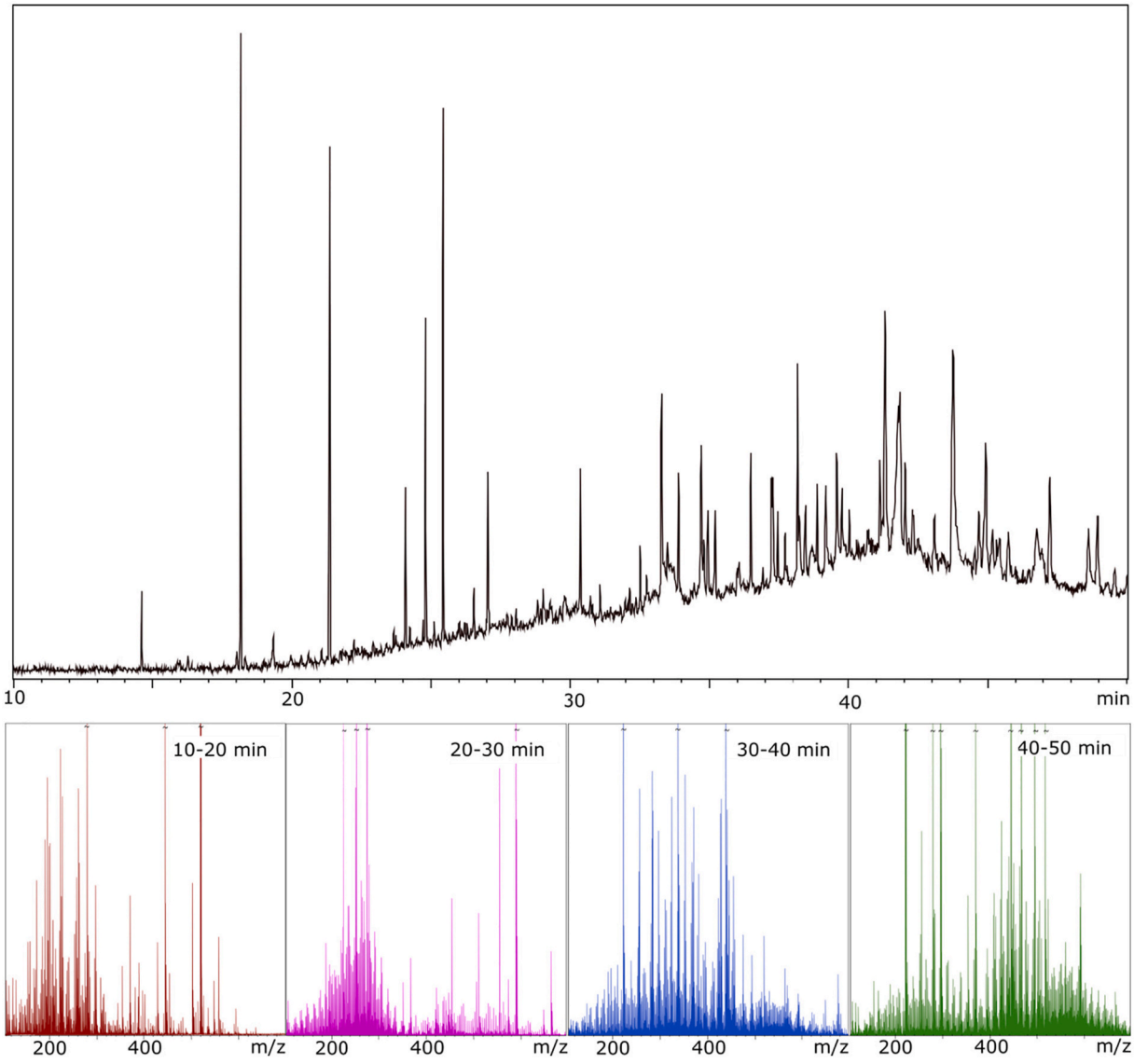

Fig. 12. Total ion chromatogram for one sampling depth (67.5–69.5 cm) and the mass spectra resulting from averaging the acquired scans over 10 min intervals. Figure extracted and caption are adapted from Ref. [131].

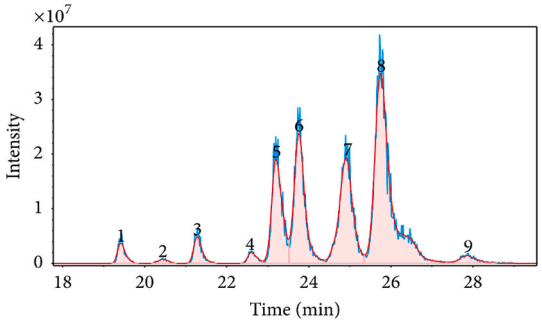

Fig. 13. Extracted ions chromatograms (*m/z* 135.081539) from a GC-APCI-FT-ICR MS analysis of pyrolysis oil from German brown coal, showing the separation of 9 propylphenol, ethylmethylphenol, and trimethylphenol isomers. Real signal is represented in blue, and Gaussian-fitted signal is represented in red. Extracted from Ref. [63].

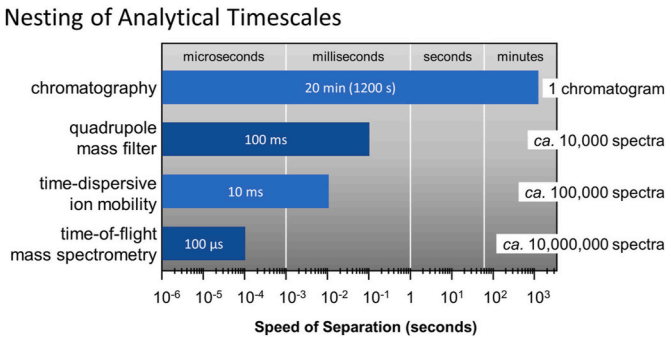

Fig. 14. Analytical timescales based on the speed of separation of analytical strategies (on the left) and on the total number of potential spectra that can be obtained in a 20-min chromatogram (on the right). Figure and caption are extracted from Ref. [139]. Copyright 2014 American Chemical Society.

UPLC to MS and MS/MS detection was once more essential to discriminate isomers with close fragmentation pattern. A total of 13 metabolites were detected and tentatively identified thanks to the high level of confidence brought by FT-ICR MS high mass measurement accuracy, contributing to a better understanding of its safety and its mechanism of action.

Metabolomic studies were performed on living organism samples to investigate the composition of their metabolome to improve the knowledge or to deduce metabolic pathways.

For example, Sun et al. [38] studied the *in vitro* metabolism of paeoniflorin in human intestinal microflora by using LC-FT-ICR MS. *In vitro* model was general anaerobic media broth mixed with fresh human feces. Thanks to the accurate mass measurements and retention times obtained in LC-FT-ICR MS 31 metabolites of paeoniflorin were highlighted and completed with the fragmentation from LC-QTOF-MS/MS experiments, 16 metabolites were identified. Thirteen metabolites were discovered for the first time in human intestinal microflora *in vitro* study extending the known metabolic reactions in the paeoniflorin pathway.

Pollier et al. [125] hyphenated LC to FT-ICR MS to study the profile of triterpene saponins in *Medicago truncatula* hairy roots. Hairy roots which are the product of an infection of *M. truncatula* make their cultivation easier and thus could be used as an alternative to phytochemicals to prevent the destruction of natural roots. In order to reduce the number of potential molecular formulae for each detected triterpene saponins, the authors compared the elemental compositions with mass errors lower than 5 ppm to the different isotopic pattern present in the FTICR mass spectra. The combination of accurate mass measurement and investigation of the isotopic pattern improved the confidence in elemental composition annotation. A total of 79 compounds in *M. truncatula* hairy roots were annotated, including 61 ones not previously detected in this plant.

The list of the untargeted metabolomic studies carried out in LC-FT-ICR MS detailed here is obviously not exhaustive, but the readers will find some complements in Table 1 on what has been done up to now in this field. This complements includes other close related "omics" such as foodomics [47,53,126,127] and lipidomics [29,74].

5.2.2. Targeted metabolites analysis

The targeted analysis focuses only on known compounds. Therefore, the data interpretation and the quantification are most of the time easier. Usually, targeted analyses are performed after untargeted analyses to have a better sight on the content of the sample in order to adapt the quantification methodology. All targeted applications of the hyphenation of a separation method to FT-ICR MS are recorded in Table 1 (for LC-FT-ICR MS) and Table 2 (for CE-FT-ICR MS). Two of them have been chosen to illustrate this paragraph.

In 2015, Nakabayashi et al. [128] developed a method to boost the sensitivity of the products ion of monoterpene indole alkaloids during LC-FT-ICR MS/MS analysis. The study focuses on the biosynthetic pathways of monoterpene indole alkaloids in *Catharanthus roseus* and *Uncaria rhynchophylla*, since those metabolites are known for their pharmaceutical activity. To boost the sensitivity of the product ions, MS/MS was performed with an increase of the product ion accumulation by 20 only for the MS/MS compared to the ion accumulation for the MS analysis. The gain of sensitivity with the MS/MS boost is illustrated in Fig. 10. This MS/MS boost strategy was then applied to targeted analyses of *Catharanthus roseus* and *Uncaria rhynchophylla*. It enabled the identification of major and minor monoterpene indole alkaloids. Moreover, the use of the LC prior to the FT-ICR MS analysis simplified the interpretation of mass spectrum by distributing the total ion population, including isomers, over the run time.

The second chosen example was the only one involving the hyphenation of FT-ICR MS with capillary electrophoresis in the area of metabolomic analysis. In 2008, the targeted analysis of cationic metabolites from *Desulfovibrio vulgaris* Hildenborough lysate was performed by Baidoo et al. [58]. *D. vulgaris* is a Gram-negative anaerobic bacterium, easily cultivable and able to oxide soluble heavy metals into insoluble forms. Therefore, the study of its metabolome is of great interest for preventing soil and water contamination. The authors developed an original method using pH-mediated stacking and transient isotachophoresis (PMS-tITP) to improve the detection of the targeted metabolites by injecting higher sample volume than in classical CE. Thanks to the separation and the reduction of ion suppression, the absolute quantification of 28 metabolites, including leucine and isoleucine which are structural isomers, was achieved with only 124 nL injected. Despite the little sacrifice in resolution and mass measurement accuracy, the hyphenation of such system was therefore crucial compared to FT-ICR MS direct infusion.

Many other studies were focused on the targeted analysis of biological samples from various matrices. As evoked, the class of metabolites involved in these studies as well as the type of matrix can be found in Tables 1 and 2.

5.3. Environmental applications

Environmental analyses cover a wide range of environments and purposes. This includes the analysis of water, soil, fauna and flora, but also different atmospheric environments. The aims of those analyses can be various, from a comprehensive study of compounds naturally present in the environment to the monitoring of an environmental pollution. The chemical and physical properties of the analyzed molecules in environmental application are wide as well. Most of the time these analyses concern volatile organic compounds (VOC) making GC the most useful separation method hyphenated to FT-ICR MS. However, LC is also widely used, particularly when the molecule polarity is increasing.

Environmental applications using separation method coupled to FT-ICR MS are summarized in Table 3 for GC, and Table 1 for LC. Some of them have been detailed in the following paragraph.

5.3.1. Food contaminants analyses

The analyses of food contaminants are a good link between the foodomic evoked in the previous paragraph and the environmental analyses as most of food pollutants may come from anthropogenic sources. The hyphenation of GC and APCI-FT-ICR MS was used by Zacs et al. [39] to assess food contamination by halogenated flame retardants. The method was developed on various food samples (meat, whole milk, eggs and cereals) and then applied on cod liver, fish liver oil and soybean meal. The study was focused on halogenated flame retardants accumulated in food chains representing potential cumulative and health risks. The high mass measurement accuracy and the ultra-high resolution of the FTICR allowed resolving the overlapping of isotopologue peaks containing ^{13}C, ^{2}H, ^{18}O, ^{15}N, $^{79}Br/^{81}Br$ and $^{35}Cl/^{37}Cl$. The interpretation of the isotopic pattern reduced the number of potential elemental composition for unknown compounds. The awareness of the number of bromine and chlorine in each assigned compound helped to discriminate brominated from chlorinated flame retardants and ensured a classification based on the number of Br and Cl atoms. The GC dimension not only highlighted the isomers during analyses but also facilitated the data interpretation compared to FT-ICR MS direct infusion. Indeed, in this study, the MS spectrum of each GC peak still contained around 5000 m/z values letting imagine what a nightmare it would have been for the data interpretation without the GC dimension. At last, the quantification of 18 brominated and chlorinated flame retardants was performed.

5.3.2. Biosphere environmental studies

Evoking environmental issues is very often linked to pollutants and the evaluation of the quality of the biosphere. The aquatic environments are very often subject to pollution, and most of the time LC-FT-ICR MS is employed because of the high polarity of the water-soluble molecules. The characterization of the dissolved organic matter in water can be used to monitor the natural organic degradation and the organic pollution in aquatic environment. For example, Qi et al. [49] have developed a LC-FT-ICR MS method to characterize dissolved organic matter in surface water samples from the Yongding River (China) and rainwater from Shanghai. Compared to direct infusion, LC helped to reduce the ion suppression phenomenon, to discriminate compounds of interest from matrix interferences and to limit the artifacts caused by the

formation of metal adduct. Four molecular classes of compounds were separated: metal salts, carboxyl-rich alicyclic molecules, organosulfates and lignins-like compounds. The use of LC was essential for the comprehensive profiling of organosulfates as they easily overlap with other compounds of the dissolved organic matter. By reducing the complexity of each recorded spectrum along the run, minority compounds were detected (20% of the elemental composition assigned with LC-FT-ICR MS were not detected in direct infusion). The semi-quantification of O_x class compounds was performed and van Krevelen diagrams with relative abundances were plotted to compare the composition of dissolved organic matter in the different water samples. Sandron et al. [54] also used LC-FT-ICR MS to characterize dissolved organic matter in seawater and natural organic matter from Suwannee River, but they added a preliminary step consisting of an offline fractionation. The combination of offline fractionation and online LC enabled a remarkable separation of the isomer species. In 2019, Kim et al. [129] used a LC-FT-ICR MS method equipped with quadrupole detection (in other words, a 2ω-detection) to characterize natural organic matter from rivers. The quadrupole detection increased by 1.4 the number of detected compounds compared to dipole detection (1ω-detection) and by 2 compared to direct infusion. This achievement was made possible through the following combination: the acquisition time with the 2ω-detection is 2 times shorter than with the 1ω-detection and the complexity of each recorded mass spectrum along the run was reduced thanks to LC separation. At last, water can also be contaminated with polar molecules when extracting bitumen from oil sands. Among these contaminations, naphthenic acids are known for their toxicity. In this case, GC is appropriate. In 2014, Ortiz et al. [130] used GC-FT-ICR MS to characterize naphthenic acids from oil sand processed water and groundwater from the Athabasca river region. Between 1300 and 2200 compounds, including many isomers, were detected in each sample and assigned thanks to the high mass measurement accuracy of the FT-ICR MS and to the Kendrick mass defect. Those compounds are distributed into 11 classes based on their heteroatom content. Thanks to GC, isomers were separated within a same class of compounds (Fig. 11). The high resolution and mass measurement accuracy of the FT-ICR MS were essential to characterize naphthenic acids due to their very close structures.

Soil and sediments are other environments potentially exposed to pollutants. In 2010, Bataineh et al. [67] developed a LC-APCI-FT-ICR MS/MS method to characterize polar mutagenic compounds in aquatic sediment. The method was developed from 55 model compounds representing all classes of polycyclic aromatic compounds basically found in sediment samples. Their tentative identification was based on accurate mass measurement, MS/MS fragmentation but also on LC retention behavior which, in addition to reveal the presence of isomers, reduced the number of candidates. Soils and sediments are witnesses of contamination over time. The different soil layers may contain various contaminations caused along the history of the site. In 2019, Thomas et al. [131] used several methods, including direct infusion on a 12 T FT-ICR MS and a 7 T FT-ICR MS coupled to GC using a 2ω-detection, for the analysis of Salt marsh soil from New York/New Jersey (NY/NJ) estuary at different depths. The 2ω-detection allowed reaching very high resolutions (300 000 for GC-APCI-FT-ICR MS against 650 000 for DI-APPI-FT-ICR MS at m/z 200) while maintaining cycle times suitable for GC. Soils are complex matrices and every mass spectrum acquired and summed on 10-min segments (Fig. 12) remains of great complexity despite the GC fractionation, and requires high resolution for their interpretation. Once again, the separation of analytes prior their detection enables the reduction of ionization competition, and several compounds containing heteroatoms were detected with higher intensities compared to direct infusion. The FT-ICR MS high resolution and mass measurement accuracy allow the classification of the different detected compounds according to their elemental composition revealing that the NY/NJ estuary may have been contaminated by petroleum, agricultural effluent, or industrial chemicals.

Flora and fauna (including humans through the foodstuffs mentioned in section 5.4.1) is the ultimate destination of the biosphere pollutants where they are bioaccumulated causing health damages. Several studies monitoring these potential contaminations have been carried out in GC-FT-ICR MS like Solouki et al. [132] on volatile organic compounds (terpenes), Taguchi et al. [133] on dioxins in extracts of plants exposed to industrial fire fallout, or Sühring et al. [134] who controlled the presence of chemical pollution in different parts of European eels (including eggs and gonads) to assess the maternal transfer of these contaminants.

5.4. Petroleomics applications

As every omics, petroleomics studies face very high sample complexity requiring mass spectrometers with ultra-high-resolution power and very high mass measurement accuracy such as FT-ICR MS. Only few of these studies involved a separation method, although isomer discrimination cannot be achieved without an additional dimension (separation method or ion mobility). Petroleomic applications using separation methods hyphenated to FT-ICR MS found in the literature are gathered in Table 1 for LC but the majority have involved GC collected in Table 3.

GC-EI-FT-ICR MS is often used to explore gasoline and fuel content [35,55]. For instance, Luo et al. [35] associated GC with a 7 T FT-ICR MS to study low concentrated gasoline samples from four retail gas stations. Over 50 compounds were chromatographically resolved among which some C_8H_{10} isomers, 9 hexene and 10 heptane isomers. Molecular formulae were confidently assigned within mass errors mostly below 5 ppm and some identifications were also confirmed with standards. Additional experiments carried out in CI succeeded in the discrimination of some coeluted isomers thanks to their different proton affinities. When samples are containing aromatic polar molecules, APCI is then involved. Zuber et al. [63] analyzed pyrolysis oils from German brown coal by GC-APCI-FTICR MS. Once again, the GC separation allowed the separation and detection of many isomers among which the nine propylphenols, ethylmethylphenols and trimethylphenols are displayed in Fig. 13.

APLI is also an interesting ionization source for PAH and Benigni et al. [65] analyzed their content in fossil oil by GC-APLI-FT-ICR MS. Various reference fossil oils standards such as shale oil, petroleum crude oil and heavy sweet crude oil were analyzed to illustrate the benefits of using GC-FT-ICR MS for the characterization of PAH. Due to the intrinsic properties of GC separations, a high mass cut off at m/z 450 was observed. Compared to direct APLI-FT-ICR MS infusion, more compounds were detected by GC-FT-ICR MS in the m/z range below m/z 450 (up to 25% are only identified with GC-FT-ICR MS). Furthermore, the hyphenation achieved the separation of isomers and increased the sensitivity and dynamic range.

If very few LC-FT-ICR MS hyphenated systems were used for petroleomics studies, in 2013 Lababidi et al. [135] developed the first online LC-APLI-FT-ICR MS method for crude oil analysis. The online LC-FT-ICR MS was more efficient in the assignment than the offline mode (480 assigned formula offline and 1438 assigned formula online) despite a degradation of the FT-ICR MS resolving power to keep compatible the acquisition in LC (resolution of 200 000 at m/z 400 online instead of 750 000 offline). Online LC-APPI-FT-ICR MS analyses of crude oil were carried out later by Rowland et al. [31] and the same statement was presented.

6. What about the future of hyphenation with FT-ICR MS?

The hyphenation of separation methods is undoubtedly a little bit trickier to implement with FT-ICR MS than with other analyzers (quadrupoles, ion traps, time of flight and even orbitraps). This issue raises questions about their future in the face of relentless progress of MS technologies. It is quite impossible to predict and plan for innovation

and particularly the diffusion of the new technologies. However, it is clear from the recent advances that, the progress goes ever faster, ever higher and ever further. This leitmotif is in line with the facilitation of hyphenation. Indeed, from recent articles [89,136–138], it is possible to envisage future commercial ICR cells enabling the detection in 3ω, 4ω, 5ω mode (and even more?) even associated with 21 T magnetic field [92]. Such progress will allow faster acquisitions in line with the requisites of online separations. Thus, maybe in a few years, the burdensome compromises between FT-ICR MS performance and acquisition time will no longer be needed to get enough acquisition points per chromatographic (from GC to UPLC) or electrophoretic peak.

The effective competition for online separation methods is ion mobility mass spectrometry. It was already evoked in this manuscript as a solution to overcome the separation of isomers (isobars do not present any real problems with FT-ICR MS). As shown in Fig. 14 [139], chromatography is extremely time-consuming compared to all other MS steps. In the full-time equivalent of the 20-min chromatogram, it is possible to collect around 100 000 spectra using time dispersive IM. The same performance is only reached at a frequency of around 84 spectra per second in hyphenation (regardless the molecular information and its precision which decreases with the acquisition time). Even if already used for the separation of phosphopeptides [140] in FT-ICR MS analysis, the coupling of time dispersive ion mobility is not suitable for the slower mass analyzers. However, more recent IMS techniques such trapped ion mobility spectrometry (TIMS) and particularly oversampling selective accumulation TIMS became effective enough (IMS resolving up to 250) to be hyphenated to FT-ICR MS without prejudice to the achievement of mass accuracy <1 ppm and mass resolution >1 million [141].

Nevertheless, achieving the detection of such a large number of *m/z* signals does not mean that the analysis a complex mixture is exhaustive. Indeed, mass spectrometers, no matter how powerful (resolution and accuracy), only detect *m/z* ratios and the analyte ions are all produced upstream from the IMS cells. This crucial step is well known to be subjected to ion suppression effects due to competition during the ionization process. It was clearly highlighted in the application section of this review that there is often a huge difference between the number of analytes detected by direct infusion FT-ICR MS and the number of analytes revealed in very complex mixtures by online separation hyphenated with FT-ICR MS. This is not only due to the presence of isomers but above all because of ion suppression. With the constant need to explore deeper and deeper complex samples, hyphenation of separation methods to FT-ICR MS will probably remain essential for years. At last, instead of confronting chromatographic methods (including capillary electrophoresis) to ion mobility, it will undoubtedly be more fruitful to associate them to go a step further in the determination of the molecular content of complex mixtures.

7. Conclusion

The purpose of this review is to provide an overview of the online hyphenation of Fourier Transform Ion Cyclotron Resonance Mass Spectrometry (FT-ICR MS) with separation methods to date. Coupling separation techniques and mass spectrometry is essentially a question of compromises. This is even truer for FT-ICR MS whose hyphenation with GC, LC or CE may appear counter-intuitive and scarcely compatible at the first sight. If the relentless progress has suppressed some apparent technical limitations (e.g. vacuum compatibility with ion sources), coupling separation techniques with FT-ICR MS still means some compromises and is not as straightforward as with other analyzers (such as QTOF-MS for instance). In a few words, FT-ICR MS needs time (ion transfer, accumulation and especially acquisition times) to reach its highest resolving power and mass measurement accuracy capabilities whereas separation methods have no time to lose to remain effective (sharp peaks for an optimal chromatographic resolving power). Fortunately, in many applications, the highest performances of both techniques are not required to achieve the level of success envisioned, the strength of the first one balancing the weakness of the second (and vice versa). “Omics” is undoubtedly the main application area of FT-ICR MS combined to online separation techniques. This can be easily understood by the huge complexity of the explored samples in this field, particularly in untargeted studies. FT-ICR MS enables to obtain the required high mass measurement accuracy to determine accurate molecular formulae and resolution for isobar distinction, while separation techniques highlight isomers. However, the separation of isomers is not the only significant advantage of online chromatography or capillary electrophoresis to FT-ICR MS. They also help to reduce ion suppression effects, enable to extend the dynamic range of detection (detection of minor compounds and quantification) and reduce the complexity of mass spectra acquired along the run, enabling easier and deeper data interpretation.

Even if their implementation is still a little bit trickier (the art of compromise), the hyphenation of separation methods with FT-ICR MS certainly has still a bright future and will probably provide unparalleled results to the scientific community (the art of the possible) for years to come.

Declaration of competing interest

The authors declare that they have no known competing financial interests or personal relationships that could have appeared to influence the work reported in this paper.

Data availability

No data was used for the research described in the article.

Acknowledgements

This work was supported by a PhD grant from the RESEX project funded by the European Regional Development Fund (FEDER), the general council of Moselle, Region Grand Est, Metz Metropole and the University of Lorraine. The graphical abstract was created with BioRender.com.

References

[1] M.B. Comisarow, A.G. Marshall, Fourier transform ion cyclotron resonance spectroscopy, Chem. Phys. Lett. 25 (1974) 282–283, https://doi.org/10.1016/0009-2614(74)89137-2.

[2] E.N. Nikolaev, I.A. Boldin, R. Jertz, G. Baykut, Initial experimental characterization of a new ultra-high resolution FTICR cell with dynamic harmonization, J. Am. Soc. Mass Spectrom. 22 (2011) 1125–1133, https://doi.org/10.1007/s13361-011-0125-9.

[3] B. Bogdanov, R.D. Smith, Proteomics by FTICR mass spectrometry: top down and bottom up, Mass Spectrom. Rev. 24 (2005) 168–200, https://doi.org/10.1002/mas.20015.

[4] M. Maia, A. Figueiredo, C. Cordeiro, M. Sousa Silva, FT-ICR-MS-based metabolomics: a deep dive into plant metabolism, Mass Spectrom. Rev. (2021) 1–22, https://doi.org/10.1002/mas.21731.

[5] M. Rychlik, B. Kanawati, C. Roullier-Gall, D. Hemmler, Y. Liu, H. Alexandre, R. D. Gougeon, L. Gmelch, M. Gotthardt, P. Schmitt-Kopplin, Chapter 21 - foodomics assessed by Fourier transform mass spectrometry, in: B. Kanawati, P. Schmitt-Kopplin (Eds.), Fundamentals and Applications of Fourier Transform Mass Spectrometry, Elsevier, 2019, pp. 651–677, https://doi.org/10.1016/B978-0-12-814013-0.00021-1.

[6] R.P. Rodgers, A.G. Marshall, Petroleomics: advanced characterization of petroleum-derived materials by fourier transform ion cyclotron resonance mass spectrometry (FT-ICR MS), in: O.C. Mullins, E.Y. Sheu, A. Hammami, A. G. Marshall (Eds.), Asphaltenes, Heavy Oils, and Petroleomics, Springer, New York, NY, 2007, pp. 63–93, https://doi.org/10.1007/0-387-68903-6_3.

[7] E.B. Kujawinski, Electrospray ionization fourier transform ion cyclotron resonance mass spectrometry (ESI FT-ICR MS): characterization of complex environmental mixtures, Environ. Forensics 3 (2002) 207–216, https://doi.org/10.1080/713848382.

[8] A. Buck, A. Ly, B. Balluff, N. Sun, K. Gorzolka, A. Feuchtinger, K.-P. Janssen, P. J. Kuppen, C.J. van de Velde, G. Weirich, F. Erlmeier, R. Langer, M. Aubele, H. Zitzelsberger, M. Aichler, A. Walch, High-resolution MALDI-FT-ICR MS imaging for the analysis of metabolites from formalin-fixed, paraffin-embedded clinical tissue samples, J. Pathol. 237 (2015) 123–132, https://doi.org/10.1002/path.4560.

[9] M. Lohse, R. Haag, E. Lippold, D. Vetterlein, T. Reemtsma, O.J. Lechtenfeld, Direct imaging of plant metabolites in the rhizosphere using laser desorption ionization ultra-high resolution mass spectrometry, Front. Plant Sci. 12 (2021), 753812, https://doi.org/10.3389/fpls.2021.753812.

[10] A.G. Marshall, C.L. Hendrickson, G.S. Jackson, Fourier transform ion cyclotron resonance mass spectrometry: a primer, 17:1<1::AID-MAS1>3.0.CO;2-K, Mass Spectrom. Rev. 17 (1998) (1998) 1–35, https://doi.org/10.1002/(SICI)1098-2787.

[11] E.B. Ledford, R.L. White, S. Ghaderi, C.L. Wilkins, M.L. Gross, Coupling of capillary gas chromatograph and Fourier transform mass spectrometer, Anal. Chem. 52 (1980) 2450–2451, https://doi.org/10.1021/ac50064a056.

[12] T.M. Sack, M.L. Gross, Pulsed valve interface for gas chromatography/Fourier transform mass spectrometry, Anal. Chem. 55 (1983) 2419–2421, https://doi.org/10.1021/ac00264a049.

[13] G.W. Stockton, J.T. Meek, W.G. Millen, R.S. Wayne, An external ion source FT-ICR mass spectrometer for ultrahigh-mass accuracy measurements and high-performance liquid chromatographic sample introduction, in: B. Asamoto (Ed.), FT-ICR/MS: Analytical Applications of Fourier Transform Ion Cyclotron Resonance Mass Spectrometry, VCH, New York, 1991.

[14] C.C. Stacey, G.H. Kruppa, C.H. Watson, J. Wronka, F.H. Laukien, J. Fred Banks, C. M. Whitehouse, R.D. Voyksner, Reverse-phase liquid chromatography/electrospray-ionization Fourier-transform mass spectrometry in the analysis of peptides, Rapid Commun. Mass Spectrom. 8 (1994) 513–516, https://doi.org/10.1002/rcm.1290080704.

[15] W. Schrader, H.-W. Klein, Liquid chromatography/Fourier transform ion cyclotron resonance mass spectrometry (LC-FTICR MS): an early overview, Anal. Bioanal. Chem. 379 (2004) 1013–1024, https://doi.org/10.1007/s00216-004-2675-1.

[16] S.A. Hofstadler, J.H. Wahl, J.E. Bruce, R.D. Smith, On-line capillary electrophoresis with Fourier transform ion cyclotron resonance mass spectrometry, J. Am. Chem. Soc. 115 (1993) 6983–6984, https://doi.org/10.1021/ja00068a070.

[17] J. Hertzog, C. Mase, M. Hubert-Roux, C. Afonso, P. Giusti, C. Barrère-Mangote, Characterization of heavy products from lignocellulosic biomass pyrolysis by chromatography and fourier transform mass spectrometry: a review, Energy Fuel. 35 (2021) 17979–18007, https://doi.org/10.1021/acs.energyfuels.1c02098.

[18] D. Ohta, S. Kanaya, H. Suzuki, Application of Fourier-transform ion cyclotron resonance mass spectrometry to metabolic profiling and metabolite identification, Curr. Opin. Biotechnol. 21 (2010) 35–44, https://doi.org/10.1016/j.copbio.2010.01.012.

[19] I.A. Boldin, E.N. Nikolaev, Fourier transform ion cyclotron resonance cell with dynamic harmonization of the electric field in the whole volume by shaping of the excitation and detection electrode assembly, Rapid Commun. Mass Spectrom. 25 (2011) 122–126, https://doi.org/10.1002/rcm.4838.

[20] P.J. Amorim Madeira, P. A C M, High resolution mass spectrometry using FTICR and orbitrap instruments, in: S. Salih (Ed.), Fourier Transform - Materials Analysis, InTech, 2012, pp. 25–44, https://doi.org/10.5772/37423.

[21] E.N. Nikolaev, Y.I. Kostyukevich, G. Vladimirov, Chapter 4 - fundamentals and simulations in FT-ICR-MS, in: B. Kanawati, P. Schmitt-Kopplin (Eds.), Fundamentals and Applications of Fourier Transform Mass Spectrometry, Elsevier, 2019, pp. 89–111, https://doi.org/10.1016/B978-0-12-814013-0.00004-1.

[22] F. Xian, C.L. Hendrickson, A.G. Marshall, High resolution mass spectrometry, Anal. Chem. 84 (2012) 708–719, https://doi.org/10.1021/ac203191t.

[23] N.L. Kelleher, M.W. Senko, M.M. Siegel, F.W. McLafferty, Unit resolution mass spectra of 112 kDa molecules with 3 Da accuracy, J. Am. Soc. Mass Spectrom. 8 (1997) 380–383, https://doi.org/10.1016/S1044-0305(97)00060-3.

[24] E.N. Nikolaev, G.N. Vladimirov, R. Jertz, G. Baykut, From Supercomputer Modeling to Highest Mass Resolution in FT-ICR, vol. 2, Mass Spectrom, Tokyo, 2013, https://doi.org/10.5702/massspectrometry.S0010. S0010.

[25] D. Huang, M. Bouza, D.A. Gaul, F.E. Leach, I.J. Amster, F.C. Schroeder, A. S. Edison, F.M. Fernández, Comparison of high-resolution fourier transform mass spectrometry platforms for putative metabolite annotation, Anal. Chem. (2021), https://doi.org/10.1021/acs.analchem.1c02224.

[26] H.N. Moseley, Correcting for the effects of natural abundance in stable isotope resolved metabolomics experiments involving ultra-high resolution mass spectrometry, BMC Bioinf. 11 (2010) 139, https://doi.org/10.1186/1471-2105-11-139.

[27] C. Stingl, C. Ihling, G. Ammerer, A. Sinz, K. Mechtler, Application of different fragmentation techniques for the analysis of phosphopeptides using a hybrid linear ion trap-FTICR mass spectrometer, Biochim. Biophys. Acta, Proteins Proteomics 1764 (2006) 1842–1852, https://doi.org/10.1016/j.bbapap.2006.09.016.

[28] J. Guillemant, M. Lacoue-Nègre, A. Berlioz-Barbier, F. Albrieux, L.P. de Oliveira, J.-F. Joly, L. Duponchel, Towards a new pseudo-quantitative approach to evaluate the ionization response of nitrogen compounds in complex matrices, Sci. Rep. 11 (2021) 6417, https://doi.org/10.1038/s41598-021-85854-7.

[29] A. Fauland, H. Köfeler, M. Trötzmüller, A. Knopf, J. Hartler, A. Eberl, C. Chitraju, E. Lankmayr, F. Spener, A comprehensive method for lipid profiling by liquid chromatography-ion cyclotron resonance mass spectrometry, J. Lipid Res. 52 (2011) 2314–2322, https://doi.org/10.1194/jlr.D016550.

[30] T.R.I. Cataldi, G. Bianco, S. Abate, Profiling of N-acyl-homoserine lactones by liquid chromatography coupled with electrospray ionization and a hybrid quadrupole linear ion-trap and Fourier-transform ion-cyclotron-resonance mass spectrometry (LC-ESI-LTQ-FTICR-MS), J. Mass Spectrom. 43 (2007) 82–96, https://doi.org/10.1002/jms.1275.

[31] S.M. Rowland, D.F. Smith, G.T. Blakney, Y.E. Corilo, C.L. Hendrickson, R. P. Rodgers, Online coupling of liquid chromatography with fourier transform ion cyclotron resonance mass spectrometry at 21 T provides fast and unique insight into crude oil composition, Anal. Chem. 93 (2021) 13749–13754, https://doi.org/10.1021/acs.analchem.1c01169.

[32] R.M. Boiteau, S.J. Fansler, Y. Farris, J.B. Shaw, D.W. Koppenaal, L. Pasa-Tolic, J. K. Jansson, Siderophore profiling of co-habitating soil bacteria by ultra-high resolution mass spectrometry, Metallomics 11 (2019) 166–175, https://doi.org/10.1039/c8mt00252e.

[33] D.G. Schmid, P. Grosche, G. Jung, High-resolution analysis of a 144-membered pyrazole library from combinatorial solid phase synthesis by using electrospray ionisation Fourier transform ion cyclotron resonance mass spectrometry, Rapid Commun. Mass Spectrom. 15 (2001) 341–347, https://doi.org/10.1002/rcm.237.

[34] M. Wetterhall, M. Palmblad, P. Håkansson, K.E. Markides, J. Bergquist, Rapid analysis of tryptically digested cerebrospinal fluid using capillary Electrophoresis−Electrospray Ionization−Fourier transform ion cyclotron Resonance−Mass spectrometry, J. Proteome Res. 1 (2002) 361–366, https://doi.org/10.1021/pr025526s.

[35] Z. Luo, C. Heffner, T. Solouki, Multidimensional GC-fourier transform ion cyclotron resonance MS analyses: utilizing gas-phase basicities to characterize multicomponent gasoline samples, J. Chromatogr. Sci. 47 (2009) 75–82, https://doi.org/10.1093/chromsci/47.1.75.

[36] Y. Iijima, Y. Nakamura, Y. Ogata, K. Tanaka, N. Sakurai, K. Suda, T. Suzuki, H. Suzuki, K. Okazaki, M. Kitayama, S. Kanaya, K. Aoki, D. Shibata, Metabolite annotations based on the integration of mass spectral information, Plant J. 54 (2008) 949–962, https://doi.org/10.1111/j.1365-313X.2008.03434.x.

[37] H. Kong, M. Wang, K. Venema, A. Maathuis, R. van der Heijden, J. van der Greef, G. Xu, T. Hankemeier, Bioconversion of red ginseng saponins in the gastro-intestinal tract in vitro model studied by high-performance liquid chromatography–high resolution Fourier transform ion cyclotron resonance mass spectrometry, J. Chromatogr. A 1216 (2009) 2195–2203, https://doi.org/10.1016/j.chroma.2008.11.030.

[38] S. Sun, L. Zhu, Y. Hu, Y. Liu, Studies on the metabolism of paeoniflorin in human intestinal microflora by high performance liquid chromatography/electrospray ionization/Fourier transform ion cyclotron resonance mass spectrometry and quadrupole time-of-flight mass spectrometry, J. Chromatogr., B 1085 (2018) 63–71, https://doi.org/10.1016/j.jchromb.2018.03.042.

[39] D. Zacs, I. Perkons, V. Bartkevics, Evaluation of analytical performance of gas chromatography coupled with atmospheric pressure chemical ionization Fourier transform ion cyclotron resonance mass spectrometry (GC-APCI-FT-ICR-MS) in the target and non-targeted analysis of brominated and chlorinated flame retardants in food, Chemosphere 225 (2019) 368–377, https://doi.org/10.1016/j.chemosphere.2019.03.047.

[40] I.A. Boldin, E.N. Nikolaev, Theory of peak coalescence in Fourier transform ion cyclotron resonance mass spectrometry, Rapid Commun. Mass Spectrom. 23 (2009) 3213–3219, https://doi.org/10.1002/rcm.4231.

[41] P.K. Jensen, L. Pasa-Tolic, K.K. Peden, S. Martinovic, M.S. Lipton, G.A. Anderson, N. Tolic, K.-K. Wong, R.D. Smith, Mass spectrometric detection for capillary isoelectric focusing separations of complex protein mixtures, Electrophoresis 21 (2000) 1372–1380.

[42] P.K. Jensen, L. Paša-Tolić, G.A. Anderson, J.A. Horner, M.S. Lipton, J.E. Bruce, R. D. Smith, Probing proteomes using capillary isoelectric focusing-electrospray ionization fourier transform ion cyclotron resonance mass spectrometry, Anal. Chem. 71 (1999) 2076–2084, https://doi.org/10.1021/ac990196p.

[43] Y. Shen, R. Zhao, M.E. Belov, T.P. Conrads, G.A. Anderson, K. Tang, L. Paša-Tolić, T.D. Veenstra, M.S. Lipton, H.R. Udseth, R.D. Smith, Packed capillary reversed-phase liquid chromatography with high-performance electrospray ionization fourier transform ion cyclotron resonance mass spectrometry for proteomics, Anal. Chem. 73 (2001) 1766–1775, https://doi.org/10.1021/ac0011336.

[44] Y. Shen, N. Tolić, R. Zhao, L. Paša-Tolić, L. Li, S.J. Berger, R. Harkewicz, G. A. Anderson, M.E. Belov, R.D. Smith, High-throughput proteomics using high-efficiency multiple-capillary liquid chromatography with on-line high-performance ESI FTICR mass spectrometry, Anal. Chem. 73 (2001) 3011–3021, https://doi.org/10.1021/ac001393n.

[45] J.T. Adamson, K. Hakansson, in: C.L. Nilsson (Ed.), Chapter 14 - Electrospray Ionization Fourier Transform Ion Cyclotron Resonance Mass Spectrometry for Lectin Analysis, Lectins, Elsevier Science B.V., Amsterdam, 2007, pp. 343–371, https://doi.org/10.1016/B978-044453077-6/50015-6.

[46] H. Gao, Y. Shen, T.D. Veenstra, R. Harkewicz, G.A. Anderson, J.E. Bruce, L. Pasa Tolic, R.D. Smith, Two-dimensional electrophoretic/chromatographic separations combined with electrospray ionization FTICR mass spectrometry for high throughput proteome analysis, 12:7<383::AID-MCS1>3.0.CO;2-S, J. Microcolumn Sep. 12 (2000) (2000) 383–390, https://doi.org/10.1002/1520-667X.

[47] F. Lelario, S. De Maria, A.R. Rivelli, D. Russo, L. Milella, S.A. Bufo, L. Scrano, A complete survey of glycoalkaloids using LC-FTICR-MS and IRMPD in a commercial variety and a local landrace of eggplant (Solanum melongena L.) and their anticholinesterase and antioxidant activities, Toxins 11 (2019) 230, https://doi.org/10.3390/toxins11040230.

[48] D. Thakur, T. Rejtar, B.L. Karger, N.J. Washburn, C.J. Bosques, N.S. Gunay, Z. Shriver, G. Venkataraman, Profiling the glycoforms of the intact α subunit of recombinant human chorionic gonadotropin by high-resolution capillary Electrophoresis−Mass spectrometry, Anal. Chem. 81 (2009) 8900–8907, https://doi.org/10.1021/ac901506p.

[49] Y. Qi, C. Ma, S. Chen, J. Ge, Q. Hu, S.-L. Li, D.A. Volmer, P. Fu, Online liquid chromatography and FT-ICR MS enable advanced separation and profiling of

organosulfates in dissolved organic matter, ACS EST Water 1 (2021) 1975–1982, https://doi.org/10.1021/acsestwater.1c00162.
[50] P. Giavalisco, K. Köhl, J. Hummel, B. Seiwert, L. Willmitzer, ^{13}C isotope-labeled metabolomes allowing for improved compound annotation and relative quantification in liquid chromatography-mass spectrometry-based metabolomic research, Anal. Chem. 81 (2009) 6546–6551, https://doi.org/10.1021/ac900979e.
[51] M. Karas, U. Bahr, T. Dülcks, Nano-electrospray ionization mass spectrometry: addressing analytical problems beyond routine, Fresenius' J. Anal. Chem. 366 (2000) 669–676, https://doi.org/10.1007/s002160051561.
[52] E. Carlsohn, J. Nyström, H. Karlsson, A.-M. Svennerholm, C.L. Nilsson, Characterization of the outer membrane protein profile from disease-related Helicobacter pylori isolates by subcellular fractionation and nano-LC FT-ICR MS analysis, J. Proteome Res. 5 (2006) 3197–3204, https://doi.org/10.1021/pr060181p.
[53] F. Lelario, G. Bianco, S.A. Bufo, T.R.I. Cataldi, Establishing the occurrence of major and minor glucosinolates in Brassicaceae by LC–ESI-hybrid linear ion-trap and Fourier-transform ion cyclotron resonance mass spectrometry, Phytochemistry 73 (2012) 74–83, https://doi.org/10.1016/j.phytochem.2011.09.010.
[54] S. Sandron, N.W. Davies, R. Wilson, A.R. Cardona, P.R. Haddad, P.N. Nesterenko, B. Paull, Fractionation of dissolved organic matter on coupled reversed-phase monolithic columns and characterisation using reversed-phase liquid chromatography-high resolution mass spectrometry, Chromatographia 81 (2018) 203–213, https://doi.org/10.1007/s10337-017-3324-0.
[55] J.E. Szulejko, T. Solouki, Potential analytical applications of interfacing a GC to an FT-ICR MS: fingerprinting complex sample matrixes, Anal. Chem. 74 (2002) 3434–3442, https://doi.org/10.1021/ac011192z.
[56] V.Y. Taguchi, R.J. Nieckarz, R.E. Clement, S. Krolik, R. Williams, Dioxin analysis by gas chromatography-Fourier transform ion cyclotron resonance mass spectrometry (GC-FTICRMS), J. Am. Soc. Mass Spectrom. 21 (2010) 1918–1921, https://doi.org/10.1016/j.jasms.2010.07.010.
[57] M. Frommberger, P. Zürbig, J. Jantos, T. Krahn, H. Mischak, A. Pich, I. Just, P. Schmitt-Kopplin, E. Schiffer, Peptidomic analysis of rat urine using capillary electrophoresis coupled to mass spectrometry, Proteonomics Clin. Appl. 1 (2007) 650–660, https://doi.org/10.1002/prca.200700195.
[58] E.E.K. Baidoo, P.I. Benke, C. Neusüss, M. Pelzing, G. Kruppa, J.A. Leary, J. D. Keasling, Capillary electrophoresis-fourier transform ion cyclotron resonance mass spectrometry for the identification of cationic metabolites via a pH-mediated stacking-transient isotachophoretic method, Anal. Chem. 80 (2008) 3112–3122, https://doi.org/10.1021/ac800007q.
[59] C. Gstöttner, S. Nicolardi, M. Haberger, D. Reusch, M. Wuhrer, E. Domínguez-Vega, Intact and subunit-specific analysis of bispecific antibodies by sheathless CE-MS, Anal. Chim. Acta 1134 (2020) 18–27, https://doi.org/10.1016/j.aca.2020.07.069.
[60] D. Baykut, M. Grapow, M. Bergquist, A. Amirkhani, I. Ivonin, D. Reineke, T. Grussenmeyer, P. Hakansson, H.-R. Zerkowski, G. Baykut, J. Bergquist, Molecular differentiation of ischemic and valvular heart disease by liquid chromatography/fourier transform ion cyclotron resonance mass spectrometry, Eur. J. Med. Res. 11 (2006) 221–226.
[61] J.E. Szulejko, Z. Luo, T. Solouki, Simultaneous determination of analyte concentrations, gas-phase basicities, and proton transfer kinetics using gas chromatography/Fourier transform ion cyclotron resonance mass spectrometry (GC/FT-ICR MS), Int. J. Mass Spectrom. 257 (2006) 16–26, https://doi.org/10.1016/j.ijms.2006.05.016.
[62] M.P. Barrow, K.M. Peru, J.V. Headley, An added dimension: GC atmospheric pressure chemical ionization FTICR MS and the Athabasca oil sands, Anal. Chem. 86 (2014) 8281–8288, https://doi.org/10.1021/ac501710y.
[63] J. Zuber, M.M. Kroll, P. Rathsack, M. Otto, Gas chromatography/atmospheric pressure chemical ionization-fourier transform ion cyclotron resonance mass spectrometry of pyrolysis oil from German Brown coal, Int. J. Anal. Chem. 2016 (2016) 1–12.
[64] M. Constapel, M. Schellenträger, O.J. Schmitz, S. Gäb, K.J. Brockmann, R. Giese, Th Benter, Atmospheric-pressure laser ionization: a novel ionization method for liquid chromatography/mass spectrometry, Rapid Commun. Mass Spectrom. 19 (2005) 326–336, https://doi.org/10.1002/rcm.1789.
[65] P. Benigni, J.D. DeBord, C.J. Thompson, P. Gardinali, F. Fernandez-Lima, Increasing polyaromatic hydrocarbon (PAH) molecular coverage during fossil oil analysis by combining gas chromatography and atmospheric-pressure laser ionization fourier transform ion cyclotron resonance mass spectrometry (FT-ICR MS), Energy Fuel. 30 (2016) 196–203, https://doi.org/10.1021/acs.energyfuels.5b02292.
[66] E. Sommella, G.M. Conte, E. Salviati, G. Pepe, A. Bertamino, C. Ostacolo, F. Sansone, F.D. Prete, R.P. Aquino, P. Campiglia, Fast profiling of natural pigments in different Spirulina (arthrospira platensis) dietary supplements by DI-FT-ICR and evaluation of their antioxidant potential by pre-column DPPH-UHPLC assay, Molecules 23 (2018) 1152, https://doi.org/10.3390/molecules23051152.
[67] M. Bataineh, U. Lübcke-von Varel, H. Hayen, W. Brack, HPLC/APCI-FTICR-MS as a tool for identification of partial polar mutagenic compounds in effect-directed analysis, J. Am. Soc. Mass Spectrom. 21 (2010) 1016–1027, https://doi.org/10.1016/j.jasms.2010.02.015.
[68] S. Lababidi, W. Schrader, Online normal-phase high-performance liquid chromatography/Fourier transform ion cyclotron resonance mass spectrometry: effects of different ionization methods on the characterization of highly complex crude oil mixtures: normal-phase HPLC/FT-ICR MS of crude oil, Rapid Commun. Mass Spectrom. 28 (2014) 1345–1352, https://doi.org/10.1002/rcm.6907.
[69] S.A. Hofstadler, F.D. Swanek, D.C. Gale, A.G. Erwing, R.D. Smith, Capillary electrophoresis-electrospray ionization fourier transform ion cyclotron resonance mass spectrometry for direct analysis of cellular proteins, Anal. Chem. 67 (1995) 1477–1480, https://doi.org/10.1021/ac00104a028.
[70] S.A. Hofstadler, J.H. Wahl, R. Bakhtiar, G.A. Anderson, J.E. Bruce, R.D. Smith, Capillary electrophoresis fourier transform ion cyclotron resonance mass spectrometry with sustained off-resonance irradiation for the characterization of protein and peptide mixtures, J. Am. Soc. Mass Spectrom. 5 (1994) 894–899, https://doi.org/10.1016/1044-0305(94)87014-4.
[71] L. Yang, C.S. Lee, S.A. Hofstadler, L. Pasa-Tolic, R.D. Smith, Capillary isoelectric focusing electrospray ionization fourier transform ion cyclotron resonance mass spectrometry for protein characterization, Anal. Chem. 70 (1998) 3235–3241, https://doi.org/10.1021/ac980224o.
[72] S. Martinovic, L. Pasa-Tolic, C. Masselon, P.K. Jensen, C.L. Stone, R.D. Smith, Characterization of human alcohol dehydrogenase isoenzymes by capillary isoelectric focusing-mass spectrometry, Electrophoresis 21 (2000) 2368–2375, https://doi.org/10.1002/1522-2683(20000701)21:12<2368::AID-ELPS2368>3.0.CO;2-F.
[73] M.J. Chalmers, C.L. Mackay, C.L. Hendrickson, S. Wittke, M. Walden, H. Mischak, D. Fliser, I. Just, A.G. Marshall, Combined top-down and bottom-up mass spectrometric approach to characterization of biomarkers for renal disease, Anal. Chem. 77 (2005) 7163–7171, https://doi.org/10.1021/ac050983o.
[74] G. Hübner, B. Lindner, Separation of R-form lipopolysaccharide and lipid A by CE-Fourier-transform ion cyclotron resonance MS, Electrophoresis 30 (2009) 1808–1816, https://doi.org/10.1002/elps.200800754.
[75] M. Boulanger, C. Delvaux, L. Quinton, B. Joris, E.D. Pauw, J. Far, Bacillus licheniformis peptidoglycan characterization by CZE–MS: assessment with the benchmark RP-HPLC-MS method, Electrophoresis 40 (2019) 2672–2682, https://doi.org/10.1002/elps.201900147.
[76] S. Pleasance, P. Thibault, J. Kelly, Comparison of liquid-junction and coaxial interfaces for capillary electrophoresis-mass spectrometry with application to compounds of concern to the aquaculture industry, J. Chromatogr. A 591 (1992) 325–339, https://doi.org/10.1016/0021-9673(92)80250-X.
[77] V. Bezy, P. Chaimbault, P. Morin, S.E. Unger, M.-C. Bernard, L.A. Agrofoglio, Analysis and validation of the phosphorylated metabolites of two anti-human immunodeficiency virus nucleotides (stavudine and didanosine) by pressure-assisted CE-ESI-MS/MS in cell extracts: sensitivity enhancement by the use of perfluorinated acids and alcohols as coaxial sheath-liquid make-up constituents, Electrophoresis 27 (2006) 2464–2476, https://doi.org/10.1002/elps.200500850.
[78] J.T. Whitt, M. Moini, Capillary electrophoresis to mass spectrometry interface using a porous junction, Anal. Chem. 75 (2003) 2188–2191, https://doi.org/10.1021/ac026380j.
[79] A.G. Marshall, M.B. Comisarow, G. Parisod, Relaxation and spectral line shape in Fourier transform ion resonance spectroscopy, J. Chem. Phys. 71 (1979) 4434–4444, https://doi.org/10.1063/1.438196.
[80] C.L. Hendrickson, J.P. Quinn, N.K. Kaiser, D.F. Smith, G.T. Blakney, T. Chen, A. G. Marshall, C.R. Weisbrod, S.C. Beu, 21 tesla fourier transform ion cyclotron resonance mass spectrometer: a national resource for ultrahigh resolution mass analysis, J. Am. Soc. Mass Spectrom. 26 (2015) 1626–1632, https://doi.org/10.1007/s13361-015-1182-2.
[81] A.G. Marshall, Theoretical signal-to-noise ratio and mass resolution in Fourier transform ion cyclotron resonance mass spectrometry, Anal. Chem. 51 (1979) 1710–1714, https://doi.org/10.1021/ac50047a029.
[82] M.F. Wahab, P.K. Dasgupta, A.F. Kadjo, D.W. Armstrong, Sampling frequency, response times and embedded signal filtration in fast, high efficiency liquid chromatography: a tutorial, Anal. Chim. Acta 907 (2016) 31–44, https://doi.org/10.1016/j.aca.2015.11.043.
[83] A.G. Marshall, T. Chen, 40 years of Fourier transform ion cyclotron resonance mass spectrometry, Int. J. Mass Spectrom. 377 (2015) 410–420, https://doi.org/10.1016/j.ijms.2014.06.034.
[84] K.P. Wanczek, B. Kanawati, Chapter 1 - historical developments in Fourier transform ion cyclotron resonance mass spectrometry, in: B. Kanawati, P. Schmitt-Kopplin (Eds.), Fundamentals and Applications of Fourier Transform Mass Spectrometry, Elsevier, 2019, pp. 3–33, https://doi.org/10.1016/B978-0-12-814013-0.00001-6.
[85] J.B. Shaw, T.-Y. Lin, F.E. Leach, A.V. Tolmachev, N. Tolić, E.W. Robinson, D. W. Koppenaal, L. Paša-Tolić, 21 tesla fourier transform ion cyclotron resonance mass spectrometer greatly expands mass spectrometry toolbox, J. Am. Soc. Mass Spectrom. 27 (2016) 1929–1936, https://doi.org/10.1007/s13361-016-1507-9.
[86] D.F. Smith, D.C. Podgorski, R.P. Rodgers, G.T. Blakney, C.L. Hendrickson, 21 tesla FT-ICR mass spectrometer for ultrahigh-resolution analysis of complex organic mixtures, Anal. Chem. 90 (2018) 2041–2047, https://doi.org/10.1021/acs.analchem.7b04159.
[87] Y.I. Kostyukevich, G.N. Vladimirov, E.N. Nikolaev, Dynamically harmonized FT-ICR cell with specially shaped electrodes for compensation of inhomogeneity of the magnetic field. Computer simulations of the electric field and ion motion dynamics, J. Am. Soc. Mass Spectrom. 23 (2012) 2198–2207, https://doi.org/10.1007/s13361-012-0480-1.
[88] E. Cho, M. Witt, M. Hur, M.-J. Jung, S. Kim, Application of FT-ICR MS equipped with quadrupole detection for analysis of crude oil, Anal. Chem. 89 (2017) 12101–12107, https://doi.org/10.1021/acs.analchem.7b02644.
[89] J.A. Driver, A. Kharchenko, I.J. Amster, Simulations of nw measurement using multiple detection electrodes in FTICR mass spectrometry, Int. J. Mass Spectrom. 455 (2020), 116372, https://doi.org/10.1016/j.ijms.2020.116372.
[90] M.L. Easterling, J.N. Agar, Chapter 3 - fundamentals, strengths, and future directions for Fourier transform ion cyclotron resonance mass spectrometry, in:

B. Kanawati, P. Schmitt-Kopplin (Eds.), Fundamentals and Applications of Fourier Transform Mass Spectrometry, Elsevier, 2019, pp. 63–88, https://doi.org/10.1016/B978-0-12-814013-0.00003-X.
[91] L.V. Tose, C.R. Weisbrod, V. Michalkova, M. Nouzova, F.G. Noriega, F. Fernandez-Lima, Following de novo triglyceride dynamics in ovaries of Aedes aegypti during the previtellogenic stage, Sci. Rep. 11 (2021) 9636, https://doi.org/10.1038/s41598-021-89025-6.
[92] J.B. Shaw, M.V. Gorshkov, Q. Wu, L. Paša-Tolić, High speed intact protein characterization using 4X frequency multiplication, ion trap harmonization, and 21 tesla FTICR-MS, Anal. Chem. 90 (2018) 5557–5562, https://doi.org/10.1021/acs.analchem.7b04606.
[93] P. Hu, D.P. Cole, Routine absorption mode FTMS data display with an ethoxylated anionic detergent as a dual-role (mass and phase) calibrant, J. Am. Soc. Mass Spectrom. 30 (2019) 468–475, https://doi.org/10.1007/s13361-018-2099-3.
[94] J. Irungu, E.P. Go, Y. Zhang, D.S. Dalpathado, H.-X. Liao, B.F. Haynes, H. Desaire, Comparison of HPLC/ESI-FTICR MS versus MALDI-TOF/TOF MS for glycopeptide analysis of a highly glycosylated HIV envelope glycoprotein, J. Am. Soc. Mass Spectrom. 19 (2008) 1209–1220, https://doi.org/10.1016/j.jasms.2008.05.010.
[95] L. Xin, L. Hou, Y. Zhou, H. Wang, H. Yu, Online effective identification of glycopeptide using liquid chromatography combined with fourier transform ion cyclotron resonance mass spectrometry (FTICR-MS), Adv. Biosci. Biotechnol. 6 (2015) 624–628, https://doi.org/10.4236/abb.2015.69065.
[96] X. Wang, M.R. Emmett, A.G. Marshall, Liquid chromatography electrospray ionization fourier transform ion cyclotron resonance mass spectrometric characterization of *N* -linked glycans and glycopeptides, Anal. Chem. 82 (2010) 6542–6548, https://doi.org/10.1021/ac1008833.
[97] M. Ramström, M. Palmblad, K.E. Markides, P. Håkansson, J. Bergquist, Protein identification in cerebrospinal fluid using packed capillary liquid chromatography Fourier transform ion cyclotron resonance mass spectrometry, Proteomics 3 (2003) 184–190, https://doi.org/10.1002/pmic.200390027.
[98] J.G. Pounds, J.W. Flora, J.N. Adkins, K.M. Lee, G.S.J.B. Rana, T. Sengupta, R. D. Smith, W.J. McKinney, Characterization of the mouse bronchoalveolar lavage proteome by micro-capillary LC–FTICR mass spectrometry, J. Chromatogr., B 864 (2008) 95–101, https://doi.org/10.1016/j.jchromb.2008.01.044.
[99] H. Kang, L. Paš-Tolić, R.D. Smith, Targeted tandem mass spectrometry for high-throughput comparative proteomics employing NanoLC-FTICR MS with external ion dissociation, J. Am. Soc. Mass Spectrom. 18 (2007) 1332–1343, https://doi.org/10.1016/j.jasms.2007.04.011.
[100] M.E. Belov, G.A. Anderson, M.A. Wingerd, H.R. Udseth, K. Tang, D.C. Prior, K. R. Swanson, M.A. Buschbach, E.F. Strittmatter, R.J. Moore, R.D. Smith, An automated high performance capillary liquid chromatography-Fourier transform ion cyclotron resonance mass spectrometer for high-throughput proteomics, J. Am. Soc. Mass Spectrom. 15 (2004) 212–232, https://doi.org/10.1016/j.jasms.2003.09.008.
[101] D. Mohan, L. Paša-Tolić, C.D. Masselon, N. Tolić, B. Bogdanov, K.K. Hixson, R. D. Smith, C.S. Lee, Integration of electrokinetic-based multidimensional separation/concentration platform with electrospray ionization-fourier transform ion cyclotron resonance-mass spectrometry for proteome analysis of shewanella oneidensis, Anal. Chem. 75 (2003) 4432–4440, https://doi.org/10.1021/ac0342572.
[102] M.S. Lipton, L. Paša-Tolić, G.A. Anderson, D.J. Anderson, D.L. Auberry, J. R. Battista, M.J. Daly, J. Fredrickson, K.K. Hixson, H. Kostandarithes, C. Masselon, L.M. Markillie, R.J. Moore, M.F. Romine, Y. Shen, E. Stritmatter, N. Tolić, H. R. Udseth, A. Venkateswaran, K.-K. Wong, R. Zhao, R.D. Smith, Global analysis of the Deinococcus radiodurans proteome by using accurate mass tags, Proc. Natl. Acad. Sci. USA 99 (2002) 11049–11054, https://doi.org/10.1073/pnas.172170199.
[103] Y.O. Tsybin, P. Håkansson, M. Wetterhall, K.E. Markides, J. Bergquist, Capillary electrophoresis and electron capture dissociation fourier transform ion cyclotron resonance mass spectrometry for peptide mixture and protein digest analysis, Eur. J. Mass Spectrom. 8 (2002) 389–395, https://doi.org/10.1255/ejms.514.
[104] L. Li, C.D. Masselon, G.A. Anderson, L. Paša-Tolić, S.-W. Lee, Y. Shen, R. Zhao, M. S. Lipton, T.P. Conrads, N. Tolić, R.D. Smith, High-throughput peptide identification from protein digests using data-dependent multiplexed tandem FTICR mass spectrometry coupled with capillary liquid chromatography, Anal. Chem. 73 (2001) 3312–3322, https://doi.org/10.1021/ac010192w.
[105] S. Lippold, S. Nicolardi, E. Domínguez-Vega, A.-K. Heidenreich, G. Vidarsson, D. Reusch, M. Haberger, M. Wuhrer, D. Falck, Glycoform-resolved FcγRIIIa affinity chromatography–mass spectrometry, mAbs 11 (2019) 1191–1196, https://doi.org/10.1080/014904099273011.
[106] S.-W. Lee, S.J. Berger, S. Martinovic, L. Pasa-Tolic, G.A. Anderson, Y. Shen, R. Zhao, R.D. Smith, Direct mass spectrometric analysis of intact proteins of the yeast large ribosomal subunit using capillary LC/FTICR, Proc. Natl. Acad. Sci. USA 99 (2002) 5942–5947, https://doi.org/10.1073/pnas.082119899.
[107] S. Martinović, T.D. Veenstra, G.A. Anderson, L. Pasa-Tolić, R.D. Smith, Selective incorporation of isotopically labeled amino acids for identification of intact proteins on a proteome-wide level, J. Mass Spectrom. 37 (2002) 99–107, https://doi.org/10.1002/jms.263.
[108] C.-X. Zhang, F. Xiang, L. Pasa-Tolic, G.A. Anderson, T.D. Veenstra, R.D. Smith, Stepwise mobilization of focused proteins in capillary isoelectric focusing mass spectrometry, Anal. Chem. 72 (2000) 1462–1468, https://doi.org/10.1021/ac9912653.
[109] L. Pasa-Tolic, P.K. Jensen, G.A. Anderson, M.S. Lipton, K.K. Peden, S. Martinovic, N. Tolic, J.E. Bruce, R.D. Smith, High throughput proteome-wide precision measurements of protein expression using mass spectrometry, J. Am. Chem. Soc. 121 (1999) 7949–7950, https://doi.org/10.1021/ja991063o.
[110] S.A. Hofstadler, J.C. Severs, R.D. Smith, F.D. Swanek, A.G. Ewing, Analysis of single cells with capillary electrophoresis electrospray ionization fourier transform ion cycloton resonance mass spectrometry, Rapid Commun. Mass Spectrom. 10 (2) (1996) 919–922, https://doi.org/10.1002/(SICI)1097-0231(19960610)10:8<919::AID-RCM597>3.0.CO.
[111] A.G. Marshall, M.W. Senko, W. Li, M. Li, S. Dillon, S. Guan, T.M. Logan, Protein molecular mass to 1 Da by ^{13}C, ^{15}N double-depletion and FT-ICR mass spectrometry, J. Am. Chem. Soc. 119 (1997) 433–434, https://doi.org/10.1021/ja9630046.
[112] S. Martinovic, S.J. Berger, L. Pasa-Tolic, R.D. Smith, Separation and detection of intact noncovalent protein complexes from mixtures by on-line capillary isoelectric focusing-mass spectrometry, Anal. Chem. 72 (2000) 5356–5360, https://doi.org/10.1021/ac0004557.
[113] Y. Jin, Z. Lin, Qingg Xu, Cexiong Fu, Zhaorui Zhang, Q. Zhang, W.A. Pritts, Y. Ge, Comprehensive characterization of monoclonal antibody by Fourier transform ion cyclotron resonance mass spectrometry, mAbs 11 (2019) 106–115, https://doi.org/10.1080/19420862.2018.1525253.
[114] L. He, L.C. Anderson, D.R. Barnidge, D.L. Murray, C.L. Hendrickson, A. G. Marshall, Analysis of monoclonal antibodies in human serum as a model for clinical monoclonal gammopathy by use of 21 tesla FT-ICR top-down and middle-down MS/MS, J. Am. Soc. Mass Spectrom. 28 (2017) 827–838, https://doi.org/10.1007/s13361-017-1602-6.
[115] L.C. Anderson, C.J. DeHart, N.K. Kaiser, R.T. Fellers, D.F. Smith, J.B. Greer, R. D. LeDuc, G.T. Blakney, P.M. Thomas, N.L. Kelleher, C.L. Hendrickson, Identification and characterization of human proteoforms by top-down LC-21 tesla FT-ICR mass spectrometry, J. Proteome Res. 16 (2017) 1087–1096, https://doi.org/10.1021/acs.jproteome.6b00696.
[116] G. Brinkmalm, An online nano-LC-ESI-FTICR-MS methodfor comprehensive characterization ofendogenous fragments from amyloidbandamyloid precursor protein in human and catcerebrospinalfluid, J. Mass Spectrom. 47 (2012) 591–603, https://doi.org/10.1002/jms.2987.
[117] B. Chen, Z. Lin, A.J. Alpert, C. Fu, Q. Zhang, W.A. Pritts, Y. Ge, Online hydrophobic interaction chromatography–mass spectrometry for the analysis of intact monoclonal antibodies, Anal. Chem. 90 (2018) 7135–7138, https://doi.org/10.1021/acs.analchem.8b01865.
[118] T.S. Collier, A.M. Hawkridge, D.R. Georgianna, G.A. Payne, D.C. Muddiman, Top-down identification and quantification of stable isotope labeled proteins from *Aspergillus flavus* using online nano-flow reversed-phase liquid chromatography coupled to a LTQ-FTICR mass spectrometer, Anal. Chem. 80 (2008) 4994–5001, https://doi.org/10.1021/ac800254z.
[119] J.D. Tipton, J.C. Tran, A.D. Catherman, D.R. Ahlf, K.R. Durbin, J.E. Lee, J. F. Kellie, N.L. Kelleher, C.L. Hendrickson, A.G. Marshall, Nano-LC FT-ICR tandem mass spectrometry for top-down proteomics: routine baseline unit mass resolution of whole cell lysate proteins up to 72 kDa, Anal. Chem. 84 (2012) 2111–2117, https://doi.org/10.1021/ac202651v.
[120] N. Lourette, H. Smallwood, S. Wu, E.W. Robinson, T.C. Squier, R.D. Smith, L. Paša-Tolić, A top-down LC-FTICR MS-based strategy for characterizing oxidized calmodulin in activated macrophages, J. Am. Soc. Mass Spectrom. 21 (2010) 930–939, https://doi.org/10.1016/j.jasms.2010.02.027.
[121] R. Lakshmanan, J.J. Wolff, R. Alvarado, J.A. Loo, Top-down protein identification of proteasome proteins with nanoLC-FT-ICR-MS employing data-independent fragmentation methods, Proteomics 14 (2014) 1271–1282, https://doi.org/10.1002/pmic.201300339.
[122] R. Nakabayashi, Y. Sawada, Y. Yamada, M. Suzuki, M.Y. Hirai, T. Sakurai, K. Saito, Combination of liquid chromatography–fourier transform ion cyclotron resonance-mass spectrometry with ^{13}C-labeling for chemical assignment of sulfur-containing metabolites in onion bulbs, Anal. Chem. 85 (2013) 1310–1315, https://doi.org/10.1021/ac302733c.
[123] Y. Ren, P. Wang, C. Wu, J. Zhang, C. Niu, Identification of the metabolites after oral administration of extract of ziziphi spinosae semen to rats or dogs by high-performance liquid chromatography/linear ion trap FTICR hybrid mass spectrometry: metabolites of ziziphi spinosae semen in rats or dogs, Biomed. Chromatogr. 27 (2013) 17–26, https://doi.org/10.1002/bmc.2742.
[124] J. Guan, Q. Zhang, R. Rong, F. Han, H. Zhu, Y. Zhao, A. Song, Z. Yu, Metabolic profile of 2-(2-hydroxypropanamido) benzoic acid in rats by ultra high performance liquid chromatography combined with Fourier transform ion cyclotron resonance mass spectrometry, J. Chromatogr., B 993 (994) (2015) 60–68, https://doi.org/10.1016/j.jchromb.2015.04.039.
[125] J. Pollier, K. Morreel, D. Geelen, A. Goossens, Metabolite profiling of triterpene saponins in *Medicago truncatula* hairy roots by liquid chromatography fourier transform ion cyclotron resonance mass spectrometry, J. Nat. Prod. 74 (2011) 1462–1476, https://doi.org/10.1021/np200218r.
[126] G. Bianco, F. Lelario, F.G. Battista, S.A. Bufo, T.R.I. Cataldi, Identification of glucosinolates in capers by LC-ESI-hybrid linear ion trap with Fourier transform ion cyclotron resonance mass spectrometry (LC-ESI-LTQ-FTICR MS) and infrared multiphoton dissociation, J. Mass Spectrom. 47 (2012) 1160–1169, https://doi.org/10.1002/jms.2996.
[127] I.I. Rockenbach, E. Jungfer, C. Ritter, B. Santiago-Schübel, B. Thiele, R. Fett, R. Galensa, Characterization of flavan-3-ols in seeds of grape pomace by CE, HPLC-DAD-MSn and LC-ESI-FTICR-MS, Food Res. Int. 48 (2012) 848–855, https://doi.org/10.1016/j.foodres.2012.07.001.
[128] R. Nakabayashi, H. Tsugawa, M. Kitajima, H. Takayama, K. Saito, Boosting sensitivity in liquid chromatography–fourier transform ion cyclotron resonance–tandem mass spectrometry for product ion analysis of monoterpene indole alkaloids, Front. Plant Sci. 6 (2015), https://doi.org/10.3389/fpls.2015.01127.

[129] D. Kim, S. Kim, S. Son, M.-J. Jung, S. Kim, Application of online liquid chromatography 7 T FT-ICR mass spectrometer equipped with quadrupolar detection for analysis of natural organic matter, Anal. Chem. (2019), https://doi.org/10.1021/acs.analchem.9b00689.
[130] X. Ortiz, K.J. Jobst, E.J. Reiner, S.M. Backus, K.M. Peru, D.W. McMartin, G. O'Sullivan, V.Y. Taguchi, J.V. Headley, Characterization of naphthenic acids by gas chromatography-fourier transform ion cyclotron resonance mass spectrometry, Anal. Chem. 86 (2014) 7666–7673, https://doi.org/10.1021/ac501549p.
[131] M.J. Thomas, E. Collinge, M. Witt, D.C. Palacio Lozano, C.H. Vane, V. Moss-Hayes, M.P. Barrow, Petroleomic depth profiling of Staten Island salt marsh soil: 2ω detection FTICR MS offers a new solution for the analysis of environmental contaminants, Sci. Total Environ. 662 (2019) 852–862, https://doi.org/10.1016/j.scitotenv.2019.01.228.
[132] T. Solouki, J.E. Szulejko, J.B. Bennett, L.B. Graham, A preconcentrator coupled to a GC/FTMS: advantages of self-chemical ionization, mass measurement accuracy, and high mass resolving power for GC applications, J. Am. Soc. Mass Spectrom. 15 (2004) 1191–1200, https://doi.org/10.1016/j.jasms.2004.03.003.
[133] V.Y. Taguchi, R.J. Nieckarz, R.E. Clement, S. Krolik, R. Williams, Dioxin analysis by gas chromatography-fourier transform ion cyclotron resonance mass spectrometry (GC-FTICRMS), J. Am. Soc. Mass Spectrom. (2010), https://doi.org/10.1016/j.jasms.2010.07.010. S1044030510005118.
[134] R. Sühring, X. Ortiz, M. Pena-Abaurrea, K.J. Jobst, M. Freese, J.-D. Pohlmann, L. Marohn, R. Ebinghaus, S. Backus, R. Hanel, E.J. Reiner, Evidence for high concentrations and maternal transfer of substituted diphenylamines in European eels analyzed by two-dimensional gas chromatography–time-of-flight mass spectrometry and gas chromatography–fourier transform ion cyclotron resonance mass spectrometry, Environ. Sci. Technol. 50 (2016) 12678–12685, https://doi.org/10.1021/acs.est.6b04382.
[135] S. Lababidi, S.K. Panda, J.T. Andersson, W. Schrader, Direct coupling of normal-phase high-performance liquid chromatography to atmospheric pressure laser ionization fourier transform ion cyclotron resonance mass spectrometry for the characterization of crude oil, Anal. Chem. 85 (2013) 9478–9485, https://doi.org/10.1021/ac400670s.
[136] S.-G. Park, G.A. Anderson, J.E. Bruce, Characterization of harmonic signal acquisition with parallel dipole and multipole detectors, J. Am. Soc. Mass Spectrom. 29 (2018) 1394–1402, https://doi.org/10.1007/s13361-018-1954-6.
[137] S.-G. Park, J.P. Mohr, G.A. Anderson, J.E. Bruce, Application of frequency multiple FT-ICR MS signal acquisition for improved proteome research, Int. J. Mass Spectrom. 465 (2021), 116578, https://doi.org/10.1016/j.ijms.2021.116578.
[138] S.-G. Park, G.A. Anderson, J.E. Bruce, Parallel detection of fundamental and sixth harmonic signals using an ICR cell with dipole and sixth harmonic detectors, J. Am. Soc. Mass Spectrom. 31 (2020) 719–726, https://doi.org/10.1021/jasms.9b00144.
[139] J.C. May, J.A. McLean, Ion mobility-mass spectrometry: time-dispersive instrumentation, Anal. Chem. 87 (2015) 1422–1436, https://doi.org/10.1021/ac504720m.
[140] X. Tang, J.E. Bruce, H.H. Hill Jr., Design and performance of an atmospheric pressure ion mobility Fourier transform ion cyclotron resonance mass spectrometer, Rapid Commun. Mass Spectrom. 21 (2007) 1115–1122, https://doi.org/10.1002/rcm.2928.
[141] P. Benigni, F. Fernandez-Lima, Oversampling selective accumulation trapped ion mobility spectrometry coupled to FT-ICR MS: fundamentals and applications, Anal. Chem. 88 (2016) 7404–7412, https://doi.org/10.1021/acs.analchem.6b01946.
[142] M.W. Senko, C.L. Hendrickson, M.R. Emmett, S.D.H. Shi, A.G. Marshall, External accumulation of ions for enhanced electrospray ionization fourier transform ion cyclotron resonance mass spectrometry, J. Am. Soc. Mass Spectrom. 8 (1997) 970–976, https://doi.org/10.1016/S1044-0305(97)00126-8.
[143] M.R. Emmett, F.M. White, C.L. Hendrickson, S.D. Shi, A.G. Marshall, Application of micro-electrospray liquid chromatography techniques to FT-ICR MS to enable high-sensitivity biological analysis, J. Am. Soc. Mass Spectrom. 9 (1998) 333–340, https://doi.org/10.1016/S1044-0305(97)00287-0.
[144] W. Li, C.L. Hendrickson, M.R. Emmett, A.G. Marshall, Identification of intact proteins in mixtures by alternated capillary liquid chromatography electrospray ionization and LC ESI infrared multiphoton dissociation fourier transform ion cyclotron resonance mass spectrometry, Anal. Chem. 71 (1999) 4397–4402, https://doi.org/10.1021/ac990011e.
[145] S.E. Martin, J. Shabanowitz, D.F. Hunt, J.A. Marto, Subfemtomole MS and MS/MS peptide sequence analysis using nano-HPLC micro-ESI fourier transform ion cyclotron resonance mass spectrometry, Anal. Chem. 72 (2000) 4266–4274, https://doi.org/10.1021/ac000497v.
[146] T.L. Quenzer, M.R. Emmett, C.L. Hendrickson, P.H. Kelly, A.G. Marshall, High sensitivity fourier transform ion cyclotron resonance mass spectrometry for biological analysis with nano-LC and microelectrospray ionization, Anal. Chem. 73 (2001) 1721–1725, https://doi.org/10.1021/ac001095q.
[147] Y. Tanaka, I. Sato, C. Iwai, T. Kosaka, T. Ikeda, T. Nakamura, Identification of human liver diacetyl reductases by nano-liquid chromatography/fourier transform ion cyclotron resonance mass spectrometry, Anal. Biochem. 293 (2001) 157–168, https://doi.org/10.1006/abio.2001.5128.
[148] M.E. Belov, G.A. Anderson, R.D. Smith, Higher-resolution data-dependent selective external ion accumulation for capillary LC-FTICR, Int. J. Mass Spectrom. 218 (2002) 265–279, https://doi.org/10.1016/S1387-3806(02)00736-4.
[149] M. Palmblad, Y.O. Tsybin, M. Ramström, J. Bergquist, P. Håkansson, Liquid chromatography and electron-capture dissociation in Fourier transform ion cyclotron resonance mass spectrometry: LC and ECD with FTICRMS, Rapid Commun. Mass Spectrom. 16 (2002) 988–992, https://doi.org/10.1002/rcm.667.
[150] R.D. Smith, G.A. Anderson, M.S. Lipton, L. Pasa-Tolic, Y. Shen, T.P. Conrads, T. D. Veenstra, H.R. Udseth, An accurate mass tag strategy for quantitative and high-throughput proteome measurements, Proteomics 2 (2002) 513–523, https://doi.org/10.1002/1615-9861(200205)2:5<513::AID-PROT513>3.0.CO;2.
[151] W. Davidson, L. Frego, Micro-high-performance liquid chromatography/Fourier transform mass spectrometry with electron-capture dissociation for the analysis of protein enzymatic digests, Rapid Commun. Mass Spectrom. 16 (2002) 993–998, https://doi.org/10.1002/rcm.666.
[152] C. Ihling, K. Berger, M.M. Höfliger, D. Führer, A.G. Beck-Sickinger, A. Sinz, Nano-high-performance liquid chromatography in combination with nano-electrospray ionization Fourier transform ion-cyclotron resonance mass spectrometry for proteome analysis, Rapid Commun. Mass Spectrom. 17 (2003) 1240–1246, https://doi.org/10.1002/rcm.1049.
[153] M. Witt, J. Fuchser, G. Baykut, Fourier transform ion cyclotron resonance mass spectrometry with NanoLC/microelectrospray ionization and matrix-assisted laser desorption/ionization: analytical performance in peptide mass fingerprint analysis, J. Am. Soc. Mass Spectrom. (2003), https://doi.org/10.1016/S1044-0305(03)00138-7.
[154] S.K. Bergström, A.P. Dahlin, M. Ramström, M. Andersson, K.E. Markides, J. Bergquist, A simplified multidimensional approach for analyqis of complex biological samples : on-line LC-CE-MS, Analyst 131 (2006) 791–798, https://doi.org/10.1039/b601660j.
[155] Y.E.M. Burgt, I.M. Taban, M. Konijnenburg, M. Biskup, M.C. Duursma, R.M. A. Heeren, A. Römpp, R.V. Nieuwpoort, H.E. Bal, Parallel processing of large datasets from NanoLC-FTICR-MS measurements, J. Am. Soc. Mass Spectrom. 18 (2007) 152–161, https://doi.org/10.1016/j.jasms.2006.09.005.
[156] H.S. Smallwood, N.M. Lourette, C.B. Boschek, D.J. Bigelow, R.D. Smith, L. Paša-Tolić, T.C. Squier, Identification of a denitrase activity against calmodulin in activated macrophages using high-field liquid Chromatography−FTICR mass spectrometry, Biochemistry 46 (2007) 10498–10505, https://doi.org/10.1021/bi7009713.
[157] A. Öhrfelt, H. Zetterberg, K. Andersson, R. Persson, D. Secic, G. Brinkmalm, A. Wallin, E. Mulugeta, P.T. Francis, E. Vanmechelen, D. Aarsland, C. Ballard, K. Blennow, A. Westman-Brinkmalm, Identification of novel α-synuclein isoforms in human brain tissue by using an online NanoLC-ESI-FTICR-MS method, Neurochem. Res. 36 (2011) 2029–2042, https://doi.org/10.1007/s11064-011-0527-x.
[158] L. Switzar, S. Nicolardi, J.W. Rutten, S.A.J.L. Oberstein, A. Aartsma-Rus, Y.E. M. van der Burgt, In-depth characterization of protein disulfide bonds by online liquid chromatography-electrochemistry-mass spectrometry, J. Am. Soc. Mass Spectrom. 27 (2016) 50–58, https://doi.org/10.1007/s13361-015-1258-z.
[159] L.C. Anderson, M. Håkansson, B. Walse, C.L. Nilsson, Intact protein analysis at 21 tesla and X-ray crystallography define structural differences in single amino acid variants of human mitochondrial branched-chain amino acid aminotransferase 2 (BCAT2), J. Am. Soc. Mass Spectrom. 28 (2017) 1796–1804, https://doi.org/10.1007/s13361-017-1705-0.
[160] K. Guo, C. Ji, L. Li, Stable-isotope dimethylation labeling combined with LC−ESI MS for quantification of amine-containing metabolites in biological samples, Anal. Chem. 79 (2007) 8631–8638, https://doi.org/10.1021/ac0704356.
[161] I. Bobeldijk, M. Hekman, J. de Vries-van der Weij, L. Coulier, R. Ramaker, R. Kleemann, T. Kooistra, C. Rubingh, A. Freidig, E. Verheij, Quantitative profiling of bile acids in biofluids and tissues based on accurate mass high resolution LC-FT-MS: compound class targeting in a metabolomics workflow, J. Chromatogr., B 871 (2008) 306–313, https://doi.org/10.1016/j.jchromb.2008.05.008.
[162] T.R.I. Cataldi, G. Bianco, S. Abate, Accurate mass analysis of N-acyl-homoserine-lactones and cognate lactone-opened compounds in bacterial isolates of *Pseudomonas aeruginosa* PAO1 by LC-ESI-LTQ-FTICR-MS, J. Mass Spectrom. 44 (2009) 182–192, https://doi.org/10.1002/jms.1479.
[163] K. Guo, L. Li, Differential ^{12}C-/^{13}C-isotope dansylation labeling and fast liquid chromatography/mass spectrometry for absolute and relative quantification of the metabolome, Anal. Chem. 81 (2009) 3919–3932, https://doi.org/10.1021/ac900166a.
[164] K. Guo, F. Bamforth, L. Li, Qualitative metabolome analysis of human cerebrospinal fluid by ^{13}C-/^{12}C-isotope dansylation labeling combined with liquid chromatography Fourier transform ion cyclotron resonance mass spectrometry, J. Am. Soc. Mass Spectrom. 22 (2011) 339–347, https://doi.org/10.1007/s13361-010-0033-4.
[165] H. Suzuki, R. Sasaki, Y. Ogata, Y. Nakamura, N. Sakurai, M. Kitajima, H. Takayama, S. Kanaya, K. Aoki, D. Shibata, K. Saito, Metabolic profiling of flavonoids in Lotus japonicus using liquid chromatography Fourier transform ion cyclotron resonance mass spectrometry, Phytochemistry 69 (2008) 99–111, https://doi.org/10.1016/j.phytochem.2007.06.017.
[166] F. Han, Y. Li, X. Mao, R. Xu, R. Yin, Characterization of chemical constituents in Rhodiola Crenulate by high-performance liquid chromatography coupled with Fourier-transform ion cyclotron resonance mass spectrometer (HPLC-FT-ICR MS): constituents in R. Crenulate by HPLC-FTICR-MS, J. Mass Spectrom. 51 (2016) 363–368, https://doi.org/10.1002/jms.3764.
[167] R. Nakabayashi, Y. Sawada, M. Aoyagi, Y. Yamada, M.Y. Hirai, T. Sakurai, T. Kamoi, D.D. Rowan, K. Saito, Chemical assignment of structural isomers of sulfur-containing metabolites in garlic by liquid Chromatography−Fourier transform ion cyclotron Resonance−Mass spectrometry, J. Nutr. 146 (2016) 397S–402S, https://doi.org/10.3945/jn.114.202317.

[168] Y. Wang, M. Zhao, Y. Ou, B. Zeng, X. Lou, M. Wang, C. Zhao, Metabolic profile of esculin in rats by ultra high performance liquid chromatography combined with Fourier transform ion cyclotron resonance mass spectrometry, J. Chromatogr., B 1020 (2016) 120–128, https://doi.org/10.1016/j.jchromb.2016.03.027.
[169] T. Liu, S. Li, X. Tian, Z. Li, Y. Cui, F. Han, Y. Zhao, Z. Yu, A plasma metabonomic analysis on potential biomarker in pyrexia induced by three methods using ultra high performance liquid chromatography coupled with Fourier transform ion cyclotron resonance mass spectrometry, J. Chromatogr., B 1063 (2017) 214–225, https://doi.org/10.1016/j.jchromb.2017.08.028.
[170] B. Li, H. Zhou, G. Yang, F. Han, Y. Li, Y. Gao, J. Gao, F. Zhang, L. Sun, In vivo study of erysolin metabolic profile by ultra high performance liquid chromatography coupleded to Fourier transform ion cyclotron resonance mass spectrometry, J. Chromatogr., B 1072 (2018) 173–181, https://doi.org/10.1016/j.jchromb.2017.11.019.
[171] T. Liu, X. Tian, Z. Li, F. Han, B. Ji, Y. Zhao, Z. Yu, Metabolic profiling of Gegenqinlian decoction in rat plasma, urine, bile and feces after oral administration by ultra high performance liquid chromatography coupled with Fourier transform ion cyclotron resonance mass spectrometry, J. Chromatogr., B 1079 (2018) 69–84, https://doi.org/10.1016/j.jchromb.2018.02.001.
[172] J. Yao, X. Jiang, Q. Liu, X. Yuan, T. Feng, K. Li, L. Zhao, An available strategy based on accurate mass by ultra high performance liquid chromatography coupled to Fourier transform ion cyclotron resonance mass spectrometry technology to characterization of metabolic profile of palbociclib in rat urine, feces and bile, J. Chromatogr., B 1124 (2019) 37–46, https://doi.org/10.1016/j.jchromb.2019.05.032.
[173] L. Müller, M.-C. Reinnig, H. Hayen, T. Hoffmann, Characterization of oligomeric compounds in secondary organic aerosol using liquid chromatography coupled to electrospray ionization Fourier transform ion cyclotron resonance mass spectrometry, Rapid Commun. Mass Spectrom. 23 (2009) 971–979, https://doi.org/10.1002/rcm.3957.
[174] Y. Shen, R. Zhao, N. Tolić, M.M. Tfaily, E.W. Robinson, R. Boiteau, L. Paša-Tolić, N.J. Hess, Online supercritical fluid extraction mass spectrometry (SFE-LC-FTMS) for sensitive characterization of soil organic matter, Faraday Discuss 218 (2019) 157–171, https://doi.org/10.1039/C9FD00011A.
[175] C.H. Kim, M.Y. Kim, S.-W. Lee, K.-S. Jang, UPLC/FT-ICR MS-based high-resolution platform for determining the geographical origins of raw propolis samples, J. Anal. Sci. Technol. 10 (2019) 8, https://doi.org/10.1186/s40543-019-0168-2.
[176] Z. Varga, E. Nicol, S. Bouchonnet, Photodegradation of benzisothiazolinone: identification and biological activity of degradation products, Chemosphere 240 (2020), 124862, https://doi.org/10.1016/j.chemosphere.2019.124862.
[177] S. Itoh, N. Kawasaki, N. Hashii, A. Harazono, Y. Matsuishi, T. Hayakawa, T. Kawanishi, N-linked oligosaccharide analysis of rat brain Thy-1 by liquid chromatography with graphitized carbon column/ion trap-Fourier transform ion cyclotron resonance mass spectrometry in positive and negative ion modes, J. Chromatogr. A 1103 (2006) 296–306, https://doi.org/10.1016/j.chroma.2005.11.043.
[178] C.W. Diehnelt, N.R. Dugan, S.M. Peterman, W.L. Budde, Identification of microcystin toxins from a strain of *Microcystis aeruginosa* by liquid chromatography introduction into a hybrid linear ion trap-fourier transform ion cyclotron resonance mass spectrometer, Anal. Chem. 78 (2006) 501–512, https://doi.org/10.1021/ac051556d.
[179] N. Hashii, N. Kawasaki, Y. Nakajima, M. Toyoda, Y. Katagiri, S. Itoh, A. Harazono, A. Umezawa, T. Yamaguchi, Study on the quality control of cell therapy products, J. Chromatogr. A 1160 (2007) 263–269, https://doi.org/10.1016/j.chroma.2007.05.062.
[180] M.W.F. Nielen, M.C. van Engelen, R. Zuiderent, R. Ramaker, Screening and confirmation criteria for hormone residue analysis using liquid chromatography accurate mass time-of-flight, Fourier transform ion cyclotron resonance and orbitrap mass spectrometry techniques, Anal. Chim. Acta 586 (2007) 122–129, https://doi.org/10.1016/j.aca.2006.08.055.
[181] F. Wang, S. Weidt, J. Xu, C.L. Mackay, P.R.R. Langridge-Smith, P.J. Sadler, Identification of clusters from reactions of ruthenium arene anticancer complex with glutathione using nanoscale liquid chromatography fourier transform ion cyclotron mass spectrometry combined with 18O-labeling, J. Am. Soc. Mass Spectrom. 19 (2008) 544–549, https://doi.org/10.1016/j.jasms.2007.12.002.
[182] C.S. Wu, Z.X. Jia, B.M. Ning, J.L. Zhang, S. Wu, Separation and identification of moxifloxacin impurities in drug substance by high-performance liquid chromatography coupled with ultraviolet detection and Fourier transform ion cyclotron resonance mass spectrometry, Chin. Chem. Lett. 23 (2012) 1185–1188, https://doi.org/10.1016/j.cclet.2012.09.001.
[183] J.H. Wahl, S.A. Hofstadler, R.D. Smith, Direct electrospray ion current monitoring detection and its use with on-line capillary electrophoresis mass spectrometry, Anal. Chem. 67 (1995) 462–465, https://doi.org/10.1021/ac00098a035.
[184] G.A. Valaskovic, N.L. Kelleher, F.W. McLafferty, Attomole protein characterization by capillary electrophoresis-mass spectrometry, Science 273 (1996) 1199–1202, https://doi.org/10.1126/science.273.5279.1199.
[185] T.D. Veenstra, S. Martinovic, G.A. Anderson, L. Pasa-Tolic, R.D. Smith, Proteome analysis using selective incorporation of isotopically labeled amino acids, J. Am. Soc. Mass Spectrom. 11 (2000) 78–82, https://doi.org/10.1016/S1044-0305(99)00120-8.
[186] A.H. Que, Y. Mechref, Y. Huang, J.A. Taraszka, D.E. Clemmer, M.V. Novotny, Coupling capillary electrochromatography with electrospray fourier transform mass spectrometry for characterizing complex oligosaccharide pools, 1680, Anal. Chem. 75 (2003) 1684, https://doi.org/10.1021/ac025985c.
[187] R. Gavard, H.E. Jones, D.C. Palacio Lozano, M.J. Thomas, D. Rossell, S.E. F. Spencer, M.P. Barrow, KairosMS: a new solution for the processing of hyphenated ultrahigh resolution mass spectrometry data, Anal. Chem. 92 (2020) 3775–3786, https://doi.org/10.1021/acs.analchem.9b05113.
[188] B. Zekavat, J.E. Szulejko, D. LaBrecque, A.D. Olaitan, T. Solouki, Efficient injection of low-mass ions into high magnetic field Fourier transform ion cyclotron resonance mass spectrometers: injection of low-mass ions for high magnetic field FTICRMS, Rapid Commun. Mass Spectrom. 28 (2014) 230–238, https://doi.org/10.1002/rcm.6768.